Dissertation submitted for the degree of Doctor of Natural Sciences

# On the Continuous Improvement of Global Planet Formation Models

–

## The Consistent Formation of Planetary Embryos

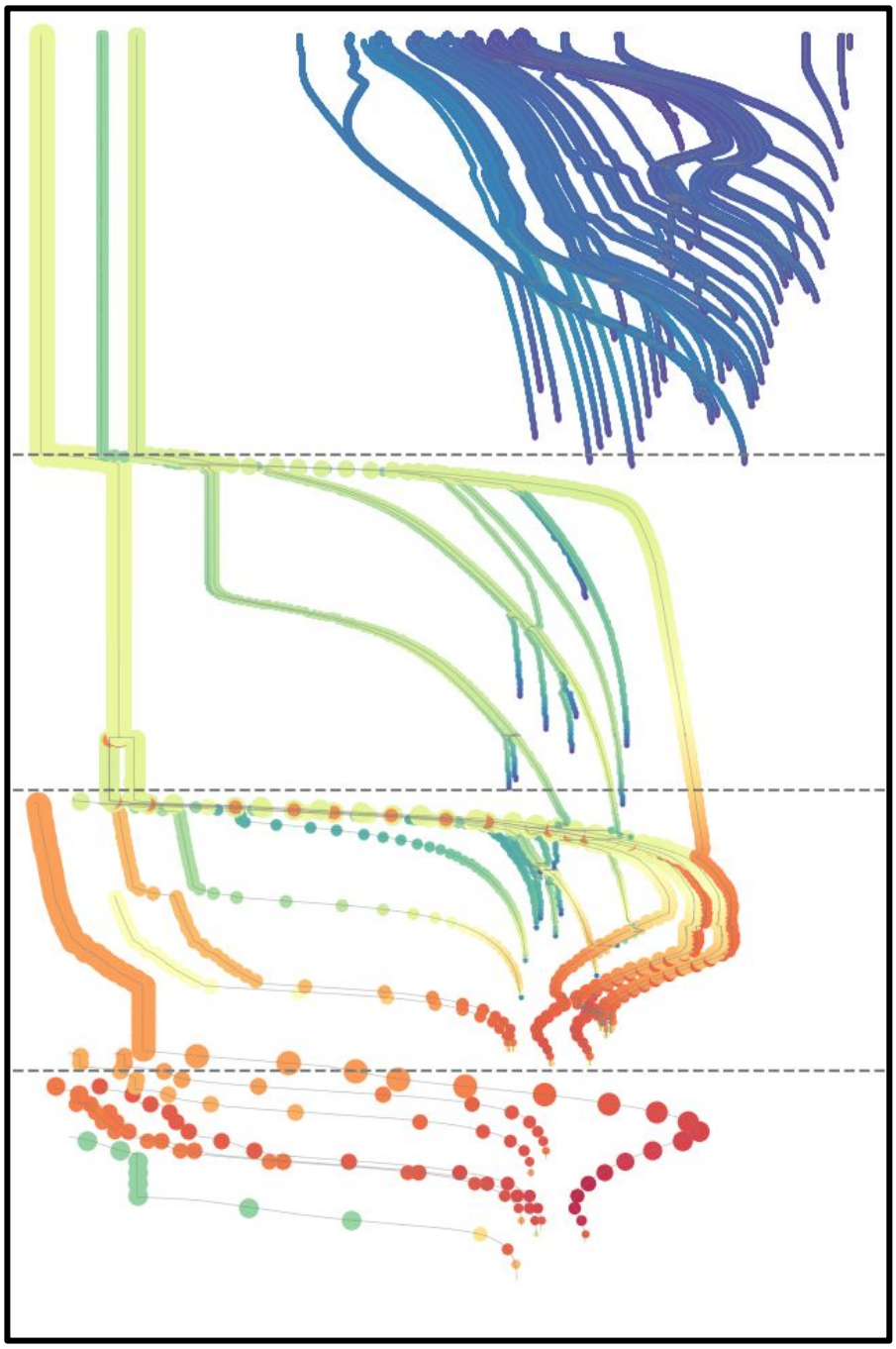

by Oliver Völkel

Dissertation
submitted to the
Combined Faculties of the Natural Sciences and Mathematics
of the Ruperto-Carola-University of Heidelberg, Germany,
for the degree of
Doctor of Natural Sciences

Put forward by
OLIVER VÖLKEL
born in Stuttgart, Germany

Oral examination: December 16, 2021

# ON THE CONTINUOUS IMPROVEMENT OF GLOBAL PLANET FORMATION MODELS

-

## THE CONSISTENT FORMATION OF PLANETARY EMBRYOS

REFEREES:
APL. PROF. DR. HUBERT KLAHR
PROF. DR. ANDREAS QUIRRENBACH

# Abstract

Our knowledge on the population of exoplanets and circumstellar disks has increased drastically in the last decades. Yet many processes during the formation of planets, especially in the intermediate size range, are unobservable. This thesis focuses on linking the evolution of a circumstellar disk with a final set of planets in a globally self consistent framework. The number of embryos and their formation in current planet formation models are subject to assumptions and not to physical modeling. This inconsistency currently marks the single largest blind spot in global planet formation modeling. Within four consecutive publications, I present key improvements in global planet formation modeling. Namely the evolution of dust and pebbles, the formation of planetesimals and the formation of planetary embryos. Within this thesis I present a global planet formation model that self-consistently tracks the formation of planets from an initial disk of gas and dust during its entire lifetime. For the first time, this is achieved without far reaching assumptions on initially placed planetesimals or planetary embryos. I show that the disk consistent treatment of planetary embryo formation results in multiple distinct embryo generations during the lifetime of the circumstellar disk. A clear dichotomy between planets that form in different generations is found. The generation from which an embryo originates has far reaching implications on its composition and final planetary properties.

# Zusammenfassung

Unser Wissen über Exoplaneten und protoplanetare Scheiben ist in den letzten Jahrzenten enorm gestiegen. Dennoch entziehen sich die meisten Prozesse bei der Entstehung von Planeten unseren Beobachgtungen. Insbesondere im Bereich zwischen Staub und bereits entstandenen detektierbaren Planeten. Die vorgelegte Dissertation verbindet die Entwicklung protoplanetarer Scheiben über ein global-selbstkonsistentes Planetenentstehungsmodell mit den daraus resultierenden Planeten. In derzeit verwendeten Planetenentstehungsmodellen sind sowohl die Anzhahl wie auch die Entstehung von planetaren Embryonen eine Annahme und nicht das Resultat physikalischer Modellierung. Diese Inkonsistent ist der derzeit größte blinde Fleck in der globalen Planetenentstehungsmodellierung. In vier aufeinander aufbauenden Publikationen lege ich essentielle Verbesserungen bzgl. globaler Planetenentstehungsmodelle vor. Diese beziehen sich auf die Entwicklung von Staub und kieselsteingroßen Partikeln, sowie der Entstehung von Planetesimalen und planetaren Embryonen. Ich präsentiere ein global-selbstkonsistentes Planetenentstehungsmodell welches die Entstehung von Planeten ausgehend von einer Staub und Gasscheibe über deren gesamte Lebensdauer beschreibt. Zum ersten Mal erfolgt dies ohne weitreichende Annahmen bzgl. anfänglicher Planetesimale, oder planetarer Embryonen. Ich zeige, dass eine scheibenkonsistente Entstehung planetarer Embryonen zu mehreren klar trennbaren Planeten-Generationen während der Lebensdauer einer protoplanetaren Scheibe führt. Es findet sich eine deutliche Dichotomie zu Planeten aus unterschiedlichen Generationen. Die Generation, aus welcher ein planetarer Embryo stammt, hat weitreichende Folgen bzgl. seiner späteren Zusammensetzung und planetarn Eigenschaften.

# Contents

# 1 | Introduction

Our home planet Earth is the only known location of life in the universe. As a potential environment for the origin and evolution of life, planets are thus among the highest priority astronomical objects to study for humankind. On the other hand, no other planet in the solar system and no other planet around any star that we observed has so far revealed itself to be a life bearing system. Is life unique to Earth or a commonly found phenomenon throughout the universe? To answer this question we need to know what makes a planet habitable and how many of those worlds exist. This requires knowledge on the present state of the planet, as much as it does on its formation history.

The current sample of observed exoplanets, while in the thousands, pales in regard to the number of known stars or galaxies in the universe and is heavily biased towards planets that are more resembled by Jupiter than Earth. Even if there were other planets like Earth out there, in many cases with current technology, we would not detect them. And even if we did, our knowledge of their formation history and their present conditions are still very limited. In parallel to continuously improving observational techniques, we need to improve our understanding of their formation to answer these questions. Only when we understand the formation of planets can we understand what events in their formation history might enable them to be a home for life.

Planet formation has long been postulated to occur from nebula like structures around stars [Kant, 1755, marquis de Laplace, 1821]. While much has changed since then in our understanding of individual processes, the conceptual idea remains. In the current paradigm, we expect planets to form in circumstellar disks. The formation of planets is therefore strongly tied to the formation of stars, as every young star forms with a disk. Yet, to this day, the formation of a planet from a circumstellar disk has never been observed (nor the complete formation of a star from a collapsing molecular cloud). Everything we see are merely snapshots in time, but never the complete story. We justify our picture, however, on the presence of numerous exoplanets around stars, the presence of the planets in the solar system and theoretical concepts that aim to explain the bottom-up formation of planets from dusty circumstellar disks.

Theory predicts timescales of up to millions of years for a planet to form [Ida and Lin, 2004]. The technology to even discover already formed planets has only been developed in the last decades. To make things even harder, numerous mechanisms involved in the formation of planets are unobservable, even with the best telescopes today (or the next generation to come). We can observe, however, fully formed planets around stars, as well as the circumstellar disks themselves from which we believe they emerge. It is specifically the intermediate size range that leaves us in the blind. This practically involves anything between dust and the fully formed planets. These processes however are indispensable in the formation of a planet and thus need to be understood. Connecting the initial structure of a circumstellar disk with a final set of planets via forward modeling is the end-goal of global planet formation models. However, this requires an in-depth and self-consistent treatment of all crucial mechanisms in the intermediate size ranges of planet formation within the same framework.

The ways planet formation is studied range over a multitude of different frameworks and concepts. From isolated analytic equations of accretion disk evolution [Shakura and Sunyaev,

1973], or collision timescales of solids in orbit around a central star [Lissauer, 1987], to complex and high resolution simulations in both a variety of isolated fields like planetesimal formation [Klahr and Schreiber, 2020] and globally coupled frameworks [Emsenhuber et al., 2020a], the theory behind planet formation has grown intensely over the past decades. A general problem in this vast field of research is to overcome the massive size range involved in the formation of a planet. This range can exceed over 40 orders of magnitude in mass from a tiny dust grain to a massive planet like Earth. As planets grow via the accretion of surrounding material, the formation of a planet requires an understanding of its local environment in the disk. Understanding the local evolution of a circumstellar disk during its entire lifetime requires an understanding of the global disk evolution as well. While isolated studies in individual components in planet formation theory are vital to its research, the entirety of the problem requires a coupled framework that combines any crucial individual physics.

Such global frameworks (or their attempts) were introduced and advanced in the last decades (Ida and Lin [2004], Alibert et al. [2005], Mordasini et al. [2009], Bitsch et al. [2015], Alessi et al. [2017], Izidoro et al. [2019], Brügger et al. [2020], Emsenhuber et al. [2020a] to mention a few ). While their differences will be highlighted later on in this thesis, they all share several vital similarities. The disk is described using one-dimensional surface densities (e.g. for the gas, or the planetesimals), instead of describing each of the many planetesimals (or gas molecules) as an individual particle. This continuum-type approach is valid on large scales and serves the purpose of computational feasibility. The surface density prescription, however, begins to break once we consider the formation of individual planets. Their evolution and formation can no longer be described with a continuum-type approach, contrary to a set of millions of planetesimals. The way global planet formation models deal with this shift in prescription is by introducing a set of individual planetary embryos in their simulation and modeling the accretion of material from the evolving surface densities. In none of the above-mentioned global planet formation frameworks is the introduction of the embryo linked with the previous evolution of the disk. The embryo is introduced as an assumption, not as the result of the disks evolution, like e.g. planetesimal growth via collisions. However, as one would expect in the core accretion scenario of planet formation, and as it has been shown in recent work [Schlecker et al., 2021], the question of where, when and how many planetary embryos form can be the most decisive parameter in modeling planet formation. Since this transition from the continuum-type surface density approach to a set of individual objects has not been done in a consistent fashion in previous global models of planet formation, it can be seen as the single largest blind spot in planet formation modeling.

My PhD project aimed to resolve this highly inconsistent shortcoming in global planet formation modeling. In the thesis presented I bridge the gap of non observability in the intermediate size range of planet formation. I present key improvements regarding the evolution of dust and pebbles, the formation of planetesimals, and the formation of planetary embryos. Those advancements on global planet formation modeling enable us to self-consistently track the size ranges from initial dust grains to a final set of planets. For the first time, this is achieved without invoking far-reaching assumptions on unobservable initially placed planetary embryos or planetesimals. It is thus possible to connect an individual disk with a distinct set of planets. Additionally, the presented framework is computationally feasible enough to compute a synthetic population of planets for statistical comparison with the observed population of exoplanets. This work reveals unknown complexity in the formation history of planets. It postulates the emergence of multiple distinct planet generations within the same circumstellar disk and manages to link final planet properties with their individual formation history.

The scientific body of this thesis has been the subject of four papers, three of which published at the time the thesis is written and one submitted. They describe individual key improvements and their effect on planet formation. In Voelkel et al. [2020] I investigate the effect of pebble flux

regulated planetesimal formation on the formation of giant planets by introducing the evolution of dust, pebbles and resulting planetesimal formation into the global planet formation model of Emsenhuber et al. [2020a]. In Voelkel et al. [2021a] and Voelkel et al. [2021b]. I investigate the formation of planetary embryos from an evolving planetesimal disk and introduce an analytic prescription for planetary embryo formation, based on the evolution of the planetesimal surface density. In Voelkel et al. [submitted to A&A] I merge the analytic embryo formation model into the global planet formation model from Voelkel et al. [2020] and study the effect of dynamic planetary embryo formation on planet formation.

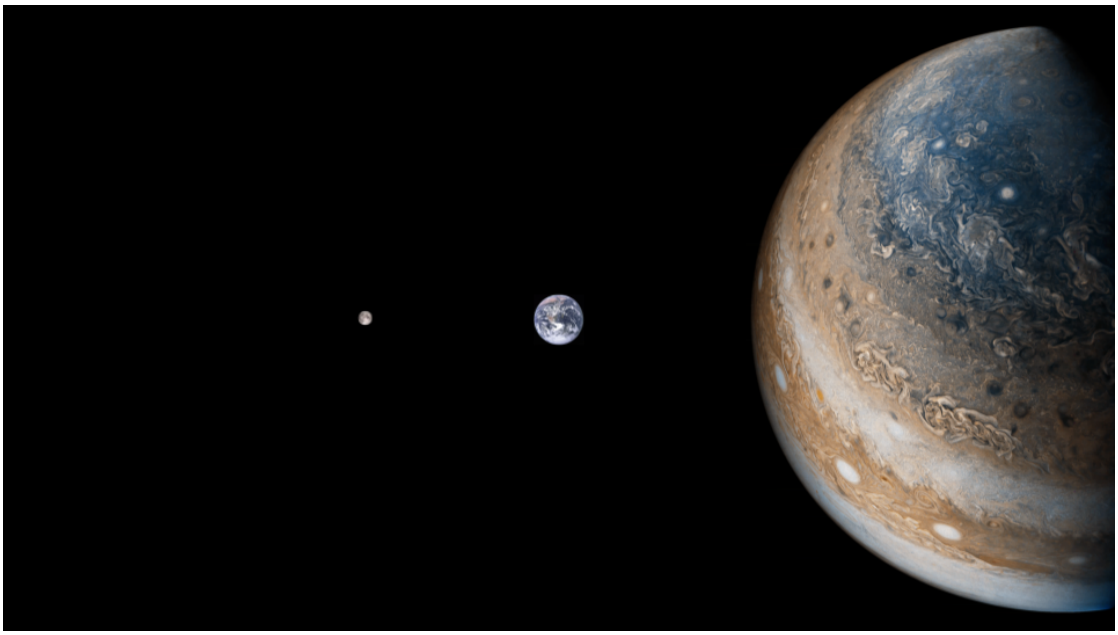

Figure 1.1: Size comparison of the Moon, Earth and Jupiter (left to right)[1].

## 1.1 Main terminology

Planets in the solar system are massive objects that orbit the Sun. Given the current definition from the IAU [2] , a planet is an object which "is in orbit around the Sun", has sufficient mass to assume "hydrostatic equilibrium" (a nearly round shape), and has "cleared the neighborhood around its orbit" . This definition refrains to make specific statements on e.g. the mass or the size of the object. However, it does implicitly so by mentioning a mass that results in a nearly round shape and the clearing of its orbital neighborhood.

### Global planet formation models

The idea behind a Global planet formation model (in the following GPFM ) is a semi-analytic prescription of the entire process. A GPFM couples multiple individual physical processes in a combined framework to model the formation of planets from a given set of initial conditions. The goal is to not only track the formation of an individual planet, but also the evolution of its environment, like the the evolution of the disk or the evolution of other simultaneously growing planets. As our understanding of the individual processes involved in the formation of a planet improves, these models begin to increase in complexity. A global model for planet formation attempts to model the entirety of the planetary system instead of the evolution of an isolated quantity within the process of planet formation (like e.g. the accretion of gas on a specifically placed planetary core). As such, they allow for studies on the effect of individual physics on planetary properties.

[1] Moon image source: https://www.nasa.gov/sites/default/files/thumbnails/image/the-moon-near-side.en_.jpg Credits: NASA / GSFC / Arizona State University. Image cropped. 02.10.2021
Earth Image "Blue Marble" source: https://www.nasa.gov/multimedia/imagegallery/image_feature_329.html Image cropped. 02.10.2021
Jupiter Image source: https://www.flickr.com/photos/132160802@N06/34724022251/ licensed under the Creative Commons Attribution 2.0 Generic license. Image cropped. 02.10.2021

[2] IAU press release on planet definition 2006, Prague
( https://www.iau.org/news/pressreleases/detail/iau0601/ 28.9.2021 )

## 1.2 A brief overview on planet formation

### The formation of a circumstellar disk

We begin our description with the formation of a star and its corresponding circumstellar disk. The star and the disk both form from a molecular cloud that is composed of gas and silicate dust. Once this cloud collapses under its own gravitational force, it begins to form a star at its center [Jeans, 1902]. A system containing more than one star is a possible outcome of this scenario as well, however, here we will focus on the formation of a single star. Stars themselves are massive objects that form as the central body of the collapsing molecular cloud. They burn via nuclear fusion [Bethe and Critchfield, 1938] and depending on their spectral type and mass their lifetimes can span from millions of years (O3 Bertulani [2013]), to trillions of years (M7 Adams et al. [2004]). They are among the most widely studied objects in astronomy, and since the discovery of the first exoplanet [Mayor and Queloz, 1995], we know that in fact many stars, not only the Sun, harbor planets. The effect of stellar properties on the formation of planets is still a very new field and all of the presented work in this thesis will refer to models and concepts that have mostly been derived for solar-type stars. The diversity within the stellar population however is gigantic. Stellar masses, luminosities, spectral types, radii, lifetimes, etc. span over orders of magnitude. To not lose ourselves within this maze of parameters, we will consider planet formation around solar-type stars within this thesis.

The cloud contains angular momentum at its collapse and as this angular momentum is conserved during the collapse, an accretion disk forms around the star. This accretion disk is what we will now refer to as the circumstellar disk. Latest observations of the dust distribution in young circumstellar disks (e.g. Andrews et al. [2018], Dullemond et al. [2018]) have revealed staggering substructures like rings and gaps, elevating these disks among the most exciting objects to study in observational astronomy. In our current understanding of planet formation, all known planets formed in such disks around stars. The initial cloud that collapsed contained some fraction of dust, beside its Hydrogen and Helium content. This amount of silicate dust is referred to as metalicity in the stellar spectrum. The same fraction of metalicity is found in the early circumstellar disk, since they both formed from the same cloud.

The evolution of the gas disk is often characterized via a viscous hydrodynamical fluid as in Lüst [1952], Weidenschilling [1977a]. Without going into too much detail on this very extensive and exciting field of research, circumstellar disks contain hydrodynamical turbulence. This turbulence is often described via a viscosity parameter and functions as a transport mechanism of angular momentum Shakura and Sunyaev [1973]. With angular momentum being transported outward, the gas disk evolves towards the star. The result is gas accretion onto the host star, which is a measurable quantity in the luminosity of young stellar objects and therefore of major importance for both star and planet formation [Manara, 2014].

### The evolution and growth of dust

In the core accretion scenario discussed herein, dust is the foundation of planet formation. Besides the gas, it is the only material that does not form within the circumstellar disk, but that directly stems from the initial molecular cloud that collapsed and formed the star. Dust behaves differently than gas, which will mark the onset of the next stage of the systems evolution. Its motion is mostly coupled to the gas, until it grows via coagulation [Birnstiel et al., 2010]. Tiny dust grains stick together and form larger agglomerates of silicate and icy particles. Once they grow sufficiently in size, their dynamic properties in relation to the surrounding gas begin to change. The dynamical evolution of particles in fluids can be characterized by their so called Stokes number [Stokes et al., 1851], which is a measure on how strongly a particle is coupled to the motion of the gas. The smaller the Stokes number, the more a particle is coupled to the gas. In the follow we will refer to the size of particles in terms of their Stokes numbers, as it it is not only the physical size

of particles that determines their dynamic motion, but also the state of its surrounding gas.

Over time, the dust in the disk will drift inward [Whipple, 1972, Adachi et al., 1976, Weidenschilling, 1977a]. This is caused by the different rotation velocity of the gas disk with respect to the dust. The gas disk around the star is stabilized by its orbital motion and its thermodynamical gas pressure. Due to the additional stabilization of the gas pressure, the gas disk rotates at a sub-Keplerian orbital speed. A dust grain, unlike a gas molecule is not supported by additional pressure and if it was not for the gas disk, a disk of dust would rotate at Keplerian speed. Tiny dust grains, however, are coupled to the motion of the gas. A dust grain in the gas disk is therefore also moving at sub-Keplerian speed. Since this dust grain is not supported by the gas pressure, its centrifugal force is not large enough to counteract the star's gravity and the grain will move closer to the star. Over time, the dust will move inward.

Once particles grow to large enough Stokes numbers they begin to move at Keplerian speed. Let's remind ourselves about the sub-Keplerian motion of the gas disk. An object moving at Keplerian speed in the sub-Keplerian disk will feel a headwind.

The headwind functions as a friction on the orbital motion of the grain. This will cause an angular momentum exchange with the disk and the particle will drift inwards. Objects with a large enough Stokes number not to be firmly coupled to the gas, but with a small enough Stokes number not to be independent of the gas are referred to as pebbles. Very small Stokes numbers result in a direct coupling of the particles motion with the surrounding gas, like cigarette dust, which stays in the air despite gravity. If the object however has a Stokes number of around unity, its motion is affected, however not entirely dominated by the motion of the surrounding gas. On Earth, a pebble is a small stone, often found close to rivers. In our context, a pebble is an object with specific aerodynamic properties. The Stokes number thus does not refer to an absolute size, but as an effective density (mass per cross section). These objects will play a major role in the growth of planets Ormel and Klahr [2010], but before that, several other things need to happen.

#### Planetesimals begin to form

Large clouds of pebbles and dust can collapse and form planetesimals Klahr and Schreiber [2020]. Like with the collapse of the cloud that forms the star and corresponding disk, gravity is the driving force for this collapse. The term planetesimal is designed to imply an infinitesimal building block for a planet. Since, as we see, even smaller material can also contribute to planetary growth this term is not necessarily the most fitting. Defining a planetesimal ist not trivial. The object has to be gravitationally bound not to be destroyed by erosion from the surrounding gas disk.

The collapse of a dust and pebble cloud can be triggered by different types of instabilities within the disk, one of them being the streaming instability [Youdin and Goodman, 2005]. This type of instability occurs if one finds a locally very high ratio of dust to gas. Usually the gas is the dominant driver of dynamics in the disk because of its higher mass. If however the ratio of dust to gas reaches values of around unity, the motion of the gas is no longer independent of the motion of the dust. The high amount of dust causes a back-reaction onto the gas, which triggers the streaming instability, resulting in the local collapse of the dust and pebble cloud. If now more outside material can contribute to the collapse, effectively weakening the streaming instability, a planetesimal can form.

The exact size of planetesimal formation is still a highly debated field of astrophysical research, see e.g. Bottke Jr et al. [2005], Walsh et al. [2017], Delbo' et al. [2017] or Zheng et al. [2017], Weidenschilling [2011], Schäfer et al. [2017]. These works refer to planetesimals as objects in the size range of several hundred meters, to several hundred kilometers. The size which will be subject to further studies regarding this thesis are 100 km in diameter as the most recent result of numerical simulations [Klahr and Schreiber, 2020]. These planetesimals are gravitationally bound objects, although their mass is not sufficient for a spherical shape, or the clearing of the

orbits. Their Stokes number, however, just like a wrecking ball in a slight summer breeze, is too large for them to feel the same interaction with the gas disk as the pebbles that formed them.

Constrainig the distribution and formation of planetesimals is far from trivial. Our own solar system delivers several vital constraints via e.g. the Asteroid belt, the Kuiper belt and the Oort Cloud. Notable here is the bottom-up theoretical modeling that aims to reproduce key findings in the solar system by Lenz et al. [2020]. Constraining the distribution in exoplanet systems via debris disks [Lagrange et al., 2000] is another viable approach. Whether planetesimals form everywhere, or only in specific regions of the circumstellar disk, like e.g. the water iceline [Drążkowska and Alibert, 2017, Schoonenberg and Ormel, 2017], remains a highly interesting question. For now at least we assume that a large amount of planetesimals has formed in the disk and we will discuss what happens next.

#### Planetesimals collide and form embryos

Going to much larger size scales in the disk than merely centimeters or kilometers, a swarm of planetesimals is not a swarm of objects on perfectly circular orbits that does not interfere with each other. Their orbital eccentricities and inclinations are affected by each other, as they begin to stir each other gravitationally. Frequent collisions are the outcome. These collisions however are not necessarily destructive, but they result in the mergers of planetesimals and as such in the growth of larger objects than the initial planetesimal forming size [Kokubo and Ida, 1996, 1998, Kobayashi et al., 2011, Walsh and Levison, 2019, Clement et al., 2020].

This planetesimal growth will result in the formation of several much larger solid objects that begin to gravitationally dominate their orbits. These larger objects then begin to scatter each other and thus increase their mutual eccentricity. Their orbits are then recircularized by the smaller planetesimals in their vicinity. The result is a stable orbital separation of the fastest growing most massive objects. These objects will become the planetary embryos. Interestingly, a higher amount of planetesimals will not result in a larger number of those embryos within a fixed spatial area. The embryos that form will only grow more massive, as their dynamics suppresses the formation of other fast growing objects in their vicinity. This stage of growth is often called oligarchic, a very well fitting term.

This process occurs much faster in the inner region of the circumstellar disk due to the shorter orbital timescales and the correspondingly higher number of collisions. Alternatively, the collapse of a pebble cloud may trigger the formation of an initially much larger object, effectively reducing the formation time of a planetary embryo at larger distances [Johansen et al., 2007, 2011, 2012, Simon et al., 2016].

#### Embryos grow by pebble and planetesimal accretion

After one of these oligarchs has reached a sufficient mass, another very efficient growth mechanism is enabled. At a mass about that of our Earths moon, the object can accrete the much smaller pebbles that drift inwards in the disk Ormel and Klahr [2010]. This pebble accretion will allow the object to grow much faster in size than the accretion of the larger planetesimals could produce. The reason lies in the dynamics of the pebbles and their interaction with the gas disk. If a large object like a planetesimal is gravitationally pulled towards our lunar mass embryo, it can either be accreted (if it manages to hit the surface) or deflected (if it misses). As large planetesimals do not feel a significant gas drag, they remain on a Keplerian orbit after their missed encounter. A pebble, however, feels a much stronger drag from the surrounding gas and as such looses angular momentum in the passage. The pebble can even be captured and spiral inwards until it finally reaches the surface of our embryo. This accretion mechanism changes the picture of planet formation drastically, giving fundamentally new constraints on the timescales involved for planet formation. Along with the accretion of planetesimals, it is the most profound growth mechanism of planets.

At this point it makes sense to highlight some of the major differences between pebble and planetesimal accretion as their individual relevance is a currently strongly debated field. The accretion of planetesimals strongly depends (among other things) on the orbital distance. As orbital timescales increase, the number of collisions and as such the planetesimal growth rate strongly decreases Lissauer [1993]. This is not the case for pebble accretion, which is why it has been a thankful concept to circumvent long formation timescales for far out giant planet cores. A distance-dependent pebble-related effect is the so called pebble isolation mass Lambrechts et al. [2014]. Once planets are massive enough to create a pressure bump in the gas disk outside their orbit, the accretion of pebbles begins to stop. The pressure bump is caused by the modification of the rotational profile of the gas disk outside the planet via gravitational torques. Up until this mass, pebble accretion can be a highly efficient growth mechanism in far-out regions where planetesimal accretion begins to reduce its efficiency. This strongly speaks for pebble accretion to form distant giant planet cores.

On the other hand, the accretion of pebbles requires the existence of a pebble reservoir, which vanishes over time due to radial drift. Planetesimals, due to their larger Stokes number, do not experience a rapid inward drift like pebbles and thus remain at their orbit (if not scattered via other planetesimals or planets). As pebbles drift inwards and larger planetesimals do not, the reservoir of pebbles at larger distances can be more rapidly depleted. Without planets or significant substructure in the disk (like e.g. the presence of rings), the lifetime of the pebble disk can be depleted in less than 1 Myrs due to accretion on the star [Birnstiel et al., 2010]. Furthermore, the accretion of pebbles requires an embryo, which is expected to be the result of planetesimal collisions. Alternatively, a single larger forming planetesimal capable of already accreting pebbles may form earlier, but even this scenario requires more time in the outer disk due to generally larger timescales. If the formation of the embryo at a larger distance takes longer than the lifetime of the pebble reservoir, the distant embryo cannot accrete pebbles. The formation of distant giant planets via pebble accretion has thus to explain the presence of the accreting embryo. Since a disk of planetesimals is expected to outlive the pebble flux at a larger distance, the accretion of planetesimals could continue for longer timescales.

#### Gas accretion leads to giant planets

During the growth of the solid core, planets begin to bind some of the surrounding gas into their atmosphere within their Hill sphere. If a planetary object has now grown to a mass about roughly ten times the mass of Earth, a gravitational collapse of the gas can occur. This stage is often referred to as runaway gas accretion [Pollack et al., 1996]. If however the accretion of solid material is larger than the accretion of gas, the runaway stage can be suppressed, as the accretion of solids heats the planetary core. This accretion heat hinders the gas from the collapse and as such from further accretion. Hot gas does not collapse as easy as cold gas due to thermodynamics. Once again, just like with the collapse of the molecular cloud that forms a star, or the collapse of the pebble cloud that forms a planetesimal, gravity is the driving force of the next growth stage.

Most of the mass in the circumstellar disk is found in gas. Let's remind ourselves, all solid material in the disk, dust, pebbles, planetesimals and planetary embryos stem from the initial tiny dust that made up only a small fraction of the initial disk mass. The efficient accretion of gas allows the planet to grow way beyond its initial solid core mass, as our own solar system gas planets Jupiter and Saturn have shown. Their formation history is expected to have undergone a stage of runaway gas accretion onto an initial solid core as well [Safronov, 1972, Perri and Cameron, 1974, Mizuno, 1980, Bodenheimer and Pollack, 1986, Pollack et al., 1996].

An alternative scenario for the formation of gas giant planets that does not involve the formation of a previous core has been introduced in Boss [1997] but found to be limited to larger distances [Rafikov, 2005]. This scenario describes the local gravitational collapse of a massive self-gravitating disk that directly forms a gas giant planet. Generally speaking, all gas giant planets

stem from the local collapse of gas in the circumstellar disk. In the core accretion scenario, however, an initial seed that triggers the collapse is required.

#### What shapes the planetary system

Up until now we have mostly discussed the main growth mechanisms and stages of a single planet, however, two main fields were not (or not specifically) mentioned. Those fields are N-body dynamics and planetary migration. During the growth and evolution of a planet it may strongly interact with both the gas disk, and other planets. These interactions mainly affect the planets orbital properties, like their semimajor axis, eccentricity and inclination. While eccentricity and inclination are dominantly affected by other planets (up to the point of scattering out of the planetary system), the change of the semimajor axis of the planet can be heavily influenced by tidal interactions with the gas disk [Goldreich and Tremaine, 1979, Ward, 1997, Tanaka et al., 2002]. Alongside this planetary migration, the gas disk can damp the eccentricity and inclination of previously excited planets and thus has a major effect on the evolution of the planetary system.

All previously discussed growth mechanisms naturally depend on the planet's environment. The dynamics of planetesimals, the properties of the gas disk and the availability of pebbles are all factors of the planets environment and orbital distance. The details of planetary migration are beyond this brief summary of planet formation, but in general the process describes the interaction of a planet with the surrounding gas disk. As angular momentum is exchanged with the gas disk, the planet changes its semimajor axis. Depending on the mass of the planet, there are different types of planetary migration and the migration rate itself depends again on the mass of the planet and its surrounding gas disk. Essential to remember however in the context of planet formation is that planets do not necessarily remain on the orbit that their initial embryo may have formed in. They can undertake large journeys during their formation which shape the final planet and the entire system.

#### On the non linearity of planet formation

We could end this (very) brief summary here but in the scope of this thesis it is worth mentioning one more thing. The above description implies a somewhat sequential character of the evolution of a planetary system. We begin with a growing dust particle, make our way to a final planet, and once the gas disk is gone, the system configures itself into a long-term stable state. However, as already mentioned in Lin and Papaloizou [1986] and as Chapter 5 of this thesis will show, the formation process of a planet may very likely end in the accretion by the host star after a period of migration. The formation of the next generation of embryos can then occur from the remaining planetesimals in the disk. The formation of planetary embryos can also occur simultaneously to the formation of a gas giant at another location in the disk. These processes raise several profound questions on planet formation as a whole. What is the survival probability of a planetary object once it has formed? How do planetary properties change depending on when (and where) the planetary embryo has formed?

The planets that in the end have survived the lifetime of the gas disk may only be the remnant later generation of planets that formed during the lifetime of the disk. This implies that the formation history of a planetary system may be far more chaotic and complex than previously assumed. Understanding this complexity however is the only way to make a statement on what conditions need to be met during the formation of a planet to allow for the presence of life.

## 1.3 Working with global planet formation models

After the brief conceptual description of planet formation in Sect. 1.2, based on our current understanding of the process, we will dive into the more technical aspects of how this picture came into place. If we ask ourselves where the properties of today's observed planetary population

come from, we need to understand every substep in the planet formation history. But even if every subfield in planet formation, like the evolution of the circumstellar disk, the evolution of the star, the coagulation of dust and its subsequent growth, was fully understood in an isolated fashion, we still do not know how planets form. In order to form a planet, these things have to be brought together and merged in the same common framework. Developing and understanding these individual processes in detail is one challenge, merging them in a common framework is the other. The coupling of the individual processes and the arising complexity is the main challenge in engineering a GPFM.

Analytic modeling quickly reaches its limitations for more complex coupled processes, which is why numerical simulations are our main approach in modeling planet formation globally. Even for the currently investigated subfields, there is no globally coupled model that brings together all individual subfields with their known complexity. In order to merge individual components, they need to be simplified in a way that enables them to be incorporated, while maintaining the essence of their implication on planet formation. This process of simplification and coupling is a challenge to balance. A model that is computationally feasible might be too simplified and may not tackle essential physics, but a model that is accurate enough might not be computationally feasible. At this point another challenge comes into play. The formation of a planet from a disk has never been observed. There is no system to which we both know the initial conditions and the final planetary system. How can we even verify (or falsify) our built model? Comparing it to an individual system can not be the final answer to that question (as the formation of a planet takes much longer than a human lifetime), so what makes a successful GPFM ?

Since the last decades, due to major improvements in observational instrumentation and methods, we can observe circumstellar disks and a multitude of exoplanetary systems. This offers us a unique way to test our GPFMs. Let's assume we are in the possession of successful GPFM for the sake of the following explanation. A model that self-consistently tracks all physics deemed crucial during the formation of a planet. This successful GPFM would predict us the planetary system that will originate from a specific disk, just like basic ballistic equations will predict the impact of a projectile, given it has all necessary initial conditions. We assume the formation of planets to be a somewhat chaotic, however still deterministic process. Now let's assume that the initial conditions for planet formation can be taken from the properties of a circumstellar disk, its stellar properties, etc. and that we are capable of observing these properties. If we now use our successful model on the many disks that we observe, and we assume that all planets formed from disks like this as well (assuming that the initial conditions did not drastically change throughout the universe), we should see a population of planets like the one we observe today. This is the idea behind planet population synthesis, a tool which will play an important role during this thesis. While the population synthesis approach requires a global planet formation model at its heart, it is in itself just another tool. In order to make statistical claims, we require a large set of parameters to be simulated. This increases the constraint on computational feasibility for the global planet formation model but allows for a quantifiable statement on the validity of the built GPFM.

Another way to verify our GPFM would be to use the solar system instead of exoplanet systems. The solar system as the best known planetary system in the universe supplies us with the most accurate constraints on a final planetary system and its individual planets. The problem here however is to choose the correct initial conditions for the solar system, as they are not exactly known. Within the current constraints, we can use MCMC simulations and see if our GPFM can reproduce a solar system analogue. If it fails, there is a good chance we lack crucial physics. For our GPFM this means that it does not only need to be verified in a statistical sense, it also has to be capable of reproducing the essential features of the solar system.

In principle there can be many successful global planet formation models (vastly different in

prescription) that allow for the above criteria. Another constraint, however, is the compliance with Occam's razor and as such the negligence of unnecessary and overly complex assumptions. In summary we can say that with our current tools and frameworks, a GPFM needs to be complex enough to include all crucial physics for planet formation and simple enough to be verified in a statistical sense without the presence of unnecessarily complex assumptions.

### 1.3.1 Current global models of planet formation

Arguably the first global planet formation model that linked the evolution of a circumstellar disk with the formation of emerging planets, including their long term evolution, is to be found in Ida and Lin [2004]. Their core accretion model describes the accretion of planetesimals that stem from an initially set disk on initially placed planetary embryos. The accretion of gas to form giant planets, as well as type II migration for massive planets, is included. The model has been subject to a large set of initial conditions, effectively computing the first synthetic population of planets and can only be described as a giant leap for global planet formation modeling.

Several other frameworks have followed a similar approach in global planet formation modeling using an initial planetesimal distribution and initial planetary embryos [Alibert et al., 2005, Mordasini et al., 2012, Alessi et al., 2017]. While each of the here mentioned frameworks would require their own individual prescription to fully be understood (or to be compared in greater detail), within the scope of this thesis I focus on their core accretion mechanism, specifically solid accretion. The most complex planet formation model that is built around the accretion of planetesimals onto initially placed planetary embryos has recently been published in Emsenhuber et al. [2020a]. It is often referred to as the NGPPS (Next Generation Planet Population Synthesis) model. The framework is the successor of Alibert et al. [2005] and Mordasini et al. [2012] and will be described in greater detail in Sect. 1.3.2.

Besides planetesimal accretion models, the accretion of pebbles [Ormel and Klahr, 2010] on planetary embryos has been subject to increasingly detailed research. Frameworks that are built around pebble accretion instead of planetesimal accretion have been introduced e.g. in Bitsch et al. [2015], Ndugu et al. [2017], Izidoro et al. [2019], Johansen et al. [2019], Bitsch et al. [2019], Brügger et al. [2020]. Using a prescription for the pebble flux and initially assumed planetary embryos, they have found that the accretion of pebbles is a highly efficient mechanism for planetary growth. Unlike the accretion of larger planetesimals [Johansen and Bitsch, 2019] due to larger orbital timescales, the accretion of pebbles remains highly efficient at larger heliocentric distances. However as already found in Bitsch et al. [2015], if an embryo is introduced at a later stage, the pebble reservoir may likely be depleted. This effectively limits growth via pebble accretion to the shorter lifetime of the pebble reservoir. This reservoir is depleted via inward drift [Birnstiel et al., 2010] and the formation of planetesimals [Lenz et al., 2019]. Without a prescription for planetesimal formation, however, the formation of a planetary embryo cannot be incorporated in a consistent fashion. Whether the embryo stems from planetesimal collisions, or is the result of a single larger forming planetesimal, both scenarios require an understanding on how much mass is transformed from pebbles to larger objects. Recent work presented in Voelkel et al. [2021b] studies the formation of planetary embryos from planetesimals that form within an evolving pebble disk. The formation of more distant embryos (>2-3 au) is found after the pebble flux has largely vanished. While the accretion of pebbles on planetesimals and planetary embryos is included, only the innermost planetary embryos can benefit from pebble accretion, as the outer embryos fail to form during the lifetime of the pebble flux.

While both pebble and planetesimal accretion are highly valuable to study individually, future modeling needs to include both mechanisms simultaneously. Models that include both the accretion of pebbles and planetesimals alike have been introduced e.g. in Alibert et al. [2018] and Guilera et al. [2020]. The work presented in Guilera et al. [2020] studies the formation of a

gas giant planet behind a pressure bump located at the water ice line. The planet formation model presented in Guilera et al. [2020] is of specific relevance, as it includes the evolution of dust and pebbles, the formation of planetesimals, and a condition for planetary embryo formation. The model assumes that once a lunar mass has formed in planetesimals (planetesimals form at 100 km in diameter) at the location of the pressure bump, a lunar mass planetary embryo is introduced at this pre-set location. While the placement on the embryo is constrained via the mass transfer from pebbles to planetesimals, the formation of the embryo remains an assumption to a specific location in the disk. Furthermore the framework did not include the growth time of planetesimals to form a lunar objects via collisions, which can take significantly longer than the formation of a lunar mass in planetesimals [Voelkel et al., 2021a]. Additionally, the study limited itself to the formation of a single embryo, neglecting potential planet-planet interactions. While the prescription presented in Guilera et al. [2020] is a large step forward in terms of consistency within global planet formation modeling, the negligence of multiple planetary embryos and planetesimal growth limits it to a local study.

Despite the differences in the above-mentioned frameworks, one striking similarity is the disk inconsistent treatment on how planetary embryos are introduced. While Guilera et al. [2020] makes a first attempt in constraining the initial formation time, the number of embryos (in their case one) and its initial location in the disk are subject to an initial assumption as well. The model presented in chapter 5 of this thesis will remove this inconsistency in global planet formation modeling.

### 1.3.2 The New Generation Planetary Population Synthesis (NGPPS)

In comparison to the models discussed in Sect. 1.3.1, the GPFM introduced by Emsenhuber et al. [2020a] is arguably the most complex and compelling GPFM in use today. It was used for population synthesis studies in Emsenhuber et al. [2020b] and is the foundation of a large set of subsequent publications that analyze said synthetic population [Schlecker et al., 2020, Burn et al., 2021, Schlecker et al., 2021, Mishra et al., 2021]. In the following I will give a description of the model that is the foundation of the continuous improvements.

Emsenhuber et al. [2020a] combines a model for stellar evolution, circumstellar disk evolution, solid and gas accretion on planetary cores, planetary evolution, planet disk interaction such as migration, and planet-planet interactions. The schematic in Fig. 1.2 is taken from Emsenhuber et al. [2020a] and gives a conceptual overview of the physics that is included in their GPFM.

The evolution of the stellar properties like the radius $R_\star$, luminosity $L_\star$, and temperature $T_\star$ for a solar mass star are taken from Baraffe et al. [2015] . The disk model in use is a one-dimensional viscously evolving gas disk on an adaptive grid Lüst [1952], Lynden-Bell and Pringle [1974]. Viscous turbulence is treated as in Shakura and Sunyaev [1973]. The vertical structure of the disk stems from Nakamoto and Nakagawa [1994] and includes viscous heating and stellar irradiation based on Fouchet et al. [2012]. Besides accretion on the host star and onto planets, the gas disk experiences photoevaporation, further decreasing its lifetime. The way photo-evaporation is included in the model is done as Mordasini et al. [2012b]. The external photo-evaporation rate for far-ultraviolet radiation follows Matsuyama et al. [2003] and the internal photo-evaporation follows Clarke et al. [2001]. The gas disk is initialized using a radial power law surface density drop-off proportional with $r^{-0.9}$ up to a critical disk radius $r_{cut,g}$ after which follows an exponential decay as in Veras and Armitage [2004].

Alongside the initial gas disk, the model in Emsenhuber et al. [2020a] contains an initial planetesimal surface density profile (something that we will strongly abbreviate from later on). The initial surface density of planetesimals follows a steeper power law index than the initial gas profile ($\propto r^{-1.5}$) as in the MMSN Hayashi [1981] to incorporate observational and theoretical findings on the solid distribution in circumstellar disks [Ansdell et al., 2018, Birnstiel and

Andrews, 2013]. As will be seen in Chapter 2, the surface density profile of planetesimals is of paramount importance for the formation of planets.

The dynamical state of planetesimals follows Fortier et al. [2013]. They are assumed to be in the oligarchic regime Ida and Makino [1993]. Important to mention here is that the continuum-type approach of a planetesimal surface density uses mean square root eccentricities and inclinations to model the dynamical state. The excitation of planetesimals can occur via self-stirring and is treated as in Ohtsuki et al. [2002]. Their excitation via protoplanets is modeled as in Guilera et al. [2010]. The latter effect greatly dominates the eccentricity and inclination distribution of planetesimals. The damping of the dynamic state of the planetesimals via the gas disk in the quadratic regime is separated into the Epstein and Stokes regime of gas drag [Adachi et al., 1976, Chambers, 2006, Rafikov, 2004, Fortier et al., 2013]. The size of planetesimals in the original Emsenhuber et al. [2020a] GPFM is set to 600m in diameter. The planetesimal size greatly affects the accretion efficiency of planetesimals and more on this field is discussed in Chapter 2.

While the GPFM in Emsenhuber et al. [2020a] also includes a compositional model based on Thiabaud et al. [2014], we will not make use of this framework, as our planetesimals will form dynamically from evolving pebbles, and as such would require specific treatment, see Chapter 2. The planetary embryos in the system are initially placed in the disk as well. The model can handle up to 100 simultaneously evolving planetary embryos.

Once embryos enter the simulation they accrete planetesimals and gas within their vicinity. The accretion of pebbles as in Chapter 5 is not part of the original Emsenhuber et al. [2020a] or the framework presented in Chapter 2. The internal structure equations of the planets in the simulation is modeled at all times to supply essential properties like the planet's radius, its luminosity and associated magnitude using a 1D approach. While this approach increases the computational effort, including effects like e.g. accretional heating by solid accretion on the luminosity can have far reaching impact on the evolution of a planet Dittkrist et al. [2014]. The more sophisticated treatment of the individual planets interior structure in combination with the global disk evolution model and interaction with other simultaneously growing planets in the same common framework elevates the GPFM in Emsenhuber et al. [2020a] to arguably be the most sophisticated planet formation model to date. The model also distinguished between the attached and detached phase of planets in the gas disk. In the attached phase, the gas envelope of the planet is in equilibrium with the surrounding gas disk and gas accretion is modeled via solving 1D radially symmetric internal structure equations [Bodenheimer and Pollack, 1986] including the effect of Deuterium burning Mollière and Mordasini [2012]. For very low surrounding gas densities or very high gas accretion rates (higher than what the gas disk can supply), the planet enters the detached phase and gas accretion is modeled via Bodenheimer et al. [2000].

In parallel to the accretion of gas, core growth occurs via the accretion of planetesimals as in Fortier et al. [2013] and the merger of other colliding planets. Planetesimals in the disk can either be accreted by the growing planets or be ejected from the system as described in Ida and Lin [2004]. The redistribution of planetesimals by scattering as in Raymond and Izidoro [2017] is not included. The structure of the core is modeled as in Mordasini et al. [2012b] to solve for its radius and density. This approach is similar to the one applied to the envelope [Seager et al., 2007]. The atmosphere around the cores can be stripped via X-ray and extreme ultraviolet radiation as in Jin et al. [2014], via Roche lobe overflow (e.g. for bloated giants very close to the star) or via collisions. As the model includes multiple planetary embryos and tracks their N-body dynamics using the mercury integrator Chambers [1999], collisions between planets are a frequent outcome. For collisions, the cores merge and and the envelope of the less massive body is ejected. The energy of the impact is included as an additional luminosity when solving the structure equations. The addition of mass and luminosity follows over the impact timescale $t_{impact}$ as in Broeg and Benz [2012].

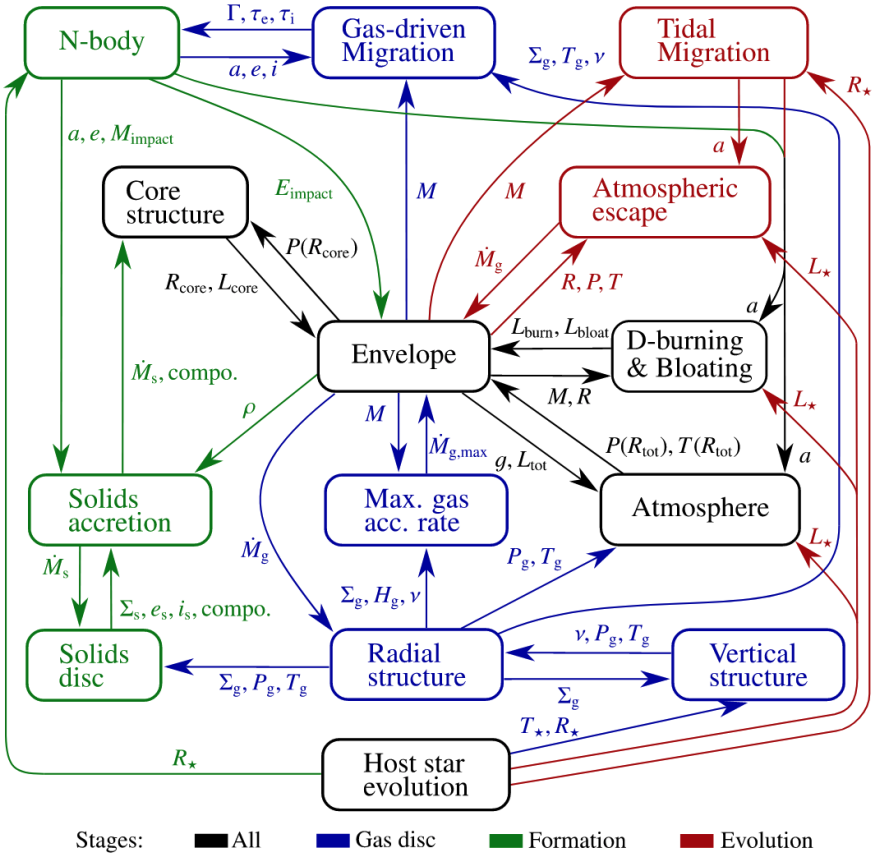


Figure 1.2: Sub-modules and most important exchanged quantities of the Generation III Bern model. The colours denote the stages at which processes are considered. Blue indicates processes active in the formation stage, but only before the dispersal of the gas disc. Green processes are considered during the entire formation stage, even after the dispersal of the gas disc. Processes in red are only considered during the evolution stage. The processes in black are included in all stages. (Figure and caption taken from Emsenhuber et al. [2020a] with kind permission of the leading author.)

Simultaneously to the evolution of the planet and the disk, planets can undergo type I and type II migration. For type I, the model follows Coleman and Nelson [2014], which includes the torque formulation of Paardekooper et al. [2011] including the possibility of attenuation of co-rotation torques via eccentricity and inclination Bitsch and Kley [2010, 2011]. Type II migration requires the formation of a gap in the gas disk and as such occurs for more massive planets. The gap-opening criterion that is chosen to switch between type I and type II migration is taken from Crida et al. [2006] and the non-equilibrium approach where the planet follows the radial velocity of the gas is taken from Dittkrist et al. [2014].

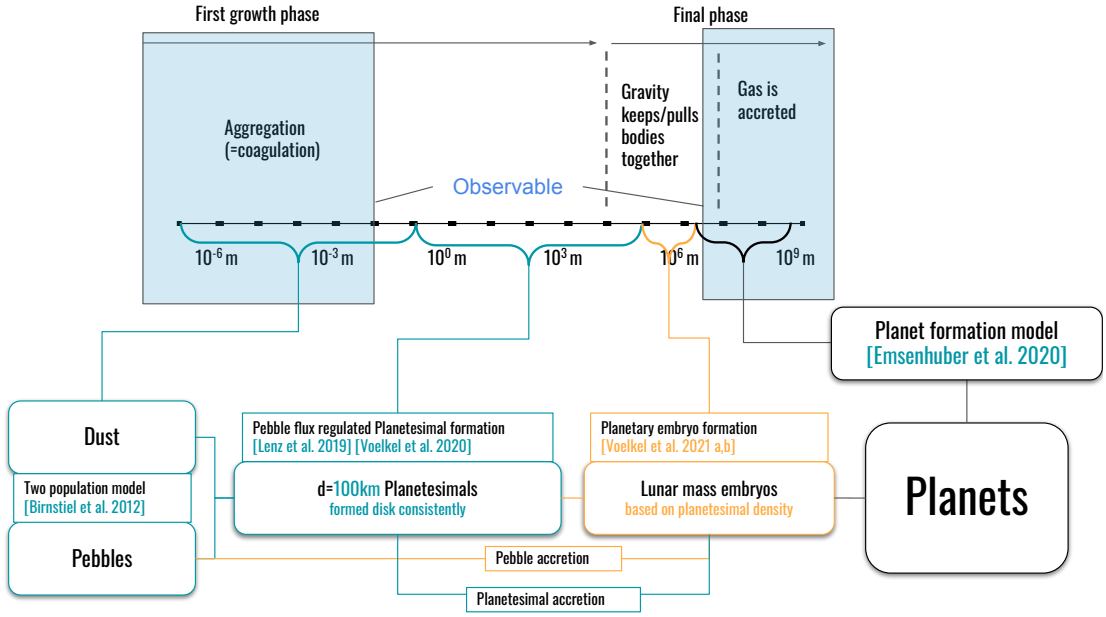


Figure 1.3: Schematic overview on the different solid evolution stages that have been added to the NGPPS model during this thesis and their corresponding size range. The evolution of dust and pebbles, the formation of planetesimals and subsequently the formation of planetary embryos in the here described form could also be coupled to other planet formation models. The evolution of the dust, pebble, and planetesimal surface density is coupled to the NGPPS gas disk evolution. The blue boxes mark the changes included in Chapter 2 and the orange boxes mark the changes included in Chapter 5. The accretion of planetesimals onto planetary embryos stems from the original Emsenhuber et al. [2020a] model. As planetary embryos can accrete pebbles and planetesimals, their back-reaction on the evolution of the dust, pebble and planetesimal disk is included. Instead of using 600 m in diameter as in the original Emsenhuber et al. [2020a], the following study will use planetesimals with 100 km in diameter. All included models run simultaneously to the other physics described in the NGPPS.

### 1.3.3 On the simplification and parameterization of physical models

As mentioned multiple times, a big challenge when engineering a GPFM is the simplification of physical models in order to be incorporated into the larger framework. I will now illustrate this process on the examples of the incorporated models within this thesis. These being the evolution of dust and pebbles, the formation of planetesimals and the formation of planetary embryos. Fig. 1.3 shows the size range involved in planet formation and gives a schematic overview on the models that have been added to the GPFM in Emsenhuber et al. [2020a]. It shows how the different size ranges and their physical prescriptions have been included. As the original model form Emsenhuber et al. [2020a] uses an initial distribution of planetesimals and planetary embryos, it only covers the larger size end of solid evolution and lacks the smaller end. As only the very small and very large end of the size spectrum can be observed however, including also the small end (here dust and pebbles) links the disk to the formation of planets and is therefore essential.

### The evolution of dust, pebbles and planetesimals

Two essential models have been included in the GPFM from Emsenhuber et al. [2020a] in Voelkel et al. [2020], and they are described in greater detail in Chapter 2.

The evolution of dust and pebbles follows a two-population approach, taken form Birnstiel et al. [2012]. Modeling the coagulation, growth, and evolution of dust in great detail, as done e.g. in Birnstiel et al. [2010], requires large computational resources and is therefore rather unfit for the population synthesis approach. Birnstiel et al. [2010] describes a full sophisticated model of dust coagulation and evolution with more than 100 different dust sizes and their relative interaction.

In order to find a computationally more feasible way to model the evolution of dust in disks, the model in Birnstiel et al. [2012] assumes that all particles can be either assigned to a larger grain size population or a smaller grain size population. The size distribution was found to be well resembled via a power law prescription and the largest size of a grain within a population. Depending on whether the local size of the particles is limited via drift or fragmentation, a fixed mass relation is applied that separates the overall solid population into small and large particles. For the case in which the size of the particles is limited by fragmentation, the model assumes that 75 % of the mass is in the larger population and in the case that growth is limited by drift, the fraction of mass in the larger size grains is given as 97 %. The mass distribution is thus top heavy in both scenarios, meaning that the majority of mass is found in objects that we can consider pebbles.

The individual sub-populations are assigned their own size and Stokes number respectively. When integrating the time evolution, one uses the mean weighted velocity between the two populations. It is shown that the global overall surface density and size evolution of the two-population model is in good agreement with the more sophisticated Birnstiel et al. [2010] model for solar mass stars. This was the motivation to incorporate the two-population solid evolution model into the GPFM framework.

Following up on the evolution of dust and pebbles, the included planetesimal formation model from Lenz et al. [2019] is again a one-dimensional parameterized approach. As a global model, it assumes local substructure in the disk that will result in particle traps. Within these particle traps, the formation of planetesimals occurs. The model does not specify which physical mechanism triggers the formation of planetesimals (e.g. streaming instability or Kelvin-Helmholtz instability) but it states that a fraction of the local pebble flux is to be transformed into planetesimals. This very basic underlying assumption is a first viable constraint on the formation timescales and spatial distribution of planetesimals because it links the formation of planetesimals to the timescales of the dust and pebble disk evolution. Planetesimals can only form from smaller material and the more small material passes through an area in the disk, the higher we expect the amount of planetesimals that form to be.

Constraining this efficiency, however, is yet to be investigated and first attempts in constraining the parameter space for the solar nebula have been taken in Lenz et al. [2020]. At this point, we can say that if the efficiency is too low, there will be no planetesimals forming. This would also result in a lack of planetary embryos, assuming that embryos form via planetesimal collision, and as such in the absence of planets in the core accretion scenario in general. If the efficiency is very high and all pebbles are rapidly transformed into planetesimals, this leaves little space for pebble accretion.

Important to mention is that the pebble-flux regulated model of planetesimal formation in Lenz et al. [2019] results in a much steeper planetesimal surface density slope than the initial gas disk. As a consequence of inward pebble drift, the amount of planetesimals in the inner region of the disk is vastly higher than initially assumed and, as shown in Chapter 2, this greatly enhances the formation of close-in giant planets.

**The formation of planetary embryos**

In Sect. 1.3.1, I mentioned that a common shortcoming of all mentioned GPFM s is the initial placement of planetary embryos and/or the placement of initial planetesimals. This means that the formation of planets is heavily influenced by our inconsistent initial assumption, as it is independent of the evolution of the disk. Nonetheless, the distribution of planetary embryos is a result of the disks evolution and if not treated consistently as such may bring incorrect results.

The formation of lunar mass embryos from 100 km sized planetesimals is a non-trivial process and numerically quite challenging to handle. Simulating a swarm of planetesimals with the necessary number to form a lunar mass object in a straightforward approach is computationally not feasible. A numerical framework called the LIPAD code that uses the workaround of tracer particles is described in Chapter 4. This very sophisticated N-body dynamics code can simulate the formation of lunar mass planetary embryos from a swarm of planetesimals for multiple million years in a locally restricted area. It is however far too complex and computationally intensive to model the formation of planetary embryos for a planet population synthesis framework. Also, only focusing only on one defined spatial area defeats the point of the global character of a GPFM.

In contrast to the sophisticated N-body code, planetesimals in the GPFM are described as a one dimensional planetesimal surface density instead of a finite number of individual objects. This simplified approach heavily decreases the computational cost of the model but does not allow for planetesimal collisions and growth as in the LIPAD code.

While the LIPAD code allows for a much more solid treatment of the dynamical evolution of planetesimals than our parameterized approach, much of that information cannot be handled by the simple one-dimensional prescription in the GPFM. The questions that we have to focus on for the formation of planetary embryos is where they form, when they form, and how many of them form. If we can reproduce these features from our one dimensional surface density evolution, then we can use this information to place planetary embryos dynamically in the simulation. Instead of coupling the N-body code, the goal is to find a simple one-dimensional prescription that tells us where, when, and how many embryos form for a given planetesimal surface density evolution. While in an ideal world we would of course use the more sophisticated prescription (in this case LIPAD), for our purpose, it is valid to use a simplified and parameterized approach.

Chapter 4 and Chapter 5 will show that using the known equations for planetesimal growth Lissauer [1993] and the orbital separation of planetary embryos Kokubo and Ida [1996, 1998] does well in reproducing the formation of planetary embryos for a given planetesimal surface density evolution. It is therefore valid to use the analytic prescription described in Voelkel et al. [2021a] as a first step to move away from an initial distribution of planetary embryos towards a more consistent treatment.

The effect of this more consistent treatment of planetary embryo formation using the GPFM presented in Emsenhuber et al. [2020a] with the pebble flux regulated planetesimal formation from Lenz et al. [2019] as implemented in Voelkel et al. [2020] is presented in Chapter 5 [Voelkel et al., submitted to A&A]. It is shown that the interplay of dynamic planetary embryo formation and planetary migration leads to the formation of multiple distinct phases of planet formation within the lifetime of the gas disk. Being able to constrain the formation time of an embryo has far reaching implications on the formation history of the resulting planet and as such on its final state. This finding vividly displays the necessity and potential of self consistent global modeling and the coupling of various physical modules within the same common framework.

### 1.3.4 The outline of this thesis

Within this thesis I present 4 consecutive publications regarding the evolution of dust and pebbles, the formation of planetesimals, and the formation of planetary embryos. Each publication is based on the results of the previous. They describe continuous improvements of global planet formation modeling and their individual implications on planet formation theory. The improvements are included into the GPFM presented in Emsenhuber et al. [2020a], arguably the mot complex and compelling GPFM to date.

In Chapter 2 [Voelkel et al., 2020] I investigate the effect of pebble flux regulated planetesimal formation on the formation of giant planets. I include the evolution of a two population model for dust and pebble evolution and the consistent formation of planetesimals into the Emsenhuber et al. [2020a] GPFM. Planetesimals form at 100km in diameter, a size often considered inefficient for planetesimal accretion. The formation of planetesimals, when done consistent with the evolution of the pebble flux, results in a steeper planetesimal surface density profile than the initial distribution of gas and dust. I show that this steep profile enables the formation of giant planets due to highly condensed planetesimal zones in the inner circumstellar disk.

In Chapter 3 [Voelkel et al., 2021a] I link the formation of planetary embryos with the formation of planetesimals. I present a parameterized semi-analytic one dimensional model for the formation of planetary embryos based on the evolution of the planetesimal surface density. Its results are compared to high resolution N-body simulations. I show that the presented model does well in reproducing the total number of planetary embryos, their spatial distribution, and formation time for a given planetesimal surface density evolution.

In Chapter 4 Voelkel et al. [2021b] I follow up on the study presented in Chapter 3 and investigate the effect of pebble accretion on the formation of planetary embryos in the terrestrial planet zone. I show that the accretion of pebbles leads to the formation of more massive planets, however less embryos form due to the larger orbital spacing as a consequence of the larger embryo mass. Since the number of embryos that form in the semi-analytic prescription of Chapter 3 is limited via the Hill radii of the growing planets, the model remains valid in the presence of pebble accretion.

In Chapter 5 Voelkel et al. [submitted to A&A] I include the dynamic embryo formation model from Chapter 3 and Chapter 4 into the GPFM presented in chapter 2. Additionally I include the accretion of pebbles alongside the accretion of planetesimals. Using the newly built framework I investigate the effect of dynamic embryo formation and pebble accretion on the formation of planetary systems. Multiple consecutive phases of embryo formation are the outcome. Massive planets form early by the accretion of pebbles and are often subject to accretion onto the host star after effective type I inward migration. Once the massive planets are accreted by the host star, a new generation of embryos begins to form in the previously populated zone. Their growth is dominated via planetesmal accretion.

Chapter 6 will close this thesis with a brief summary of the obtained results, their discussion and an outlook to future possibilities and challenges with the newly obtained GPFM.

# 2 | Dust to planetesimals

This chapter resembles the work published in Voelkel et al. [2020]. The title of the publication is "Effect of pebble flux-regulated planetesimal formation on giant planet formation". I am the leading author of the manuscript. The model description in Sect. 2.3.1 has been written by Alexandre Emsenhuber. The rest of the document, including all figures and corresponding analysis have been conducted by me, taking into account the input of all listed co-authors. The implementation of the additional code and the execution of the corresponding simulations has been conducted by me. Alexandre Emsenhuber and Christian Lenz supported the code development with discussions. Hubert Klahr, Christoph Mordasini, Alexandre Emsenhuber and Christian Lenz supported the interpretation of the results with discussions.

The formation of gas giant planets by the accretion of 100 km diameter planetesimals is often thought to be inefficient. A diameter of this size is typical for planetesimals and results from self-gravity. Many models therefore use small kilometer-sized planetesimals, or invoke the accretion of pebbles. Furthermore, models based on planetesimal accretion often use the ad hoc assumption of planetesimals that are distributed radially in a minimum-mass solar-nebula way. Voelkel et al. [2020] uses a dynamical model for planetesimal formation to investigate the effect of various initial radial density distributions on the resulting planet population. In doing so, Voelkel et al. [2020] highlights the directive role of the early stages of dust evolution into pebbles and planetesimals in the circumstellar disk on the subsequent planet formation. Voelkel et al. [2020] implemented a two-population model for solid evolution and a pebble flux-regulated model for planetesimal formation in our global model for planet population synthesis. This framework was used to study the global effect of planetesimal formation on planet formation. As reference, Voelkel et al. [2020] compared their dynamically formed planetesimal surface densities with ad hoc set distributions of different radial density slopes of planetesimals. Even though required, it is not the total planetesimal disk mass alone, but the planetesimal surface density slope and subsequently the formation mechanism of planetesimals that enables planetary growth through planetesimal accretion. Highly condensed regions of only 100 km sized planetesimals in the inner regions of circumstellar disks can lead to gas giant growth. Pebble flux-regulated planetesimal formation strongly boosts planet formation even when the planetesimals to be accreted are 100 km in size because it is a highly effective mechanism for creating a steep planetesimal density profile. Voelkel et al. [2020] finds that this leads to the formation of giant planets inside 1 au already by pure 100 km planetesimal accretion. Eventually, adding pebble accretion regulated by pebble flux and planetesimal-based embryo formation as well will further complement this picture.

## 2.1 Introduction

A current conundrum of planetesimal accretion in the core-accretion scenario of planet formation is that for 100 km planetesimals it appears to require an unreasonably high disk mass to be an effective mechanism for giant planet formation within the lifetime of a circumstellar disk [Fortier et al., 2013]. The accretion of smaller objects with a higher effective cross section, such as either kilometer (km)-sized planetesimals [Ida and Lin, 2004] or centimeter (cm)-sized bodies known as pebble accretion [Ormel and Klahr, 2010] is often described as the solution for giant planet formation and has been studied widely by Klahr and Bodenheimer [2006], Lambrechts and Johansen [2012], Levison et al. [2015], and Bitsch et al. [2015], to name just a few. While we refrain from making a statement on the efficiency of pebble accretion, the scenario of a planetary core that accretes inward-drifting pebbles also lacks an explanation on how, where, and when this planetary core first forms. Planetesimals are typically too small for efficient pebble accretion [Ormel and Klahr, 2010], therefore a pebble-accreting embryo might well have formed from planetesimal collisions. This crucial step adds room for discussing the formation of planetesimals and subsequently their role in planetary core and planet formation. From Tanaka and Ida [1999] we know that the accretion rate of planetesimals depends on the planetesimal size and linearly on the planetesimal surface density. Constraining the size of planetesimals is an active field of research. While some studies infer that the current size of asteroid belt objects is well constrained and that they are about 100 km in diameter [Bottke Jr et al., 2005, Walsh et al., 2017, Delbo' et al., 2017], other studies reported that the size distribution found today merely reflects the sizes that are most resilient to clearing and therefore suggest a smaller primordial size [Zheng et al., 2017]. The observed size distribution might also arise from the growth of planetesimals that originally measured 100 m [Weidenschilling, 2011]. In the Kuiper belt, the size distribution has a similar shape as predicted by simulations that include the streaming instability between 10 and 100 km [Schäfer et al., 2017], which indicates large initial sizes. On the other hand, recent discoveries of Kuiper belt objects through stellar occultations rather indicate a size of 1-2 km [Arimatsu et al., 2019]. Small initial sizes of 0.4 - 4 km have also been inferred theoretically by Schlichting et al. [2013]. The surface density profile of planetesimals for extrasolar systems is likewise unknown. Studies of our own Solar System motivated the minimum-mass solar-nebula (mmsn) hypothesis [Weidenschilling, 1977b, Hayashi, 1981], which results in a power-law drop of the planetesimal surface density with a decay of $\Sigma_P \propto r^{-1.5}$. Observations of solid material in disks [Andrews et al., 2010] and the widely used $\alpha$-disk model for the viscous evolution of an accretion disk [Shakura and Sunyaev, 1973] suggest a shallower density distribution of $\Sigma_P \propto r^{-0.9}$ for radially constant $\alpha$. The observed solid material is not planetesimals, however, but the dust in the circumstellar disk, as the distribution of planetesimals in protoplanetary disks is currently unobservable. Lenz et al. [2019] modeled the formation of planetesimals based on the solid evolution of a viscously evolving disk, assuming that planetesimals form proportional to the time-dependent local radial pebble flux. They reported that the profile of the planetesimal surface density becomes significantly steeper ($\Sigma_P \propto r^{-2.1}$) than the initial dust, pebble, and gas density ($\Sigma \propto r^{-0.9}$). This mass transfer results in an increase in the planetesimal surface density in the inner circumstellar disk by several orders of magnitude without increasing the total mass in planetesimals. Because the accretion rate of planetesimals is proportional to the local planetesimal surface density, these highly condensed planetesimal zones are promising candidates to exert a drastic effect on planetary growth.

Before we discuss some of the previous work, we distinguish between a global planet formation model and a model for planet population synthesis. While a model for planet population synthesis contains (or should contain) a global formation model, this does not apply vice versa. Key to the population synthesis approach is that the model is complex enough to take the physical effects into account that are deemed crucial for planet formation, but its single-system computational

cost is low enough for it to be used to study a wide range of parameters. Only this will enable a statistical comparison with observational data. For this purpose, it is vital to find ways to simplify complex physical processes and merge them to a more complex framework without loosing the essence of their nature. The formation of planetesimals is such a process, and the one-dimensional formation model by Lenz et al. [2019] is such an attempt.

Previous work on the accretion of planetesimals for planetary growth such as Johansen and Bitsch [2019], Mordasini [2018], or Ida and Lin [2004] used initial distributions of planetesimals and initially placed planetary embryos, while neglecting the presence of pebbles. Other formation models such as those of Bitsch et al. [2015] or Brügger et al. [2018] modeled planetary growth by the accretion of pebbles and initially set planetary embryos, while neglecting the formation, or accretion, of planetesimals. A model that contains both pebble and planetesimal accretion while also taking the formation of planetesimals and planetary embryos into account is still pending.

We therefore chose to improve our planet population synthesis model by a "disk-consistent"[1] model for solid evolution [Birnstiel et al., 2012] and planetesimal formation [Lenz et al., 2019] to take the early stages of the disk evolution into account. This early phase determines the planetesimal surface density distribution, the radial pebble-flux evolution, and the formation of planetary cores and therefore planet formation as a whole. For our study, we focus on the formation and accretion of planetesimals. We display the effect of the planetesimal surface density and its formation on the population of planets. We show that the accretion by 100 km sized planetesimals is in fact a highly efficient growth mechanism for planets because of the highly condensed planetesimal regions in the disk. Furthermore, we give an overview of future possibilities that arise from our newly implemented modules.

This paper is structured as followed: in Sect. 2.2 we explain the planetesimal formation model together with the newly implemented solid-evolution model on which it is based. Sect. 2.3 provides insight into the population synthesis framework and how it was modified for our purpose. The changes in $\Sigma_P$ in the population synthesis code and the newly computed synthetic populations, are presented in Sect. 2.4. Sect. 2.5 discusses the results, followed by a brief summary and an outlook on our new possibilities and future work in Sect. 2.6.

## 2.2 Planetesimal formation model

### 2.2.1 Two-population solid-evolution model

The two-population model for solid evolution by Birnstiel et al. [2012] is a parameterized approach to model the evolution and growth of dust and cm sized bodies in circumstellar disks. A detailed description of the model can be found in Birnstiel et al. [2012] and Lenz et al. [2019]. We briefly outline the assumptions here and list the most important reasons for choosing it in our framework. Our goal is to implement a fast-computing, one-dimensional, parameterized algorithm for solid evolution that is well tested and agrees well with more sophisticated models. Key for the performance of the two-population approximation is a parameterized mass ratio $f_m(r)$ as a function of orbital distance $r$ between two populations of solids, which depends on whether the growth of the particles is limited by drift or by fragmentation. In each time step, the model solves one advection-diffusion equation that is given by

$$\frac{\partial \Sigma_s}{\partial t} + \frac{1}{r}\frac{\partial}{\partial r}\left[ r\left( \Sigma_s \bar{u} - D_g \Sigma_g \frac{\partial}{\partial r}\left(\frac{\Sigma_s}{\Sigma_g}\right)\right)\right] = 0, \tag{2.1}$$

where $\Sigma_s$ is the total solid-surface density without planetesimals, $\Sigma_g$ is the gas surface density, $D_g$ is the gas diffusion coefficient, and $t$ and $r$ are time and radial distance. $\bar{u}$ describes the weighted

[1] "disk-consistent" means that both dust evolution and planet formation use the same disk model, including viscosity, density, and temperature evolution.

velocity of the total solid density and is defined as

$$\bar{u} = (1 - f_m(r)) \cdot u_0 + f_m(r) \cdot u_1, \tag{2.2}$$

where $f_m$ is the fit parameter for the mass ratio between the two populations. $u_0$ and $u_1$ describe their velocities, while the surface densities of the two populations are given as

$$\Sigma_0(r) = \Sigma_s(r) \cdot (1 - f_m(r)) \tag{2.3}$$
$$\Sigma_1(r) = \Sigma_s(r) \cdot f_m(r). \tag{2.4}$$

The two populations are defined by their Stokes number. Particles with a small Stokes number of $\mathrm{St} << 1$ are strictly coupled to the evolution of the gas, whereas particles with $\mathrm{St} \geq 1$ are not. $\Sigma_0$ describes the smaller population, which can be seen as dust, subject to diffusion and transport with the gas, while $\Sigma_1$ describes the larger population, which can be seen as pebbles, which in addition to being diffused by the gas are also sedimenting toward the midplane and drifting toward pressure maxima, for instance, toward the star. The fit parameter $f_m$ was derived by comparing the two-population model to the more sophisticated dust model from Birnstiel et al. [2010]. The values for $f_m$ that were the best fit are given as

$$f_m = \begin{cases} 0.97, & \text{drift-limited case} \\ 0.75, & \text{fragmentation-limited case} \end{cases}. \tag{2.5}$$

These are also the values that we used in our simulations. The effect of this implementation is shown in Fig. 2.1, where the ratio between dust and pebbles varies with space and time. This is shown by the two blue curves.

### 2.2.2 Pebble flux-regulated planetesimal formation

The full model and its results are described in Lenz et al. [2019] in greater detail. We therefore outline here only the basic physical assumptions of this one-dimensional approach and summarize the most important equations and results. The principle behind this parameterized model is that planetesimals form by a local continuous mechanism that converts a certain fraction of the pebbles that drift by into planetesimals. In principle, it thus acknowledges that pebbles will drift inward and that more planetesimals can be formed when more material comes by. Many different planetesimal formation prescriptions can therefore be parameterized in this way. Wheter in the framework of turbulent clustering [Cuzzi et al., 2010, Hartlep and Cuzzi, 2020], streaming instabilities [Johansen et al., 2009, Schäfer et al., 2017], local trapping in zonal flows [Johansen et al., 2007, 2011, Dittrich et al., 2013, Drążkowska and Alibert, 2017], or in vortices [Raettig et al., 2015, Lyra et al., 2018], the formation is always limited by the number of fresh pebbles that a region receives after consuming the locally available pebbles. Our parameterization is thus by definition model independent. Different scenarios might lead to the same conversion rates for the pebble flux. The parameters we need is the fraction $\varepsilon$ of pebbles that is converted into planetesimals after having drifted over a distance of $d$ within the disk. We can motivate these parameters easily in our paradigm of trapping zones that slowly evolve coherent flow structures in protoplanetary disks, such as vortices and zonal flows [Schreiber, 2018], which can form everywhere, live only for a limited time, and thus only trap a fraction of drifting pebbles. In these traps, pebbles become sufficiently concentrated for planetesimal formation to be triggered, regulated by streaming and Kelvin Helmholtz instabilities. The planetesimal formation rate is generally proportional to the radial pebble flux,

$$\dot{M}_{\mathrm{peb}} := 2\pi r \sum_{\mathrm{St}_{\mathrm{min}} \leq \mathrm{St} \leq \mathrm{St}_{\mathrm{max}}} |v_{\mathrm{drift}}(r, \mathrm{St})| \Sigma_s(r, \mathrm{St}), \tag{2.6}$$

where $v_{\text{drift}}$ is the drifting velocity of the particles and $\text{St}_{\text{min}}$ and $\text{St}_{\text{max}}$ are the minimum and maximum Stokes number for which a particle is considered a pebble. $v_{\text{drift}}$ is given as

$$v_{\text{drift}}(r,\text{St}) = \frac{\text{St}}{\text{St}^2+1}\frac{h_g(r)}{r}\frac{\partial lnP(r)}{\partial lnr}c_s(r), \tag{2.7}$$

where $P(r)$ is the gas pressure, $h_g(r)$ is the gas pressure scale height ($h_g(r) = c_s(r)/\Omega(r)$), and $c_s(r)$ is the sound speed. $\Omega(r)$ is given as the orbital frequency at the radial distance $r$. The source term for planetesimals, that is, for $\Sigma_P$ , is then given as [Lenz et al., 2019]

$$\dot{\Sigma}_{\text{p}}(r) = f_{\text{ice}}(T)\frac{\varepsilon}{d(r)}\frac{\dot{M}_{\text{peb}}}{2\pi r,} \tag{2.8}$$

where $d(r)$ is the radial separation of the pebble traps and $\varepsilon$ is the efficiency parameter that describes how much of the pebble flux is transformed into planetesimals after drifting over a distance of $d$. We chose a constant value of $\varepsilon = 0.05$ as a good value to form a sufficient number of planetesimals, as was found in Lenz et al. [2019] for $d(r) = 5.0$ pressure scale heights, motivated by our findings in the detailed numerical simulations of zonal flows [Dittrich et al., 2013]. Generally, we can change $\varepsilon$ locally when the formation of planetesimals might follow a different underlying mechanism, for instance, around the water-ice line, as described by Drążkowska and Alibert [2017] or Schoonenberg and Ormel [2017]. This flexibility allows us to study a broad range of planetesimal formation scenarios, using the same implementation. Our two-population implementation currently has no proper treatment of the processes of evaporation and possible recondensation. The only effect of the existing ice line is incorporated into the parameter $f_{\text{ice}}(T)$:

$$f_{\text{ice}}(T) = \begin{cases} 1 & \text{for } T <= 170\text{K} \\ \frac{1}{3} & \text{for } T > 170\text{K} \end{cases}, \tag{2.9}$$

in effect to reduce the pebble flux inside the ice line to compensate for the evaporation of water ice. Therefore the ice line is visible in the distribution of planetesimals, even though it is not visible in the pebbles themselves (see Fig. 2.1). We also used a fixed planetesimal size of 100 km in diameter as in Lenz et al. [2019]. As a consequence, a threshold of transformed mass must be reached to build at least one planetesimal. From this we can derive a critical pebble flux that is required for $\Sigma_P$ to change. It is given as [Lenz et al., 2019]

$$\dot{M}_{\text{cr}} := \frac{m_p}{\varepsilon\tau_t,} \tag{2.10}$$

where $\tau_t$ describes the average lifetime of a trap, which is given as 100 local orbits, and $m_P$ is the mass of a single planetesimal. For simplicity, we assumed spherical planetesimals with a uniform density of $\rho_s = 1.0\text{g/cm}^3$. The mass that is transformed into planetesimals arises as a sink term in the advection-diffusion equation (Eq. 2.1). The new advection-diffusion equation is then given as

$$\frac{\partial\Sigma_s}{\partial t} + \frac{1}{r}\frac{\partial}{\partial r}\left[r\left(\Sigma_s\bar{u} - D_g\Sigma_g\frac{\partial}{\partial r}\left(\frac{\Sigma_s}{\Sigma_g}\right)\right)\right] = L, \tag{2.11}$$

where the sink term $L$ is defined as

$$L = (1 - f_m(r))\cdot L_0 + f_m(r)\cdot L_1, \tag{2.12}$$

with

$$\begin{aligned} L_0 = &\frac{\varepsilon}{d(r)}\cdot v_{\text{drift}\,0}\Sigma_0\cdot\theta\left(\dot{M}_{\text{peb}} - \dot{M}_{\text{cr}}\right) \\ &\times\theta\left(\text{St}_0 - \text{St}_{\text{min}}\right)\cdot\theta\left(\text{St}_{\text{max}} - \text{St}_0\right) \end{aligned} \tag{2.13}$$

and

$$L_1 = \frac{\varepsilon}{d(r)} \cdot v_{\text{drift }1}\Sigma_1 \cdot \theta\left(\dot{M}_{\text{peb}} - \dot{M}_{\text{cr}}\right) \times \theta\left(\text{St}_1 - \text{St}_{\text{min}}\right) \cdot \theta\left(\text{St}_{\text{max}} - \text{St}_1\right), \tag{2.14}$$

where $\theta(\cdot)$ is the Heaviside function. This combines the conditions described above for planetesimal formation. The surface density can only change while a critical mass is transformed ($\theta\left(\dot{M}_{\text{peb}} - \dot{M}_{\text{cr}}\right)$) and when the Stokes numbers of the particles are within $\text{St}_{\text{min}}$ and $\text{St}_{\text{max}}$ ($\theta\left(\text{St}_0 - \text{St}_{\text{min}}\right) \cdot \theta\left(\text{St}_{\text{mas}} - \text{St}_0\right)$).

## 2.3 Planet formation and evolution model

### 2.3.1 Model components

The current version of our planet population synthesis model can be found in Emsenhuber et al. [2020a]. It is an update of the model presented in Mordasini [2018]. This model combines planet formation [Alibert et al., 2005, 2013] and evolution [Mordasini et al., 2012]. Descriptions of the model can be found in Benz et al. [2014], Mordasini et al. [2015], Mordasini [2018], and in upcoming work by Emsenhuber et al. [2020a]. We provide here an overview of the physical processes that are tracked in the model and focus on the solid components of the protoplanetary disk model in Sect. 2.3.2.

The formation part of the model follows the core-accretion scenario of planetary embryos in viscously evolving circumstellar disks [Lüst, 1952, Lynden-Bell and Pringle, 1974]. The macroscopic viscosity is given by the $\alpha$ parameterization [Shakura and Sunyaev, 1973]. Planetesimals are assumed to be in the oligarchic regime [Ida and Makino, 1993, Thommes et al., 2003, Chambers, 2006, Fortier et al., 2013]. The structure of the envelope is retrieved by solving the internal structure equations [Bodenheimer and Pollack, 1986]. During the initial phase, gas accretion is governed by the ability to radiate the potential energy gained by the accretion of both solids and gas [Pollack et al., 1996, Lee and Chiang, 2015]. The efficiency of cooling increases with the planetary mass, and when the gas-accretion rate is limited by the supply of the gas disk, the planet contracts [Bodenheimer et al., 2000].

Planets embedded in a gas disk will undergo migration [e.g., Baruteau et al., 2014]. The model uses the prescription of Dittkrist et al. [2014]. For type I migration, it is based on the work by Paardekooper et al. [2010], while for type II migration, planets move in equilibrium with the gas disk. The switch between the two follows the criterion of Crida et al. [2006].

The formation stage lasts for the entire lifetime of the protoplanetary disk, but for 10 Myr at least. When this is completed, the model switches to the evolution stage [Mordasini et al., 2012], in which the planets are followed until 10 Gyr. This stage follows the thermodynamical evolution of the planets, with atmospheric escape [Jin et al., 2014] and tidal migration.

To perform population synthesis, we used a method similar to that of Mordasini et al. [2009], with several adaptations. The distribution of disk gas masses and the relationship between the mass and the exponential cutoff radius follow Andrews et al. [2010]. The inner radius was fixed to 0.03 au. The initial embryo mass was $0.0123\,M_\oplus$ and the location was random, with a uniform distribution in the logarithm of the distance between 0.06 and 40 au. Embryos were placed directly at the beginning of the simulations.

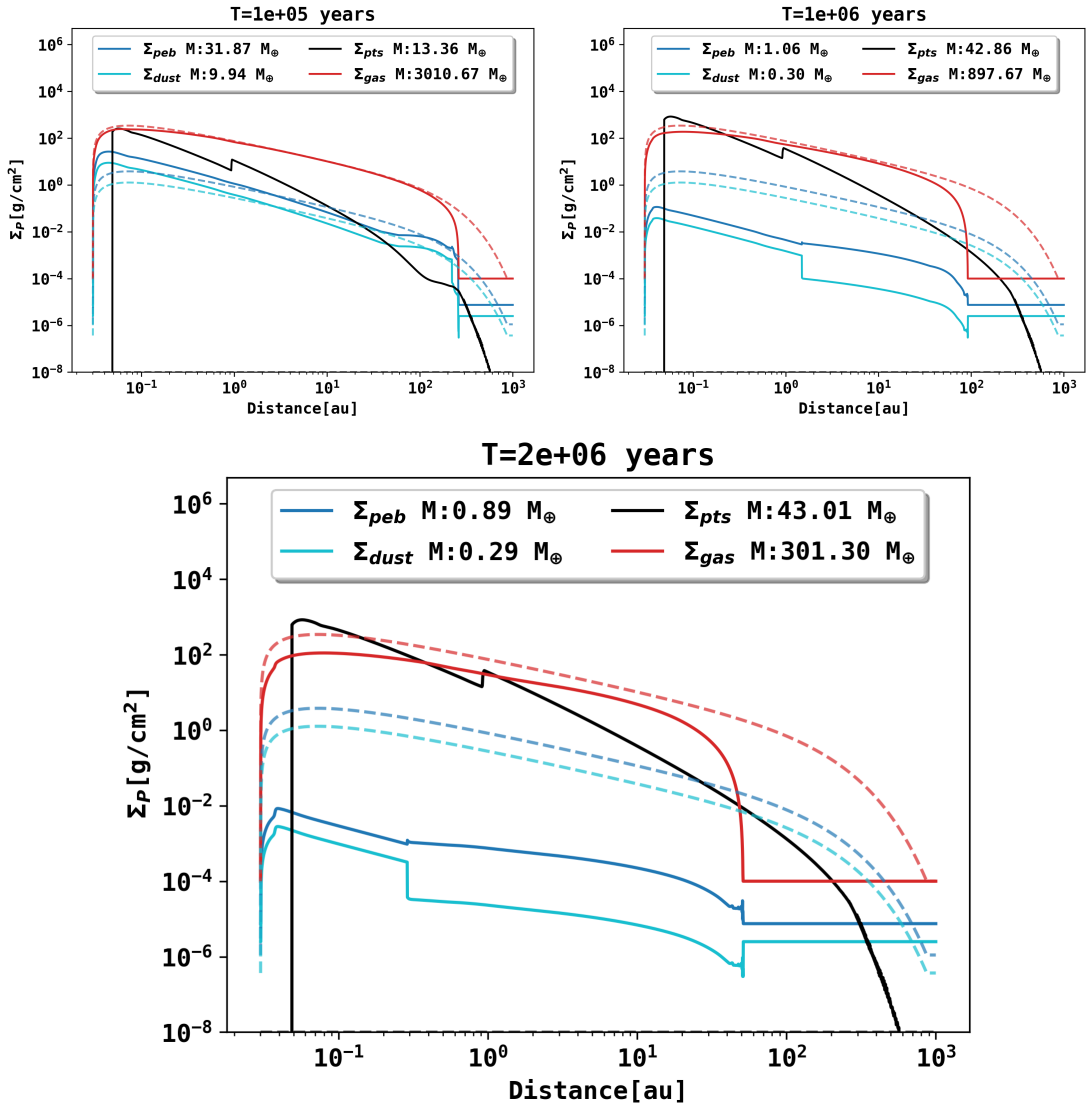


Figure 2.1: Exemplary disk evolution including our dynamical model for planetesimal formation after 0.1 Myr, 1 Myr, and 2 Myr. We show the surface density for the dust, pebbles, planetesimals, gas, and their individual disk masses. The dashed lines refer to the initial profile of the corresponding density. This run does not contain a planetary embryo, it only evolves the disk dynamically. The total disk gas mass is given as $0.012\,M_\odot$ with a dust-to-gas ration of 1.5% and $\alpha = 10^{-3}$. The exponential cutoff radius of the disk is at 137 au, the inner radius at 0.03 au, and the evaporation rate is given as $2.87 \times 10^{-5}$ $M_\odot$/year. The planetesimal and solid-evolution parameters can be found in table 5.1. The effect of the ice line is visible in the kink in the planetesimal distribution around 1 au and the effect of drift vs. fragmentation-limited pebble size in the radially varying dust-to-pebble ratio.

**Solid evolution stages of our formation model:**
**Origin model without planetesimal formation [Mordasini, 2018]**

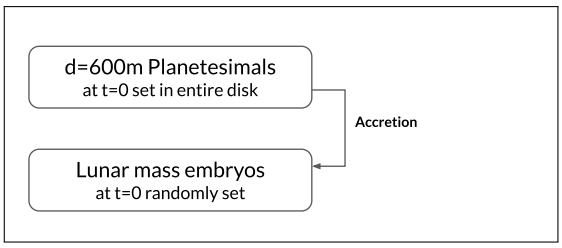


**Solid evolution as described in Sect. 2.2**

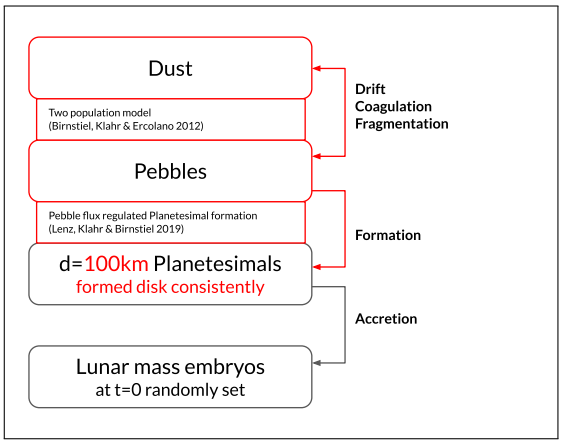


**Future possibilities**

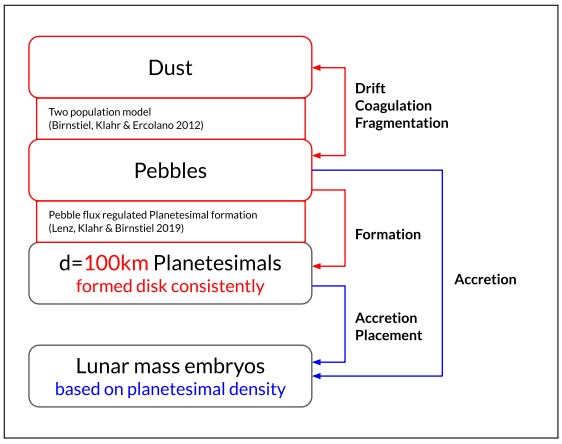


Figure 2.2: Schematic display of the different stages in the formation model for solid-evolution development. The upper panel describes the previously published model from Mordasini [2018]. The middle panel shows the currently improved version in this work, including the two-population solid evolution for dust and pebbles, as well as the formation of planetesimals (see Sec. 2.2). The lower panel presents an outlook on possible future development stages. The new modules and functions are highlighted in red, and future possibilities are highlighted in blue.

### 2.3.2 Solid component

A schematic overview of the different modules is shown in Fig. 2.2. Previous generations of the model, including the upcoming version of Emsenhuber et al. [2020a], used an initial planetesimal surface density slope that was set either to be equal to the initial gas-density slope [Mordasini et al., 2009] or used a $\Sigma_P \propto r^{-1.5}$ mmsn-like distribution [Emsenhuber et al., 2020a]. For the first case, this gave a planetesimal surface density distribution of $\Sigma_P \propto r^{-0.9}$ up to an exponential cutoff radius, which depends on the given disk size. The total mass in planetesimals was chosen to be the metalicity (in the following, dust-to-gas ratio $d_g$) of the host star times the total gas disk mass, modulo the effect of condensation fronts. The size of the planetesimals was chosen to be uniform and with a radius of $r_P = 300\,\mathrm{m}$. Importantly, $\Sigma_P$ only evolved while being accreted or ejected by embryos. Planetesimal formation or drift were not included, which left us with a static distribution of planetesimals and a complete lack of a physical description of the early phases of planet formation.

With our newly implemented model for planetesimal formation we proceed beyond the standard implementation in Emsenhuber et al. [2020a]. We now include two additional solid quantities (dust and pebbles) that evolve along with the gas evolution of the disk model. The initial mass in dust and pebbles is given as the metallicity of the host star times the gas-disk mass. Their density slope is set to be equal to that of the gas disk, giving an initial solid density profile of $\Sigma_s \propto r^{-0.9}$. There are no initially placed planetesimals. Planetesimals only form based on the evolution of dust and pebbles. This ensures that planetesimals form consistently with the disk evolution. Not only is the final distribution of planetesimals highly different than the static assumption of the previous disk model (see Sect. 2.4.1), but planetesimals now also form over time, which opens a completely new level of dynamical interaction with the disk. The size of planetesimals that we assumed in the following simulations is given as 100 km in diameter.

The main differences between Emsenhuber et al. [2020a] and this paper therefore are the size of planetesimals ($r_P = 300\,\mathrm{m}$ vs. $r_P = 50\,\mathrm{km}$) and the option for dynamic planetesimal formation, which is not yet implemented in Emsenhuber et al. [2020a]. Emsenhuber et al. [2020a], on the other hand, include an N-body integration for multiple simultaneously evolving cores. We did not use this option here because we wished to focus on the effect of dynamical planetesimal formation.

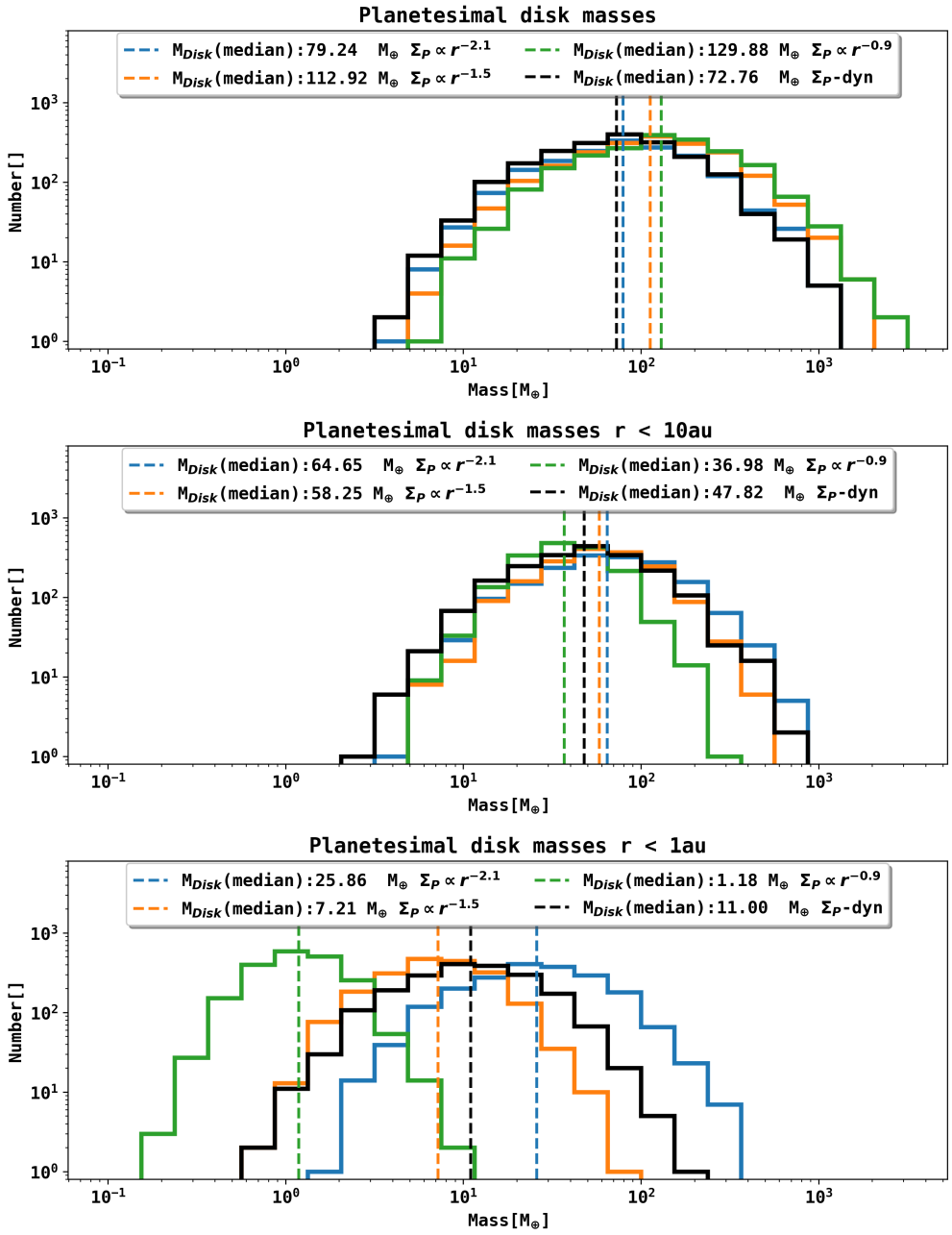


Figure 2.3: Planetesimal disk masses within 1 au, 10 au, and the complete disk for three different analytic density slopes and the dynamically formed planetesimal mass. The analytic masses are given at the start of the simulation, while the dynamically formed disk masses are shown after one million years, after most planetesimals have already formed. The dynamic runs do not contain a planetary embryo, they only simulate the disk evolution. The disk parameters, however, are the same as in the population in Fig. 2.5. We show the mass in planetesimals in the whole disk in the upper panel, the planetesimal mass within 10 au in the middle panel, the planetesimal mass within 1 au in the lower panel, and the corresponding median masses for every setup.

## 2.4 Results

### 2.4.1 Disk evolution

Previous simulations with our model used an initial $\Sigma_P$ of $d_g \cdot \Sigma_g$ , where $d_g$ is the dust-to-gas ratio. The slope in $\Sigma_P$ was therefore given as the slope of the initial gas surface density.
The density slope that arises from the pebble flux-regulated model for planetesimal formation can have a slope as steep as $\Sigma_P \propto r^{-2.1}$, and it generally depends on the individual evolution of the disk. Because of the steeper slope, we find a remarkable increase in $\Sigma_P$ in the inner regions of a protoplanetary disk and a corresponding decrease farther out. Another profound difference to the previous implementation of our model is the total mass in planetesimals. The initial mass in dust in the planetesimal formation runs is equal to the initial mass in planetesimals with the analytically given planetesimal surface density, but only a fraction of this is transformed into planetesimals. We therefore always undershoot the total mass in planetesimals for our dynamically formed simulations compared to the previous implementation. Choosing higher values for the planetesimal formation efficiency can result in a shallower density profile, similar to that of the initial gas distribution. The initial dust density is given as a fraction of the gas surface density. If we were to consider $\varepsilon/d > 1$, this would lead to local pebble-to-planetesimal conversion and the outer material would be unable to drift into the inner regions of the disk, which would have changed the density profile. For a more detailed treatment of this behavior, we refer to Lenz et al. [2019]. To find similar densities to the analytic $\Sigma_P \propto r^{-2.1}$ runs, we would have to increase our disk masses to match the final mass in planetesimals.
The total disk masses for the different density distributions are shown in Fig. 2.3, as well as the masses within 10 au and 1 au. We find that the mean total disk masses are lower for the steeper density profiles by a factor of $M_{tot}^{-2.1}/M_{tot}^{-0.9} \approx 0.62$ or $M_{tot}^{-1.5}/M_{tot}^{-0.9} \approx 0.87$. This is to be expected as more material is inside the ice line, which is taken care of in these models. The masses within 1 au of the steeper models are still higher by several orders of magnitude ($M_{1au}^{-2.1}/M_{1au}^{-0.9} \approx 21,58$ or $M_{1au}^{-1.5}/M_{1au}^{-0.9} \approx 6,01$). $M_{tot}$ and $M_{1au}$ refer to the median masses from Fig. 2.3. The lowest total median mass ratios of planetesimals can be found in the dynamically formed simulation with $M_{tot}^{\mathrm{dyn}}/M_{tot}^{-0.9} = 0.504$, the mass ratio within 1 au, however, is the second highest with $M_{1au}^{\mathrm{dyn}}/M_{1au}^{-0.9} = 8.27$. The lower total masses for the steeper planetesimal surface density can be explained by the smaller number of icy planetesimals in these setups. Choosing a steeper density slope for the same mass as in the $\Sigma_P \propto r^{-0.9}$ shifts material (icy planetesimals and silicate planetesimals) from farther out regions to the inner disk. This would evaporate the icy planetesimals within the ice line, leaving only the silicate planetesimals, therefore effectively loosing mass. The mass loss here is therefore only due to icy planetesimals within the ice line, whereas the amount of silicate planetesimals remains the same. Regardless of this mass loss, we find that the mass in the inner disk (r<1 au) is significantly higher for the steeper density slopes. The lifetimes of the gas disks studied in our case are shown in Fig. 2.4 The global effect on planet formation of these changes in $\Sigma_P$ is presented in Sect. 2.4.2.

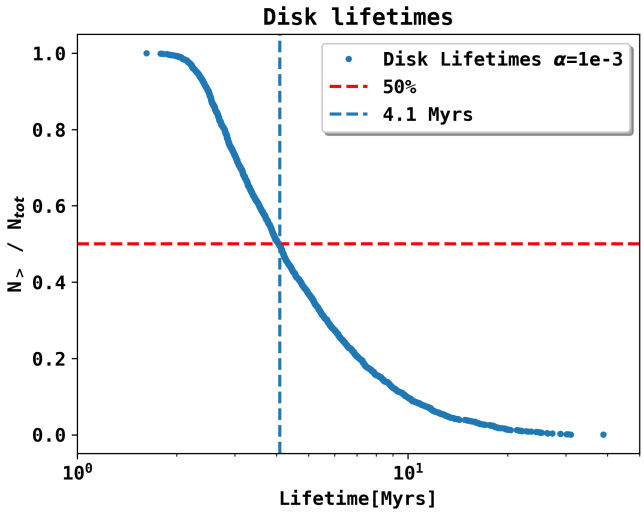


Figure 2.4: Cumulative distribution of gas-disk lifetimes for our synthetic population. We used a constant value of $\alpha = 10^{-3}$ in our runs. We find that 50% of the lifetimes are shorter than 4.1 Myr.

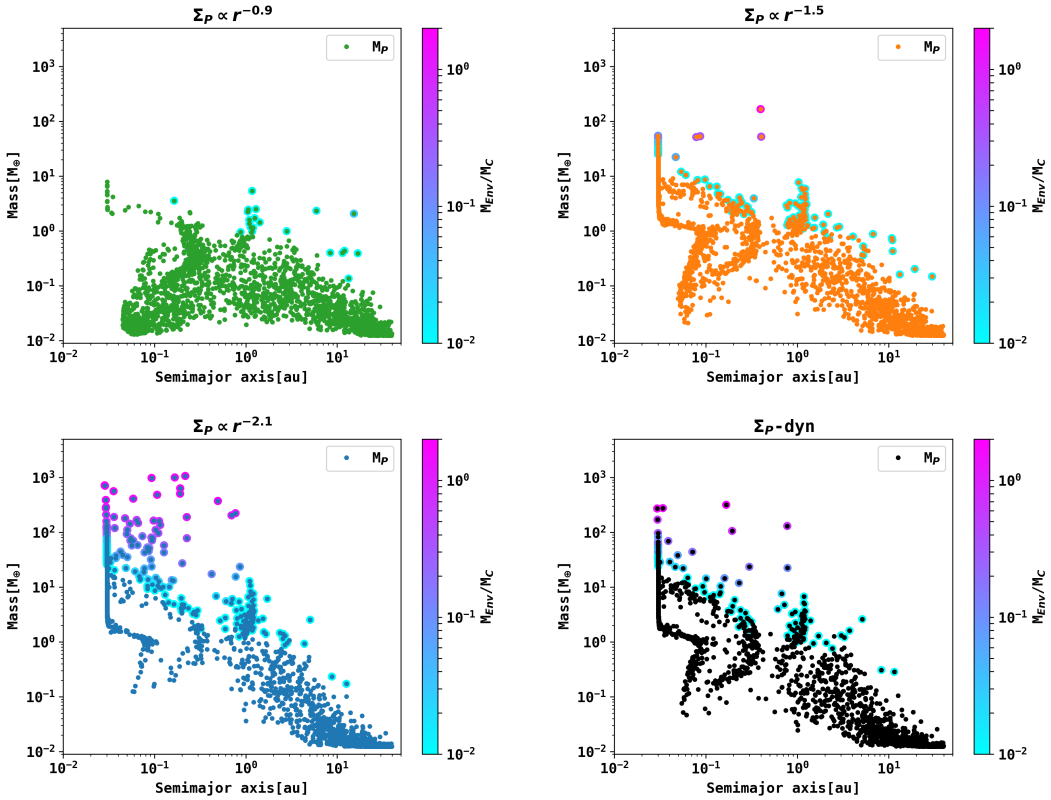


Figure 2.5: Mass vs. semimajor axis of synthetic planet populations for different $\Sigma_P$ distributions after 100 million years. Each setup contains one single planetary embryo. The initially set distributions for $\Sigma_P$ are $\Sigma_P = \Sigma_0 \cdot r^{-0.9}$ (initial gas density slope), $\Sigma_P = \Sigma_0 \cdot r^{-1.5}$ (mmsn) and $\Sigma_P = \Sigma_0 \cdot r^{-2.1}$ [Lenz et al., 2019]. The bottom right panel shows the population in which planetesimals form over time using the model described in Sec. 2.2. The circles given around the data points show the mass fraction of envelope mass over core mass. The numbers of systems are 1999 ($\Sigma_P \propto r^{-0.9}$), 1990 ($\Sigma_P \propto r^{-1.5}$), 1961 ($\Sigma_P \propto r^{-2.1}$), and 1945 ($\Sigma_P$- dyn).

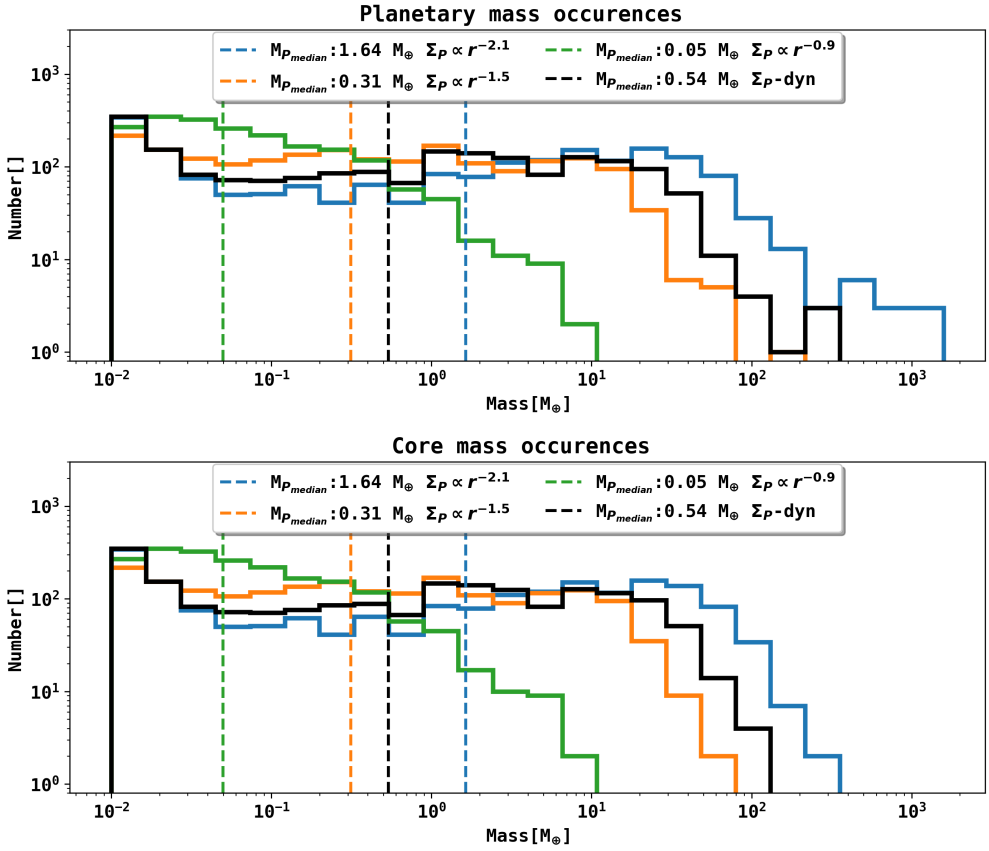


Figure 2.6: Planetary and core-mass occurrences of the four different populations. Every planet in each systems starts with a core mass of $0.0123\,M_\oplus$ and no envelope. The quantities that arise from the three analytical planetesimal surface density profiles are shown in blue ($\Sigma_P \propto r^{-2.1}$), orange ($\Sigma_P \propto r^{-1.5}$), and green ($\Sigma_P \propto r^{-0.9}$), whereas the properties of the planetesimal formation population are shown in black. The dashed lines in the plots show the median planet and median core masses. The histograms show clear shifts toward the higher mass ranges for steeper planetesimal surface densities and for the dynamically formed planetesimals than the $\Sigma_P \propto r^{-0.9}$ or even the $\Sigma_P \propto r^{-1.5}$ distribution.

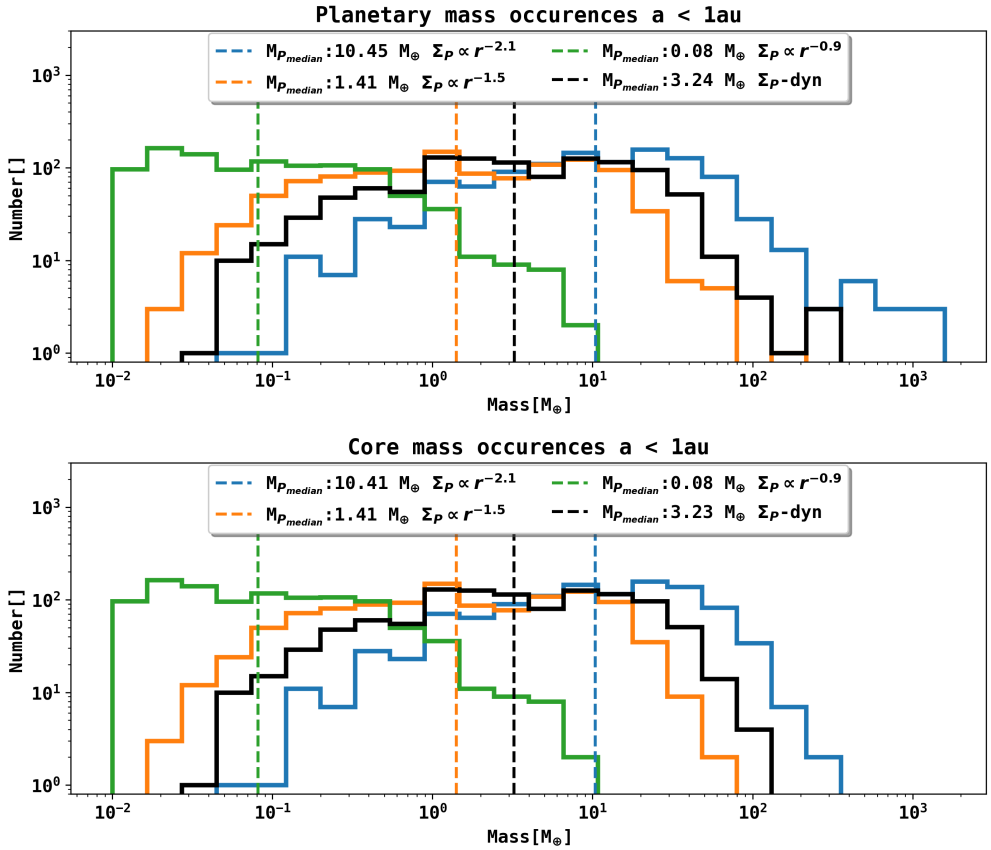


Figure 2.7: Planetary mass and core-mass occurrences of the four different populations within 1 au. Fig. 2.5 shows that the higher mass planets are located in the inner disk because these are the regions with the highest planetesimal surface density. The dashed lines in the plots show the median planet and median core masses within 1 au.

### 2.4.2 Synthetic populations

In the following we present several synthetic populations that were computed with different initial planetesimal surface density profiles and the dynamic planetesimal formation model from Lenz et al. [2019]. It is important to mention that the growth of planetary embryos by the accretion of solids is only given by the accretion of planetesimals in these simulations. To ensure the correct comparison of planetesimal accretion with different slopes of $\Sigma_P$, we neglect the accretion of pebbles for this part of our study. We also consider systems with one embryo each because our focus lies on the changes to the previous implementation. Although populations with a much higher number of embryos are possible in the new version of the model [Emsenhuber et al., 2020a], we chose to stay with one embryo per run for our study because mixing our study with effects of multiple planets in that forthcoming paper avails us nothing. We therefore focus on the general distribution of masses and semimajor axes and on the overall mass occurrences of planets.

#### Mass semimajor axis distributions

Fig. 2.5 shows the mass and semimajor axis distribution of four synthetic populations around a solar-type star using one planetary embryo of lunar mass ($0.0123\,M_\oplus$) for each system. We simulated a total number of 1999 systems for the $\Sigma_P \propto r^{-0.9}$ distribution, 1990 for $\Sigma_P \propto r^{-1.5}$, 1961 for $\Sigma_P \propto r^{-2.1}$ , and 1945 for the dynamic planetesimal formation run. The initial conditions of the four populations are the same, except for the initial $\Sigma_P$ and the formation of planetesimals. The upper left green panel refers to an initial $\Sigma_P$ of $\Sigma_P \propto r^{-0.9}$, the upper right orange to $\Sigma_P \propto r^{-1.5}$ and the lower left blue to $\Sigma_P \propto r^{-2.1}$. The lower right panel in black refers to the final planets that formed using the pebble flux-regulated model for planetesimal formation. We find a large number of planets that exceed a mass of ten earth masses (necessary for runaway gas accretion, see Pollack et al., 1996) and sometimes even reach several hundreds of earth masses when the slope of $\Sigma_P$ is given with a slope of $r^{-2.1}$. The simulation in which the slope is given with the $r^{-0.9}$ does not even produce one single planet with a mass higher than that of ten earth masses. Overall, this plot shows an immense increase in planetary masses for steeper planetesimal density profiles. It is important to mention here that the high-mass gas giant planets all end up within 1 au, which is due to the high masses in planetesimals in the inner disk and planetary migration. In our synthetic runs we do not see gas giants farther out, for example, beyond the water-ice line, as can be observed in the population of exoplanets [Winn and Fabrycky, 2015]. This will probably change when recondensation of water vapor is included, which effectively boosts the birth of planetesimals that is regulated by pebble flux.

#### Mass occurrences

For a more quantitative analysis, we studied the mass occurrences for the different planetesimal density slopes. Here we focus on the planetary mass and the core mass. Fig. 2.6 and Fig. 2.7 show histograms with the occurrences of the different masses for the various populations from Fig. 2.5. As Fig. 2.5 shows, most of the high masses are found in the inner parts of the protoplanetary disk, whereas embryos placed farther out fail to grow. We therefore also focused our study on the inner region within 1 au. Fig. 2.6 takes the complete population into account, whereas Fig. 2.7 only contains planets with a semimajor axis smaller than 1 au. We also give the median masses for the planets and their cores. A cumulative function of the planetary masses is shown in Fig. 2.8. We find that the number of planets above $10\,M_\oplus$ is given as 0 ($\Sigma_P \propto r^{-0.9}$), 159 ($\Sigma_P \propto r^{-1.5}$), 565 ($\Sigma_P \propto r^{-2.1}$), and 301 ($\Sigma_P$- dyn). The number of planets above $20\,M_\oplus$ is given as 31 ($\Sigma_P \propto r^{-1.5}$), 383 ($\Sigma_P \propto r^{-2.1}$), and 138 ($\Sigma_P$- dyn).

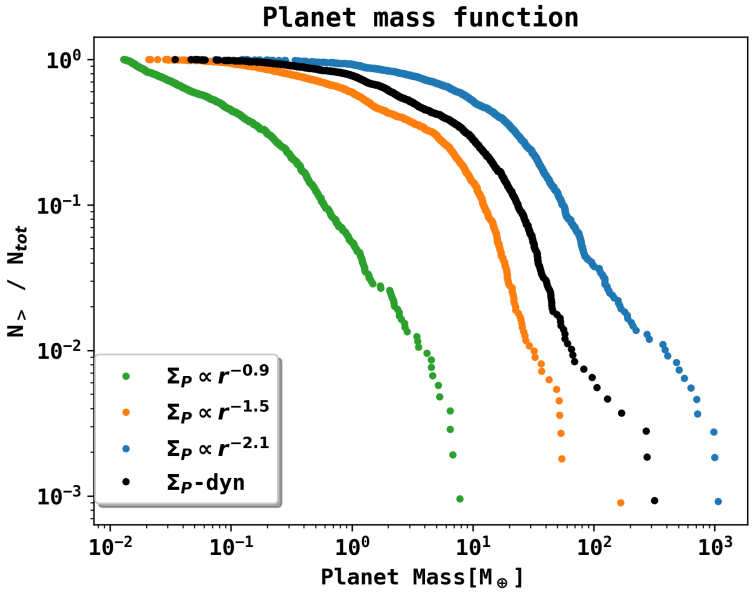


Figure 2.8: Cumulative function of planetary masses within 1 au for the four different synthetic populations from Fig. 2.5. The y-axis shows how many planets for each density profile are above the current planetary mass, normalized by the total number for planets in each population. The planets that have formed in the $\Sigma_P \propto r^{-0.9}$ run are shown in green, the $\Sigma_P \propto r^{-1.5}$ population is shown in orange, and the $\Sigma_P \propto r^{-2.1}$ population is shown in blue. The dynamic planetesimal formation population is shown in black.

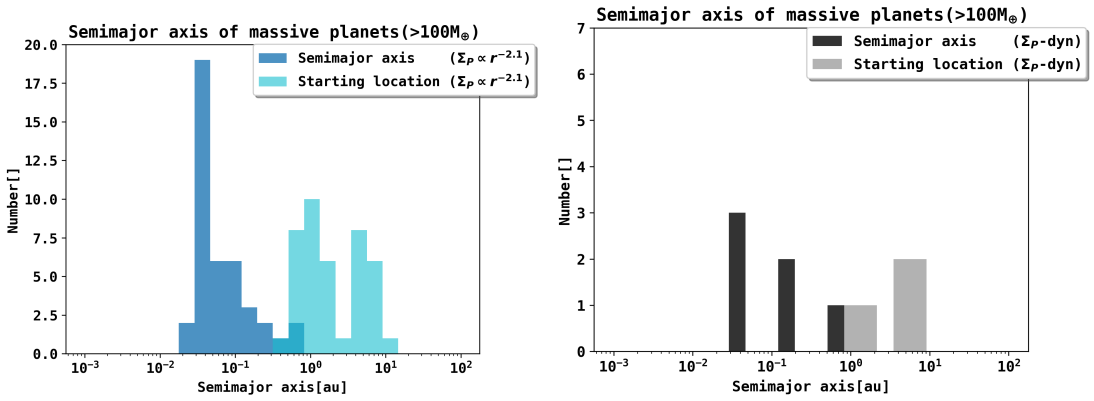


Figure 2.9: Semimajor axis distribution and starting location of planets that have grown to gas giant masses ($M_P > 100\mathrm{M}_\oplus$) in the $\Sigma_P \propto r^{-2.1}$ and the planetesimal formation runs. We find that most massive planets end up at the inner edge of the disk. The total number of planets that have reached over $100\mathrm{M}_\oplus$ in the $\Sigma_P \propto r^{-2.1}$ runs is given as 41 out of 1961. This is heavily biased by the placement of the planetary seeds, however, which also occurs in far out regions with low planetesimal surface densities.

### 2.4.3 Effect of the starting location

In Fig. 2.9 we show the semimajor axis distribution and the initial starting location distribution of high-mass planets in the $\Sigma_P \propto r^{-2.1}$ run and the dynamic formation model. We find that planets with the highest masses end up at the inner edge of the disk due to migration. There is no in situ giant formation, but rather a preferential zone in which planetary embryos need to be placed in order to grow to giant planets. This preferential area appears to be around 1 au and from around 4 au to 10 au for the $\Sigma_P \propto r^{-2.1}$ run and mostly from around 4 au to 10 au for the dynamical formation model. Embryos that are placed at a distance from 2 au to 4 au appear to have a lower probability of becoming gas giant planets in both cases, but because the probability of their formation at this location is also low because of the local deficiency in planetesimals, they should not have been placed there in the first place. Now that we have a distribution of planetesimals, we can use this information to also model the generation of embryos in a consistent fashion. Ultimately, the effect of recondensation beyond the ice line described above can further change this picture.

### 2.4.4 Gas giant growth

Here we focus on a system that forms a 997.6 $M_{\oplus}$ mass planet for the $\Sigma_P \propto r^{-2.1}$ density distribution and a 281.7 $M_{\oplus}$ planet for the dynamical planetesimal formation run. The initial disk parameters for the setup are given in Table 5.1. Fig 2.10 shows planetary growth tracks, the mass growth over time, and the corresponding semimajor axis evolution. The embryo in these systems was placed initially at 8.2 au, which seems to be a preferential starting location for giant planets, see Fig. 2.9. The higher planetesimal surface density has a drastic effect on the early stages of planetary growth. The planets in the $\Sigma_P \propto r^{-2.1}$ setup and the dynamical planetesimal formation run can grow fast enough to undergo runaway gas accretion, whereas the planet in system $\Sigma_P \propto r^{-1.5}$ fails to do so, even though its core reaches a core mass of 43 $M_{\oplus}$. The planet in system $\Sigma_P \propto r^{-0.9}$ fails to build a large enough core for significant gas accretion and ends up at 4,64 $M_{\oplus}$. The 43 $M_{\oplus}$ planet does not end up as a gas giant because of planetary migration and the continuous accretion of planetesimals during the migration phase. Continuous planetesimal accretion reduces the gas-accretion rate due to accretional heating, and while the accretion rate of solids surpasses the accretion rate of gas, the planet cannot proceed into runaway gas accretion [Pollack et al., 1996]. We find that it is not the total mass available or the accretion timescales for 100 km planetesimals that prevent giant planet formation, but fast type I migration. The upper right panel of Fig. 2.5 shows that most planets above 10 $M_{\oplus}$ end up at the inner edge of the gas disk. Their evolution is similar to that of the planet in the $\Sigma_P \propto r^{-1.5}$ system in Fig. 2.10 in the sense that they grow well above 10 $M_{\oplus}$ , but then migrate too quickly to the inner edge of the disk. Fig. 2.9 also shows that most massive planets in the $\Sigma_P \propto r^{-2.1}$ run end up at the inner edge of the disk due to migration as well. The change in migration type allows the planets in the $\Sigma_P \propto r^{-2.1}$ and the dynamical run in Fig. 2.10 to undergo runaway gas accretion. They switch from type I to type II migration before they end up too close to the star. The planet in the $\Sigma_P \propto r^{-1.5}$ run also transitions from type I to type II migration at 0.26 au, but this is already too close to the star, and type II migration continues to transport the planet to the disk edge before entering runaway gas accretion. The planet in the $\Sigma_P \propto r^{-2.1}$ run switches to type II migration at 0.65 au, giving it enough time to enter runaway gas accretion before migrating too closely to the star. When the migration rate from type I to type II is slowed down, a decrease in the accretion rate of planetesimals is caused that reduces the accretional heating and thus enables runaway gas accretion if the planet has not already migrated too closely to the star as in the $\Sigma_P \propto r^{-1.5}$ case of Fig. 2.10. The limitation for the formation of gas giant planets by 100 km planetesimal accretion is therefore mostly given by planetary migration and not by growing 10 $M_{\oplus}$ planets within the lifetime of a gaseous disk.

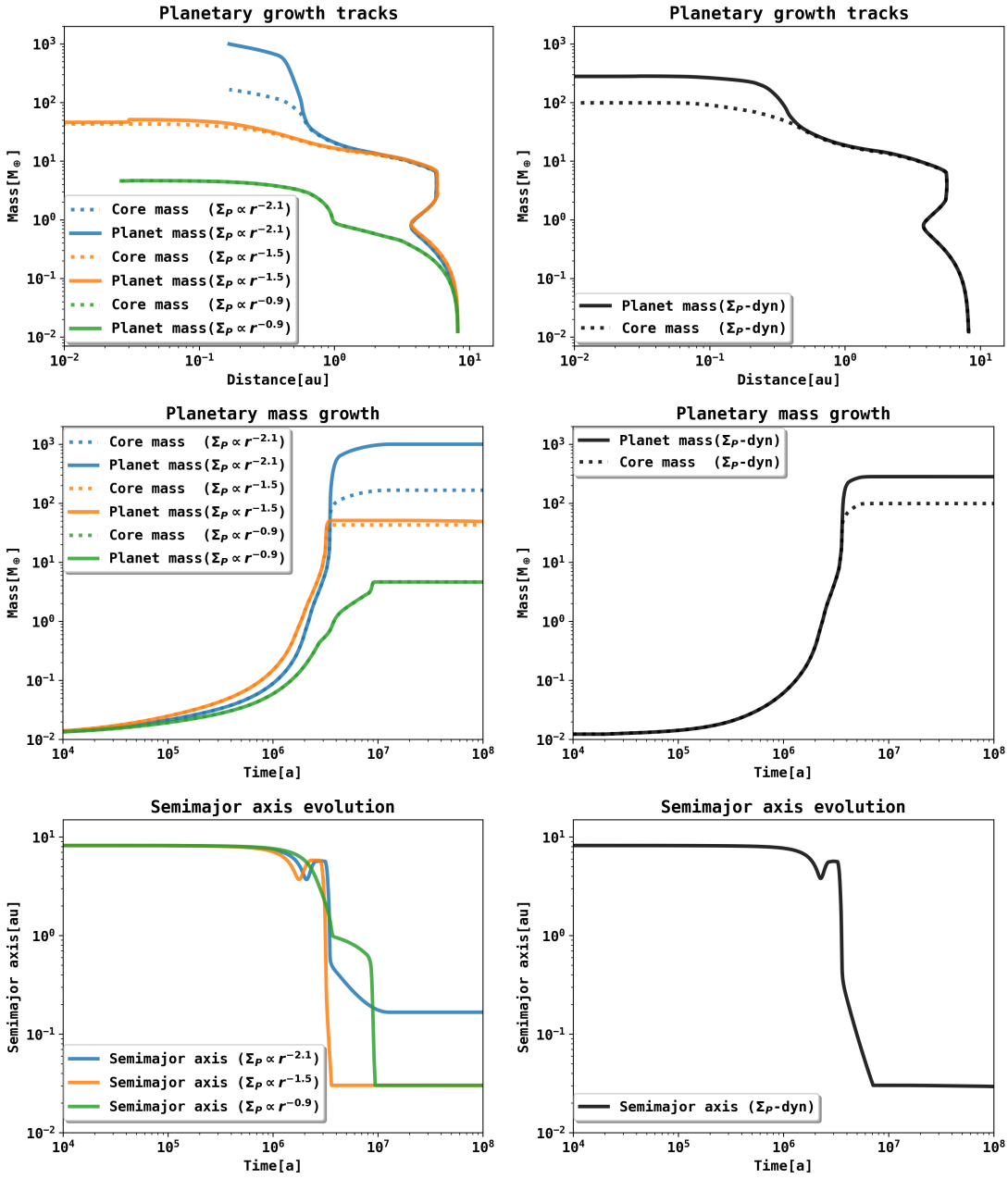


Figure 2.10: Planetary growth tracks, mass over time, and semimajor axis evolution for a giant planet system. The system that is studied leads to a gas giant planet of $997.6\,M_\oplus$ for the $\Sigma_P \propto r^{-2.1}$ density distribution and a $281.7\,M_\oplus$ planet for the dynamic model. The other systems lead to $51.1\,M_\oplus$ for $\Sigma_P \propto r^{-1.5}$ and $4.64\,M_\oplus$ for $\Sigma_P \propto r^{-0.9}$. The upper panel shows the mass and semimajor axis change during the evolution of the system, while the middle panel shows the growth of the embryo over time. The lower panel shows the semimajor axis evolution over time. On timescales of million years, the giant planet in the dynamical planetesimal formation and the $\Sigma_P \propto r^{-1.5}$ simulation falls into the star due to tidal forces, which is no longer shown in the lower right panel.

## 2.5 Discussion

In our models with a fixed initial density slope for the planetesimals we find that we cannot form gas giant planets from planetesimal accretion with 100 km sized planetesimals when we assume that the surface density distribution of the planetesimals is shallow and varies as $r^{-0.9}$. This agrees with studies from Johansen and Bitsch [2019], in which planetesimal accretion of large planetesimals is an inefficient accretion mechanism for low-mass planetary embryos. On the other hand, we can clearly show that a change in the planetesimal surface density slope has a drastic effect on the global evolution of planetary systems. A steeper profile in the initial planetesimal surface density distribution can lead to gas giant growth in the inner region of protoplanetary disks when only 100 km sized planetesimals are used, while also forming a large number of terrestrial planets and super-Earths. This result indicates that planetesimal accretion alone can be a very effective mechanism for planetary growth in the inner regions of circumstellar disks and can explain large diversities in the population of planets.

More importantly, however, we find that pebble flux-regulated planetesimal formation leads automatically from a shallow distribution of dust to a steep planetesimal distribution. This in turn leads to much higher planetary masses than in the $\Sigma_P \propto r^{-1.5}$ density profile.

The largest planets still can be formed using the $\Sigma_P \propto r^{-2.1}$ density slope and reach 1062.8 $M_\oplus$. The most massive planet in the $\Sigma_P \propto r^{-1.5}$ run reaches only 166.2 $M_\oplus$ and 7.8 $M_\oplus$ for $\Sigma_P \propto r^{-0.9}$. The maximum planetary mass for our dynamic simulation peaks at 317.1 $M_\oplus$. By comparing the mmsn ($\Sigma_P \propto r^{-1.5}$) profile with the dynamic formation model, we find that we increase the number of planets above 10 $M_\oplus$ by 89% (from 159 to 301) and the number of planets above 20 $M_\oplus$ by 345% (from 31 to 138) when we choose the formation of planetesimals to be consistent with the disk evolution.

We recall that the total mass in planetesimals is lowest for the dynamical planetesimal formation model because only a fraction of the dust and pebbles is transformed into planetesimals. The slope of the planetesimals that form over time, however, is steeper than the $r^{-1.5}$ slope. The total mass that is available for accretion is therefore lower in the planetesimal formation run because pebble accretion onto protoplanets is currently neglected.

We also find that our current models assuming 100 km sized planetesimals do not form cold giants around the water-ice line in any scenario due to orbital migration, although giant planets migrate through this area, as a study of the initial embryo location in Fig. 2.9 shows. This might also indicate that the formation of planetesimals could be enhanced by the mechanisms around the ice line, as has been predicted by Drążkowska and Alibert [2017] and Schoonenberg and Ormel [2017].
These authors suggested that sublimation and recondensation of icy pebbles at the ice line can have a drastic effect on the formation of planetesimals. This effect on planetesimal formation can be incorporated with our implementation by locally adapting the formation efficiency $\varepsilon$ and promises to have a significant effect on the formation of high-mass planets around the ice line. Finally, we find that the placement of planetary embryos appears to be a strong component for giant planet formation, see Fig. 2.9. The effect of the starting location of planetary embryos in combination with the formation of planetesimals can be studied in future work in greater detail, including the dynamical placement of planetary seeds during the evolution of the disk. In combination with the increased planetesimal formation around the ice line and pebble accretion, these features have a drastic effect on our synthetic planet populations. We expect this to explain the abundance of cold or hot giants and the diversity of terrestrial planets.

## 2.6 Summary and outlook

Using the two-population solid-evolution model by Birnstiel et al. [2012] and the model for pebble flux-regulated planetesimal formation by Lenz et al. [2019], we have studied the effect of planetesimal formation using our model for planetary population synthesis. By comparing the dynamical planetesimal formation with different ad hoc planetesimal surface density distributions, we find strong differences for the formation of planets in the inner parts of circumstellar disks for a planetesimal size of 100 km. This can be linked directly to the steeper slope in $\Sigma_P$ , as reference simulations with shallower surface density profiles show. We hereby show the effect of the planetesimal surface density distribution and formation on the population of planets. The main results of planetesimal formation for single embryo planet population synthesis are listed below

- Planetesimal accretion with 100 km sized planetesimals can be a very efficient planetary growth mechanism in the inner regions of circumstellar disks and creates a large variety of planets.
- Pebble flux-regulated planetesimal formation enables gas giant formation by accreting only 100 km sized planetesimals because of highly condensed planetesimal areas in the inner regions of circumstellar disks.
- Pebble flux-regulated planetesimal formation fails to form cold giant planets beyond the ice line. The reason is not a core-accretion timescale that is too long compared to the disk lifetimes, but orbital migration that removes the cores faster than they can grow.
- We no longer rely on an ad hoc assumption such as the mmsn model for the distribution of planetesimals in protoplanetary disks, but can start with much shallower mass distributions that agree with observations of disks around young stars.
- Dynamic planetesimal formation increases the number of planets above $10\,M_E$ by 89% and the number of planets above $20\,M_E$ by 345% compared to the mmsn hypothesis.

The greatest technical advantages that the newly implemented solid evolution model brings are listed below.

- Pebble accretion can be included next to planetesimal accretion into our population synthesis framework to study their individual contributions to planetary growth.
- Locally adapting the planetesimal formation efficiency $\varepsilon$ gives us the opportunity of studying increased planetesimal formation around the ice line, or other dynamically evolving planetesimal surface density profiles such as rings in disks.
- Planetary embryo formation based on the local planetesimal surface density evolution can be incorporated.

These improvements will enable us to consistently study the full size range of planet formation in a globally coupled framework, beginning from a disk of gas and dust.

# 3 | Planetesimals to embryos

This chapter resembles the work published in Voelkel et al. [2021a]. The title of the publication is "Linking planetary embryo formation to planetesimal formation. I. The effect of the planetesimal surface density in the terrestrial planet zone". I am the leading author of the manuscript. The model description in Sect. 3.3.1 has been written by Rogerio Deienno. The rest of the document, including all figures and corresponding analysis have been conducted by me, taking into account the input of all listed co-authors. The simulations have been conducted by Rogerio Deienno and me, their analysis and discussion have been conducted by me. The embryo formation model presented has been developed and compared with the simulations by me. Rogerio Deienno, Katherine Kretke and Hubert Klahr supported the interpretation of the results with discussions.

The growth-timescales of planetary embryos and their formation process are imperative for our understanding on how planetary systems form and develop. They determine the subsequent growth mechanisms during the life stages of a circumstellar disk. Voelkel et al. [2021a] quantifies the timescales and spatial distribution of planetary embryos through collisional growth and fragmentation of dynamically forming 100 km sized planetesimals. In our study, the formation timescales of viscous disk evolution and planetesimal formation are linked to the formation of planetary embryos in the terrestrial planet zone. Voelkel et al. [2021a] connects a one-dimensional model for viscous gas evolution, dust and pebble dynamics, and pebble flux-regulated planetesimal formation to the N-body code LIPAD. Our framework enabled us to study the formation, growth, fragmentation, and evolution of planetesimals with an initial size of 100km in diameter for the first million years of a viscous disk. Our study shows the effect of the planetesimal surface density evolution on the preferential location and timescales of planetary embryo formation. Only the innermost embryos (<2 au) in our study form well within the lifetime of an active pebble flux for any disk studied. Higher planetesimal disk masses and steeper planetesimal surface density profiles result in more massive embryos within a larger area, rather than in a higher number of embryos. A one-dimensional analytically derived model for embryo formation based on the local planetesimal surface density evolution is presented. This model can reproduce the spatial distribution, formation rate, and total number of planetary embryos at a fraction of the computational cost of the N-body simulations. The formation of planetary embryos in the terrestrial planet zone occurs simultaneously with the formation of planetesimals. The local planetesimal surface density evolution and the orbital spacing of planetary embryos in the oligarchic regime are good constraints for modeling planetary embryo formation analytically. Our embryo formation model is a valuable asset in future studies of planet formation.

## 3.1 Introduction

The core-accretion scenario is currently the most widely used theory for planet formation. It states that at first, planetary cores form in protoplanetary disks, which then continue to grow by various forms of accretion [Pollack et al., 1996]. The formation of these planetary cores clearly shapes the general picture of planet formation. To fully model the process of planet formation, we need to track the different growth processes involved, beginning from dust coagulation, pebble and dust dynamics, the formation of planetesimals, the formation of planetary embryos, and their subsequent growth until the circumstellar disk has vanished. A global model of planetesimal formation [Lenz et al., 2019] that is regulated by the local pebble flux [Birnstiel et al., 2012] was introduced into a global model of planet formation [Emsenhuber et al., 2020a] in Voelkel et al. [2020]. While this approach tracks the consistent formation and accretion of planetesimals on planetary embryos, the embryos themselves remain an ad hoc assumption. In this paper we investigate the formation of planetary embryos using N-body simulations [Levison et al., 2012], based on the evolution of the planetesimal surface density. Additionally, we construct an analytic one-dimensional parameterized prescription of planetary embryo formation that can be included in a global model of planet formation. In our companion paper, we add the effect of pebble accretion on the formation of planetary embryos.

Global models for planet formation that study planetary growth by solid accretion (Mordasini et al. [2012a], Emsenhuber et al. [2020a], Bitsch et al. [2015], and Ida and Lin [2004], to mention just a few) generally begin with the initial presence of massive objects in the circumstellar disk. These objects are mostly referred to as embryos. Once an embryo has formed, it can grow by the accretion of solids and eventually, by the accretion of gas. While the accretion of gas onto planets begins to be important at higher masses of around $10\,M_\oplus$ [Pollack et al., 1996], these $10\,M_\oplus$ objects in the disk are the consequence of a previous phase of solid accretion onto smaller embryos. For clarity, we define planetary embryos as objects of at least the mass of the Earth's Moon ($M = 0.0123\,M_\oplus$). These objects are massive enough to accrete planetesimals and pebbles from their surrounding orbits, but they are far from massive enough to effectively accrete gas.

The growth of planetary embryos depends on the local disk environment, for instance, the availability of planetesimals and pebbles. These quantities change throughout the disk evolution and depend on the global evolution of the disk. Understanding where and when planetary embryos form based on the circumstellar disk evolution is of vital relevance because the evolution stage of the disk determines the subsequent growth of the embryos. While the size range from lunar-mass embryos to gas giant cores already spreads approximately 4 orders of magnitude in mass, we recall that these lunar-mass embryos themselves are the product of long-term planetesimal growth [Kokubo and Ida, 1998, Kobayashi et al., 2011, Walsh and Levison, 2019, Clement et al., 2020]. The manner, the location, and the time at which these planetary embryos form out of much smaller planetesimals are the main subjects of this paper.

Despite all the uncertainties regarding the initial sizes at which planetesimals were formed [Schlichting et al., 2013, Schäfer et al., 2017, Walsh et al., 2017, Morbidelli et al., 2009] based on observational or theoretical arguments, here we assumed for simplicity that planetesimals all formed with a diameter of 100 km (Morbidelli et al. [2009]). Even though this planetesimal size is much larger than the one inferred by other studies [Schlichting et al., 2013], we find 5 orders of magnitude in mass between a lunar-mass object and that of a 100 km planetesimal. Large planetesimals of 100 km are currently favored to explain the size distribution of asteroids and other minor bodies of the Solar System [Morbidelli et al., 2009]. One hundred kilometers also seems to be the most likely size in simulations of planetesimal formation [Klahr and Schreiber, 2020, Johansen et al., 2009, Abod et al., 2019], and as recent work suggests, this size is limited by diffusion [Klahr and Schreiber, 2020]. While 100 km planetesimals from gravitational collapse are larger than the small pebbles out of which they form, they are not massive enough to undergo

pebble accretion. The formation of lunar-mass objects from 100 km planetesimals is therefore far from trivial and lays the foundation of subsequent planetary growth.

Forming massive planetary cores of $10\,M_\oplus$ at larger distances to the star within the lifetime of a gaseous disk is currently a challenge for planetesimal accretion models [Johansen and Bitsch, 2019]. A solution to this conundrum has appeared in the form of pebble accretion onto distant planetary embryos [Klahr and Bodenheimer, 2006, Ormel and Klahr, 2010, Lambrechts and Johansen, 2012, Bitsch et al., 2015, Ndugu et al., 2017]. This process describes the accretion of vastly smaller objects that radially drift toward the star, and it has been shown to be an effective planetary growth mechanism, even at larger distances up to the so-called pebble isolation mass [Lambrechts et al., 2014].

Similar to the case in which gas is accreted onto a $10\,M_\oplus$ core, the accretion of pebbles also requires the presence of a massive body to effectively be accreted [Ormel and Klahr, 2010]. The previously discussed planetesimal sizes of up to 100 km are not thought to be large enough for significant pebble accretion. Assuming that pebble accretion can grow a lunar-mass object over 4 orders of magnitude to the mass of a gas giant core therefore requires the ad hoc assumption of an initial planetary embryo at a given location. This approach is commonly used in planet formation studies that form gas giants from pebble accretion, but it lacks any description of the initial solid evolution of a circumstellar disk that would form the necessary embryo. While pebble accretion requires an active radial pebble flux that is believed to decay faster than the gas disk due to radial drift [Birnstiel et al., 2012], we face a similar conundrum as before.

The question is under which circumstances a planetary embryo at a given radial distance can form within the lifetime of a radial pebble flux. To answer this question, we need a global study that models the formation of planetesimals from pebbles and tracks their following growth up to the size of lunar-mass objects. Because lunar-mass objects are not thought to form from the spontaneous collapse of a pebble cloud, numerous studies have investigated the growth from planetesimals to planetary embryos in a circumstellar disk. The timescales of planet formation from a disk of planetesimals have been estimated first by Safronov and Zvjagina [1969] and Lissauer [1987]. It was later shown that the growth of planetary embryos can be split into different growth phases, such as runaway growth [Kokubo and Ida, 1996] and eventually oligarchic growth [Kokubo and Ida, 1998] after the embryo enhances the eccentricity of its surrounding planetesimals, effectively decreasing the accretion onto the planet. Not only is the accretion of planetesimals suppressed in the runaway regime, the embryos also arrange themselves around stable orbital separations when expressed in their mutual Hill radii (Kokubo and Ida [1998], Walsh and Levison [2019]). While more has been done on the formation of planetary embryos, their growth-timescales and orbital separation are main subject of our study.

Planetary embryo formation depends on the spatial distribution of planetesimals within the circumstellar disk because these are the building blocks of planetary embryos. Models for the viscous evolution of the gas suggest a shallow planetesimal surface density ($\Sigma_P$) profile of $\Sigma_P \propto r^{-0.9}$ [Shakura and Sunyaev, 1973]. The minimum mass solar nebula hypothesis suggests a steeper density profile of $\Sigma_P \propto r^{-1.5}$ [Weidenschilling, 1977b], Hayashi [1981]. However, when we consider that planetesimal formation is proportional to the radial pebble flux, the surface density profile can be as steep as $\Sigma_P \propto r^{-2.1}$ [Lenz et al., 2019].

The effect on planet formation of these different distributions under the assumption of initial embryo placement has recently been studied. It was suggested that the global planetesimal surface density distribution has major consequences for planet formation [Voelkel et al., 2020]. Studying the formation of planetary embryos based on the planetesimal surface density slope is therefore the next logical step.

Our goal is to determine the effect of the planetesimal surface density evolution on planetary embryo formation and derive an analytic recipe for planetary embryo formation. To do this, we

conduct N-body simulations and model the dynamical evolution, growth, and fragmentation of planetesimals with an initial size of $d = 100$km. Our study ranges from the initial gas and dust distribution to pebble and planetesimal formation up to the finally formed planetary embryos within 0.5 au and 5 au of a protoplanetary disk around a solar-type star. In order to make this possible, we have connected a one-dimensional model for pebble-flux-regulated planetesimal formation [Lenz et al., 2019] with the N-body code LIPAD [Levison et al., 2012]. This setup enables us to study the growth over multiple orders of magnitude in mass over $10^6$ years with reasonable computational effort, allowing multiple simulations that cover a range of initial parameters. Based on analytic assumptions and numerical results, we present a one-dimensional model for the formation of planetary embryos as a function of the local planetesimal surface density evolution.

In the following section, we explain the physical models that we used in our study and our prescription on planetary embryo formation. (Sect. 3.2). The connection between the one-dimensional planetesimal formation model and LIPAD can be found in Sect. 3.3, where we also explain the connection. Results and their discussion can be found in Sect. 3.4 and Sect. 3.5. Sect. 3.6 contains a brief summary of our study and an outlook on how we proceed with our results.

## 3.2 Planetesimal and embryo formation

Our goal is to consistently model the growth-timescales of planetary embryos from an initial disk of gas and dust. While this endeavor ranges over multiple orders of magnitude in mass, we have chosen to split it into two components. First we formed planetesimals of 100 km in diameter, using a one-dimensional parameterized description while considering pebble-flux-regulated planetesimal formation. Then we modeled the growth and fragmentation of the planetesimals in N-body simulations. Because both processes take place at the same time, it was necessary to connect our one-dimensional parameterized model with the N-body simulation, as described in Sec. 3.3. We focus on the description of the one-dimensional planetesimal formation and disk evolution model, as well as on the equations of the following planetesimal growth.

### 3.2.1 Disk evolution and planetesimal formation

We have chosen to use a one-dimensional viscous disk with an $\alpha$ prescription for turbulence [Shakura and Sunyaev, 1973], to which we added a two-population model for solids [Birnstiel et al., 2012]. Based on the radial drift of the solids, we formed planetesimals with a parameterized efficiency. An exact description of the two population model can be found in Birnstiel et al. [2012]. We outline the basic equations and assumptions. The model uses a fixed mass relation between a smaller and a larger population of dust grains. These two populations are distinguished by whether particle growth is limited by radial drift or fragmentation, respectively. Each time step solves one advection diffusion equation of the combined solid density.

$$\frac{\partial \Sigma_s}{\partial t} + \frac{1}{r}\frac{\partial}{\partial r}\left[ r\left( \Sigma_s \bar{u} - D\Sigma_g \frac{\partial}{\partial r}\left(\frac{\Sigma_s}{\Sigma_g}\right)\right)\right] = 0, \tag{3.1}$$

with $\Sigma_s$ the solid density, $\Sigma_g$ the gas density, and $D = D_{gas}/(1+St^2)$ the diffusion coefficient. This contains the diffusion coefficient of the gas $D_{gas}$ and the Stokes number $St$ of the particles. $\bar{u}$ is given as the weighted velocity of the two populations. The weighted velocity is given as

$$\bar{u} = (1 - f_m(r)) \cdot u_0 + f_m(r) \cdot u_1, \tag{3.2}$$

where $f_m(r)$ is given as the mass relation described above that separates the two populations with their corresponding velocities $u_0$ and $u_1$. The individual populations are then given as

$$\Sigma_0(r) = \Sigma_s(r) \cdot (1 - f_m(r)) \tag{3.3}$$
$$\Sigma_1(r) = \Sigma_s(r) \cdot f_m(r). \tag{3.4}$$

The mass relation $f_m$ was derived by fitting the two-population model to more sophisticated simulations of dust coagulation by Birnstiel et al. [2010]. The values that showed the best results are given as

$$f_m = \begin{cases} 0.97, & \text{drift-limited case} \\ 0.75, & \text{fragmentation-limited case.} \end{cases} \tag{3.5}$$

The decision whether a particle is within $\Sigma_0$ or $\Sigma_1$ was made according to its Stokes number [Birnstiel et al., 2012]. $\Sigma_0$ contains particles with a small Stokes number ($St \ll 1$). The motion of these particles is coupled to the motion of the gas. $\Sigma_1$ contains larger particles with $St \geq 1$, which are no longer coupled to the gas. In the following we refer to $\Sigma_0$ as dust and to $\Sigma_1$ as pebbles. Planetesimals are formed based on the radial drift of the solid material in our disk. A detailed description of the planetesimal formation model can be found in Lenz et al. [2019]. For our purpose, we assumed planetesimals to form with an initial size of 100 km in diameter. This choice is supported by numerical simulations of planetesimal formation by Klahr and Schreiber [2020] and observations of asteroid and Kuiper belt objects (Morbidelli et al. [2009], Schäfer et al. [2017], Walsh et al. [2017]).

The formation of planetesimals as described in Lenz et al. [2019] occurs in trapping zones in which disk instabilities can trigger planetesimal formation. These zones are distributed within the whole disk. The formation rate of planetesimals is then given proportional to the radial pebble flux and can be written as

$$\dot{\Sigma}_{\mathrm{p}}(r) = \frac{\varepsilon}{d(r)} \frac{\dot{M}_{\mathrm{peb}}}{2\pi r,} \tag{3.6}$$

with $\varepsilon$ the formation efficiency, $d(r)$ the radial separation of pebble traps, and $r$ the radial distance to the star. We chose $d(r)$ to be five gas pressure scale heights and $\varepsilon = 0.05$ in our simulations. $\dot{M}_{\mathrm{peb}}$ is the radial pebble flux, which in our model is defined as

$$\dot{M}_{\mathrm{peb}} := 2\pi r \sum_{\mathrm{St}_{\mathrm{min}} \leq \mathrm{St} \leq \mathrm{St}_{\mathrm{max}}} |v_{\mathrm{drift}}(r, \mathrm{St})| \Sigma_{\mathrm{s}}(r, \mathrm{St}), \tag{3.7}$$

with $v_{\mathrm{drift}}$ as the radial drift velocity. The pebble-flux-regulated model for planetesimal formation results in a steeper radial planetesimal surface density profile ( $\Sigma_p \propto r^{-2.1}$, Lenz et al. [2019]), as suggested by the minimum mass solar nebula hypothesis ($\Sigma_P \propto r^{-1.5}$) or the gas surface density profile of a viscously evolving disk ($\Sigma_P \propto r^{-0.9}$).

Because we did not specify the physical process that forms planetesimals (e.g., streaming instability or Kelvin-Helmholtz instability), this one-dimensional planetesimal formation description can be considered independent of a model. The formation of planetesimals is regulated by the local pebble flux, which in turn is regulated by dust coagulation and disk evolution [Birnstiel et al., 2012]. This approach enables us to connect the timescales of the dynamical pebble evolution of the disk with the timescales of planetesimal formation. In our study, we chose to focus on three planetesimal surface density profiles while applying the formation rate from the pebble flux regulated model because it connects the viscous timescales of the disk with the formation of planetesimals.

The gas disk in our study used an initial profile as in Lynden-Bell and Pringle [1974], using $\alpha = 2 \cdot 10^{-3}$, a cutoff radius of $r_c = 46$ au, and an initial gas surface density profile of $\Sigma_g \propto r^{-0.9}$.

The relative mass gain of the planetesimal disk between 0.5 au and 5 au was then scaled to match a total mass of 6 $M_\oplus$, 13$M_\oplus$ and 27$M_\oplus$ after 1 Myr, respectively. This was done in a post-processing fashion. The same post-processing was applied to the density slopes of the planetesimal surface density that is given to the N-body simulation. A more detailed description is found in Sect. 3.3.2.

### 3.2.2 Planetesimal growth and embryo formation

In the following we describe the one-dimensional analytical model that determines where and when lunar-mass planetary embryos are formed (based on the local evolution of the planetesimal surface density). The model connects analytic growth rates with the orbital separation of planetary embryos in the oligarchic regime. The mass of the largest object at an orbital distance $r$ to the star at a time $t$ is given as $M_p(r,t)$. When planetesimals have formed at a time $t_0$ at a distance $r$, we introduce

$$M_p(r,t_0) = M_{100\,km.} \tag{3.8}$$

We set the initial mass to that of a planetesimal with a diameter of 100 km with a solid density of $\rho_s = 1.0\,\mathrm{g/cm^3}$. During the evolution of the planetesimal disk, we integrated the mass growth rate of $M_p$ within a swarm of planetesimals at every time step. The local mass growth rate is then given as [Lissauer, 1993]

$$\frac{dM_p(r,t)}{dt} = \frac{\sqrt{3}}{2}\Sigma_P(r,t)\cdot\Omega(r)\pi {r_b}^2\left(1+\frac{v_{\mathrm{esc}}^2(M_p,r_b)}{v_\infty^2(r,t)}\right), \tag{3.9}$$

with $\Omega$ as the orbital Kepler frequency, $v_{\mathrm{esc}}$ the escape velocity of an object with mass $M_p$ and radius $r_b$ , and $v_\infty$ as the mean dispersion velocity within the swarm of planetesimals. We chose $v_\infty(r) = e(r,t)\cdot v_k(r)$ with $e(r,t)$ as the local mean planetesimal eccentricity in our analytical model computation. $v_k(r)$ is the Keplerian velocity at an orbital distance $r$. Eq. 3.9 was integrated at every time step with the updated values for $\Sigma_P$, $v_{\mathrm{esc}}$ , and $v_\infty$, therefore new planetesimals form over time. When $M_p$ has reached the minimum mass of a planetary embryo $M_{emb}$ (which in our study is given as a lunar mass) at a distance $r$, we determined this to be the location at which a lunar-mass planetary embryo can be formed. We did not track the subsequent evolution of the embryo. Our approach is solely designed to estimate the local timescales involved in forming an embryo-mass object within an evolving planetesimal disk. The eccentricity for the analytical model computation is given as $e(r,t) = 5\cdot 10^{-4}(1+r^{0.8})$, which results in a good fit to the numerical simulations. It is known that the size of planetesimals has a significant effect on the accretion rate [Fortier et al., 2007]. The planetesimal size appears in $v_\infty$, $v_{\mathrm{esc}}$ , and $M_p(r,t=0)$. Our model runs in Sect. 3.4 considered all planetesimals, including $M_p(r,t=0)$ to be 100 km in diameter. Eq. 3.9 is still valid for different planetesimal sizes by adapting $v_\infty$, $v_{esc}$ , and $M_p(r,t=0)$, however.

Our one-dimensional embryo formation model can be described by two criteria. The first criterion refers to the necessary growth time at a distance $r$ as a function of the planetesimal surface density evolution. The second criterion concerns the orbital separation to already present embryos. Criterion I for the embryo formation model can be written as

$$M_p(r,t) \geq M_{\mathrm{emb.}} \tag{3.10}$$

The second criterion for the formation of a planetary embryo at $r_i$ is the orbital separation to other planetary embryos at $r_j$. As suggested in numerical studies by Kokubo and Ida [1998], Kobayashi et al. [2011], Walsh and Levison [2019] and Clement et al. [2020], we find an orbital separation of planetary embryos in the oligarchic growth regime of $\Delta r_{\mathrm{orbit}} \sim$10-20$R_{\mathrm{Hill}}$. We chose a randomized Gaussian distribution for the orbital separation of about 17 $R_{\mathrm{Hill}}$ with a standard

deviation of $\sigma_{\Delta r} = 2.5 R_{\rm Hill}$ in our analytic model runs. The mass for the computation of the Hill radius is always given as the mass of the embryos that have already been placed. Criterion II is then given as

$$\Delta r_{\mathrm{orbit}i,j} \geq \Delta r_{\mathrm{min}}, \tag{3.11}$$

where $\Delta r_{\mathrm{orbit}i,j}$ is the orbital distance of an embryo at $r_i$ to an embryo at $r_j$. $\Delta r_{\mathrm{min}}$ was chosen from the Gaussian. As our analytic model does not track the subsequent dynamical evolution of a placed embryo, mergers and scattering were not accounted for. The embryos that are formed with the one-dimensional analytic model are compared to the results of the N-body simulations in Sect. 3.4.3.

## 3.3 LIPAD and the growth of planetesimals

### 3.3.1 LIPAD

The Lagrangian integrator for planetary accretion and dynamics (LIPAD) [Levison et al., 2012]), is a particle-based (i.e., Lagrangian) code. LIPAD was developed to follow the collisional, accretional, and dynamical evolution of a large number of meter- to kilometer-sized objects throughout the entire growth process of becoming planets, making it ideal for our study. A detailed description, as well as an extensive suite of tests of LIPAD can be found in Levison et al. [2012]. In addition, LIPAD has been successfully employed in previous studies of planet formation, as well as in the collisional evolution of meter- to kilometer-sized planetesimals interacting with planets or protoplanets [Kretke and Levison, 2014, Levison et al., 2015, Walsh and Levison, 2016, 2019, Deienno et al., 2019, 2020].

LIPAD uses the concept of tracer particles to represent a large number of small bodies with roughly the same orbit and size. Tracers are characterized by three numbers: the physical radius, the bulk density, and the constant total mass of the disk particles that it represents.

Collisional routines are employed to determine when collisions between tracers occur. In this event, following a probabilistic outcome based on a fragmentation law by Benz and Asphaug [1999], tracers can be assigned new physical radii. Therefore a distribution of tracers in LIPAD represents the size distribution of the evolving planetesimal population. The interaction among tracers results from statistical algorithms for viscous stirring, dynamical friction, and collisional damping.

Tracers that are large enough can become planetary embryos. Planetary embryos interact among themselves, as well as with tracers, through normal N-body routines [Duncan et al., 1998].

LIPAD also contains a prescription of the gaseous nebula from Hayashi [1981]. This gas disk provides aerodynamic drag, eccentricity, and inclination damping on every object.

### 3.3.2 Planetesimal formation in LIPAD

We investigated different total masses of planeteimals and surface density profiles while taking their formation timescales into account. For this purpose, we applied the formation rate from our one-dimensional model and scaled it to the total masses after $10^6$ years between 0.5 au and 5 au. The formation of planetesimals as described in Sect. 3.2 scales linearly with the planetesimal formation efficiency $\varepsilon$, therefore we chose the same qualitative formation rate for our various setups. The normalized disk mass change is shown in Fig. 3.1. Our planetesimal formation model uses a surface density distribution to describe planetesimals in the disk, whereas LIPAD uses tracer particles. We therefore transformed our surface density into a discrete number of tracer particles. We initially defined a total number of tracer particles $N_{Tracer} \mathcal{O}(\approx 10^4)$ to be generated in the simulation within $10^6$ years. To obtain the mass of the individual tracers $M_{Tracer}$ , we used

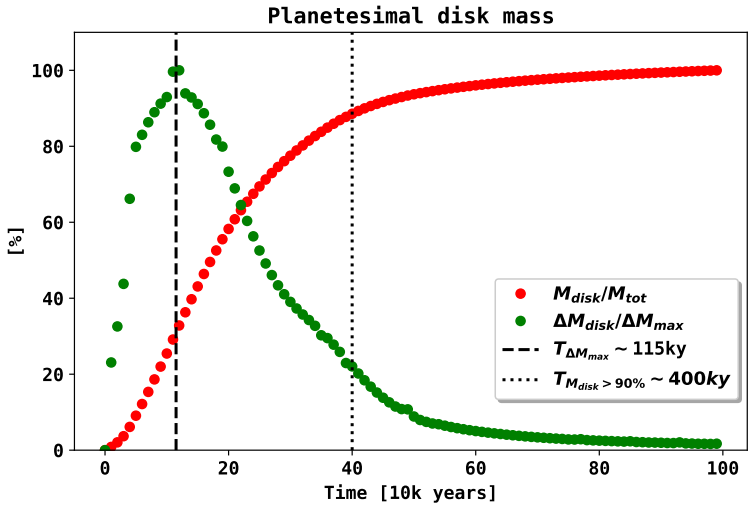


Figure 3.1: Qualitative change in planetesimal disk mass $M_{disk}$ (red dots), normalized by the total disk mass after $10^6$ years that we use in the analytic setups. The green dots indicate the disk mass increase every $10^4$ years $\Delta M_{disk}$, normalized by the maximum mass change $\Delta M_{max}$.

the final mass that is in planetesimals $M_{Pts}$ after $10^6$ years:

$$M_{Tracer} = \frac{M_{Pts}}{N_{Tracer}}. \tag{3.12}$$

The domain of the one-dimensional surface density is split into individual rings of mass. Every $10^4$ years we added new planetesimal tracers to the LIPAD simulation according to the formation of the planetesimal surface density $\Delta M_{disk}$. Each of these newly formed tracers was assigned a heliocentric distance that was chosen randomly between the inner and outer edge of the ring in which it formed. By repeating this at every time step and in every ring, we ensured that the overall heliocentric distribution of planetesimal tracers in the LIPAD simulations matched the density slope and planetesimal distribution of the one-dimensional model. LIPAD then continues with the newly included planetesimal tracers in addition to the previously included objects that by then have grown and fragmented until the next group of tracers is included. Using this setup, we connected the timescales of pebble growth and drift, the formation of planetesimals, and their simultaneous growth. The qualitative mass change in individual setups is shown in Fig. 3.1. The peak of the planetesimal formation rate occurs at $T_{\Delta M_{max}} \sim 115$ky. Because the formation of planetesimals requires a radial pebble flux, we can reach conclusions from the planetesimal formation rate onto the remaining pebbles. About 90 % of planetesimals have formed within 400 ky of our setup.

## 3.4 Numerical results

In the following we present the results of nine different setups in which we varied the total mass within 0.5 au to 5 au and the surface density slope with which planetesimals enter the simulation. The total masses after $10^6$ years were $6\,M_\oplus$, $13\,M_\oplus$ , and $27\,M_\oplus$ and for each we varied the density slope with $\Sigma_p \propto r^{-1.0}$, $\Sigma_p \propto r^{-1.5}$ , and $\Sigma \propto r^{-2.0}$ , respectively. The planetesimal formation rate for these analytic setups is shown in Fig. 3.1. We focused on the mass and semimajor axis evolution of planetary embryos in LIPAD (Fig. 3.2 - Fig. 3.4, Sect. 3.4.1). The embryo mass occurrences are shown in Fig. 3.5, Sect. 3.4.2. The LIPAD results are compared to the analytic

model for embryo placement in Fig. 3.6, Sect. 3.4.3. Following up on this, we display the cumulative number of embryos formed (Fig. 3.7, Sect. 3.4.4), their orbital separation (Fig. 3.8, Sect. 3.4.5), and the active embryo number as well as the total mass in embryos (Fig. 3.9, Sect. 3.4.6).

### 3.4.1 Mass and semimajor axis evolution

Fig. 3.2 to Fig. 3.4 show the evolution of the N-body system within 1 Myr. We show the time and semimajor axis evolution of objects that were classified as planetary embryos in the LIPAD simulation. The classification of an embryo occurs after a tracer particle represents a single object of lunar mass. The tracer is then promoted to a planetary embryo and is treated as a single N-body object with an initial lunar mass. The subsequent growth of a given embryo is represented by the color bar and its semimajor axis evolution by a gray line. The time at which a tracer is promoted to an embryo is shown as black dots.

Because embryos can collide and eventually merge during their evolution, we distinguished active embryos and initial embryos. The number of initial embryos are the events in which tracers have been promoted to planetary embryos (number of black dots), and the number of active embryos is the number of embryos at a given time $t$. The red line in the plots refers to the analytic model. It indicates where $M_P$ has surpassed a lunar mass (criterion I) when the same analytic planetesimal surface density evolution is assumed as in the N-body simulation. The red line is shown only for reference, comparing the N-body simulation with the analytical result. Even though all planetesimals that enter the LIPAD simulation have an initial semimajor axis larger than 0.5 au, we also find embryo formation within 0.5 au. This is due to dynamical interactions or scattering of the LIPAD tracer particles that lead to a nonzero planetetsimal distribution within the edge of its original formation. Because this effect is not taken into account in the analytical model density distribution, we cannot see a change in the red line within 0.5 au. This effect also has to be considered when the cumulative number of initial embryos is compared (see Fig. 3.7). Finally, our results show that the more massive disks (Fig. 3.4) form embryos earlier at close distance. Additionally, embryos in massive disks can form at larger heliocentric distances than in their less massive counterparts (Fig. 3.2).

### 3.4.2 Embryo mass occurrences

Fig. 3.5 shows the number of embryo masses at $T_{M_{disk}>90\%}(400\,\mathrm{ky})$ and at 1 Myr from the simulations of Fig. 3.2 to Fig. 3.4. Most embryos in each simulation are found at the higher mass end of their simulation. Embryos that have low masses ($\approx 0.0123\,\mathrm{M}_\oplus$) are less abundant than embryos that share the highest possible masses in the system. No single embryo grows substantially larger than the others in the system, in agreement with standard oligarchic growth models [Kokubo and Ida, 1998].

### 3.4.3 Comparison with the analytical model

Fig. 3.6 shows the time and location at which an object has reached the mass of a planetary embryo for both the LIPAD simulation and the analytical model from Sect. 3.2.2 (Eq. 3.9, 3.10, 3.11). We show the inner edge of planetesimal formation in LIPAD at 0.5 au and give the time by which the planetesimal disk mass has reached 90% of its total value ($T_{M_{disk}>90\%} = 400\mathrm{ky}$). The randomization of the semimajor axis in our analytical model is given by $2.5R_{Hill}$ , as explained in Sec. 3.3.2. We find that the overall time and semimajor axis distribution of the analytical model agree well with the larger N-body simulations from LIPAD. The randomization of the semimajor axis reproduces the stochastic nature of the N-body process well, as does the analytic growth equation for the time it takes until embryo formation (based on the local planetesimal surface density evolution at a given distance from the star).

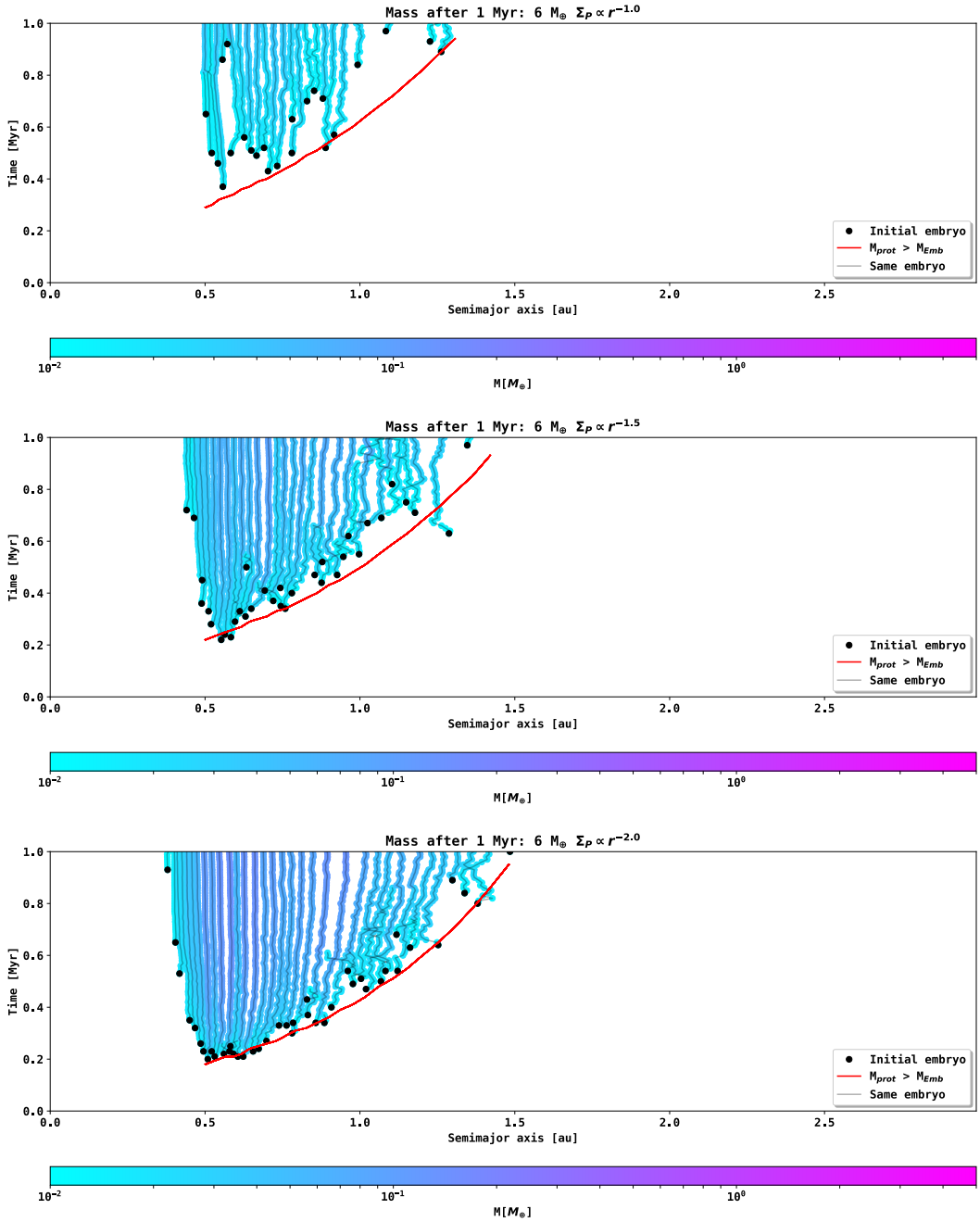


Figure 3.2: Time over semimajor axis evolution of the N-body simulation in LIPAD. The time and location at which an object has first reached lunar mass is indicated by the black dots in the plot. The subsequent growth of the embryo is tracked and connected with the gray lines (its mass is given by the color bar). The mass after one million years in planetesimals is 6 $M_\oplus$ in these runs. The planetesimal surface density slope is varied ($\Sigma_P \propto r^{-1.0}$, $\Sigma_P \propto r^{-1.5}$ , and $\Sigma_P \propto r^{-2.0}$ ). The red line indicates where $M_{prot}$ surpasses the mass of a lunar-mass planetary embryo in the analytical model from Sect. 3.2.2, assuming the same evolution of the planetesimal surface density that is given to the N-body simulation.

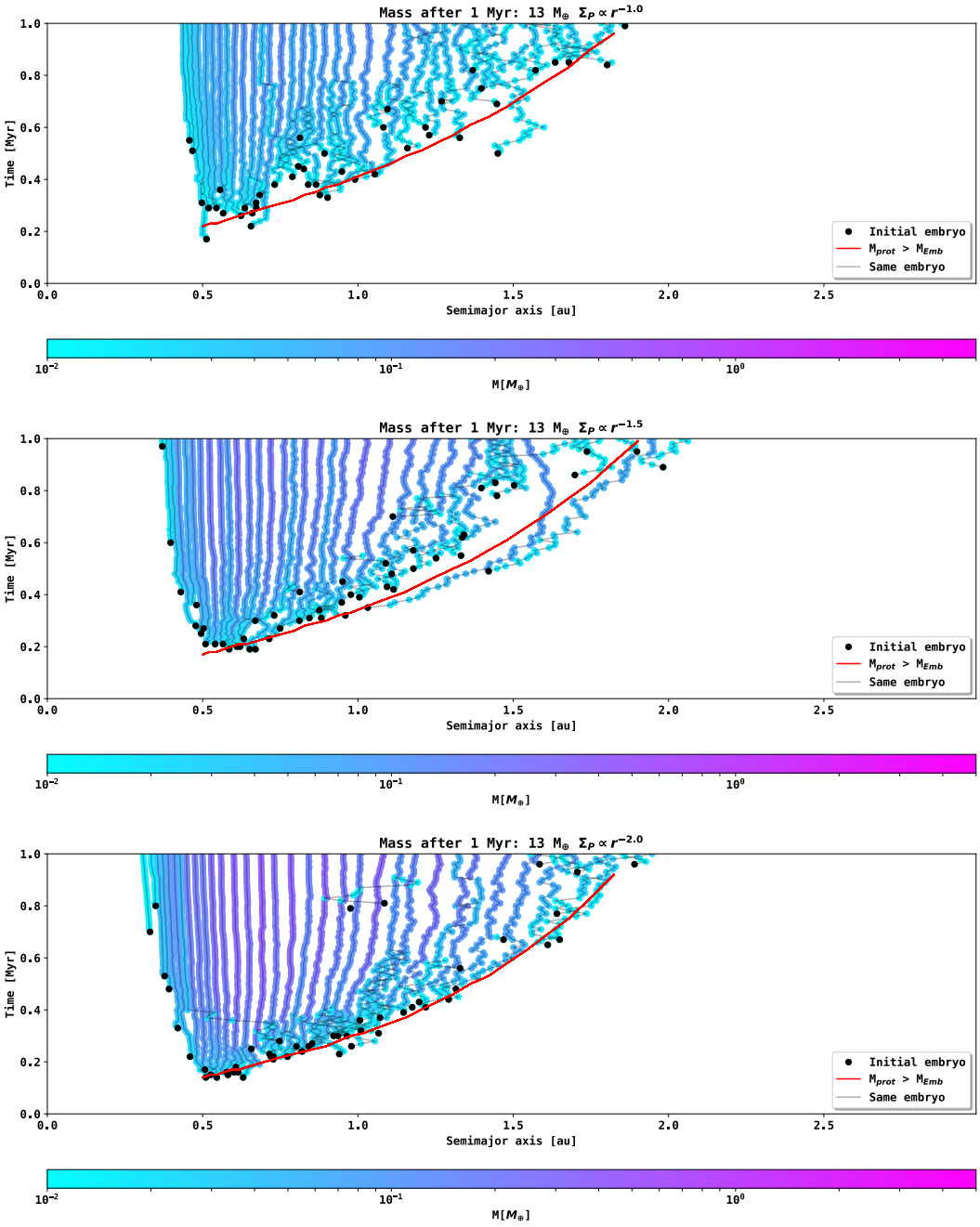


Figure 3.3: Time over semimajor axis evolution of the N-body simulation in LIPAD. The time and location at which an object has first reached lunar mass is indicated by the black dots in the plot. The subsequent growth of the embryo is tracked and connected with the gray lines (its mass is given by the color bar). The mass after one million years in planetesimals is 13 $M_\oplus$ in these runs. The planetesimal surface density slope is varied ($\Sigma_P \propto r^{-1.0}$, $\Sigma_P \propto r^{-1.5}$ , and $\Sigma_P \propto r^{-2.0}$ ). The red line indicates where $M_{prot}$ surpasses the mass of a lunar-mass planetary embryo in the analytical model from Sect. 3.2.2, assuming the same evolution of the planetesimal surface density that is given to the N-body simulation.

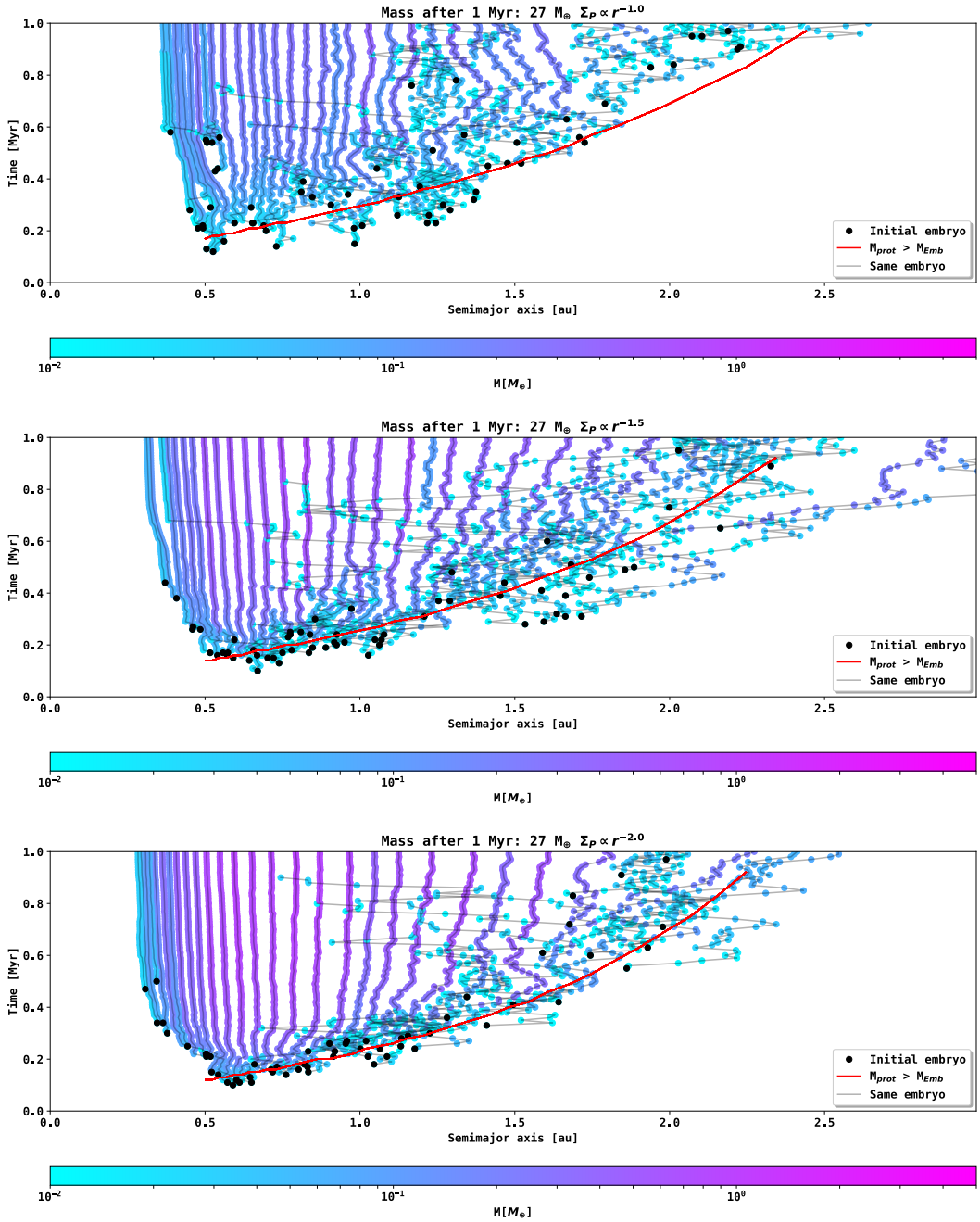


Figure 3.4: Time over semimajor axis evolution of the N-body simulation in LIPAD. The time and location at which an object has first reached lunar mass is indicated by the black dots in the plot. The subsequent growth of the embryo is tracked and connected with the gray lines (its mass is given by the color bar). The mass after one million years in planetesimals is 27 $M_\oplus$ in these runs. The planetesimal surface density slope is varied ($\Sigma_P \propto r^{-1.0}$, $\Sigma_P \propto r^{-1.5}$ , and $\Sigma_P \propto r^{-2.0}$ ). The red line indicates where $M_{prot}$ surpasses the mass of a lunar-mass planetary embryo in the analytical model from Sect. 3.2.2, assuming the same evolution of the planetesimal surface density that is given to the N-body simulation.

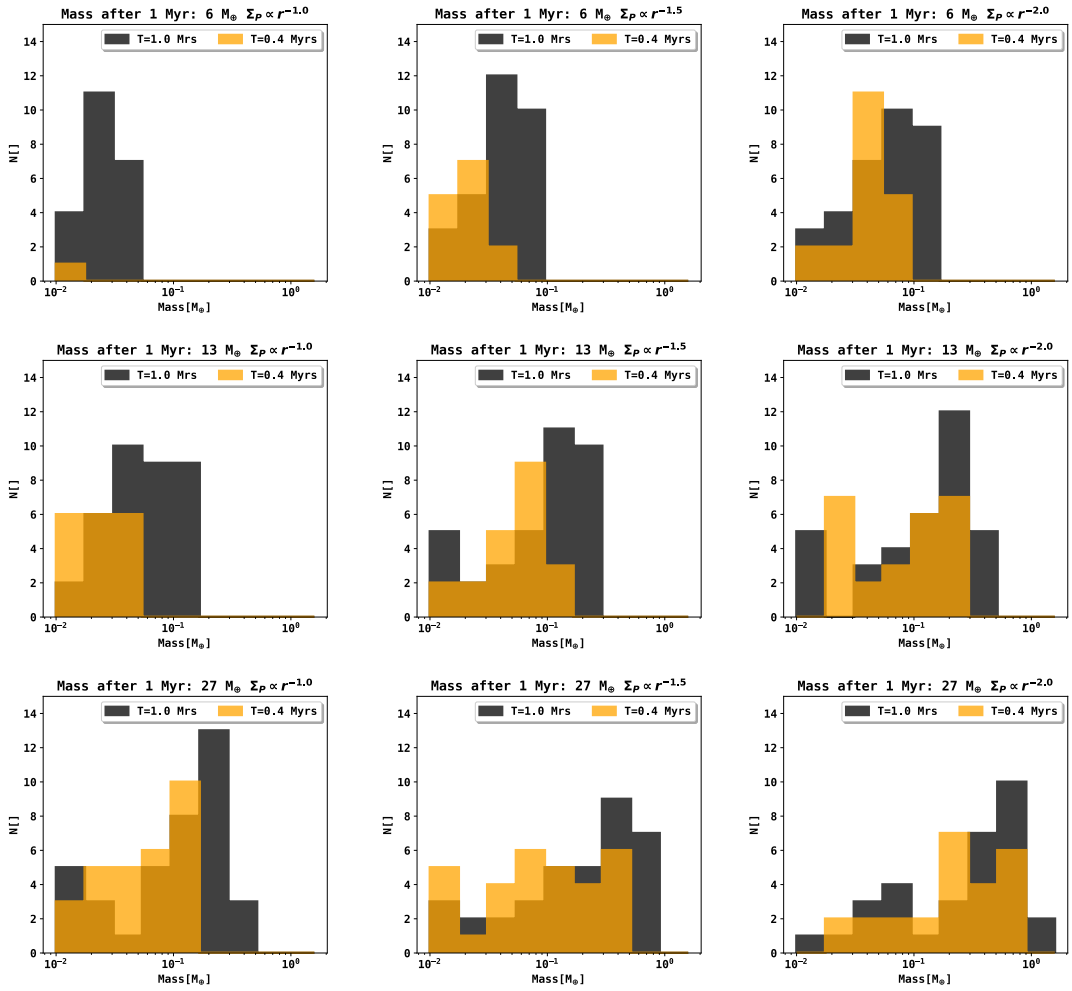


Figure 3.5: Number of embryos within a given mass bin at T = 400 ky ($T_{M_{disk}>90\%}$) and T = 1 Myr from the simulations of Fig. 3.2 to Fig. 3.4.

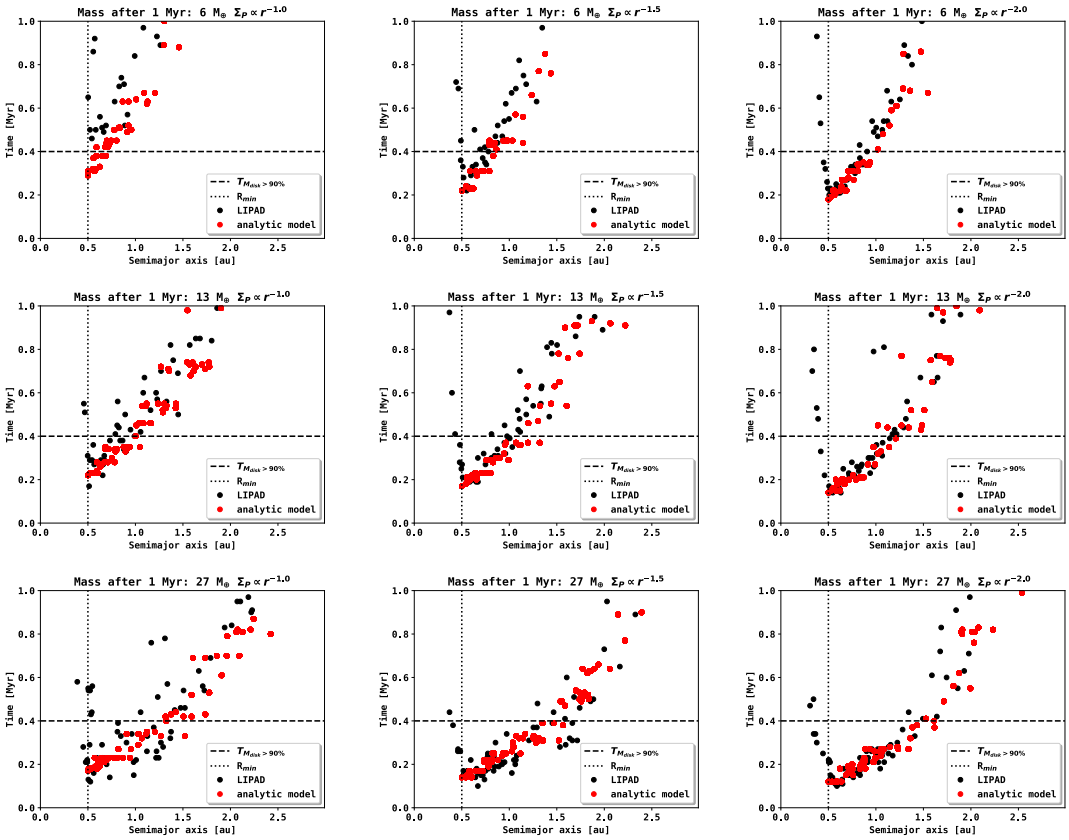


Figure 3.6: Analytical model for embryo formation and embryo formation in LIPAD. The black dots indicate the time and location at which an object reached planetary embryo mass in the LIPAD simulations. The red dots indicate the time for each distance from the star at which a planetary embryo is placed using our analytical model. The orbital separation as input to the analytical model is given as 17 $R_{Hill}$ , with a randomization of 2.5 $R_{Hill}$ The inner edge of planetesimal formation in the LIPAD runs was chosen to be at 0.5 au for numerical performance. We vary the total mass in planetesimals after $10^6$ years from 0.5 au to 5 au ($6M_\oplus$,$13M_\oplus$, and $27M_\oplus$) and the planetesimal surface density slope ($\Sigma_P \propto r^{-1.0}$, $\Sigma_P \propto r^{-1.5}$, and $\Sigma_P \propto r^{-2.0}$).

The innermost embryos (0.5 au to 1 au) in every setup form well below $T_{M_{disk}>90\%}$, but no embryo outside 2 au forms within $T_{M_{disk}>90\%}$. The implications for possible pebble accretion from this behavior are discussed in Sect. 3.5.2.

### 3.4.4 Cumulative number

Fig. 3.7 shows the cumulative number of initial embryos from the LIPAD simulation and the analytic model. The orbital separation of the embryos in the analytic model scales linearly with their Hill radius, which again scales linearly with their distance to the star. The cumulative number of planetary embryos in the analytic model therefore scales logarithmically with distance. Because the orbital separation of embryos in the N-body simulation converges to the same amount of Hill radii, we also find a logarithmic trend in the cumulative number of embryos formed in LIPAD. The total number of initial embryos is related to the total mass in planetesimals after 1 Myr. The reason for this is that embryos can form at larger distances in more massive disks.

The N-body simulations show embryo formation within 0.5 au, which is not possible in the analytic model because the planetesimal formation within 0.5 au is neglected. The innermost embryos that form in the N-body simulation are therefore due to planetesimals that moved within

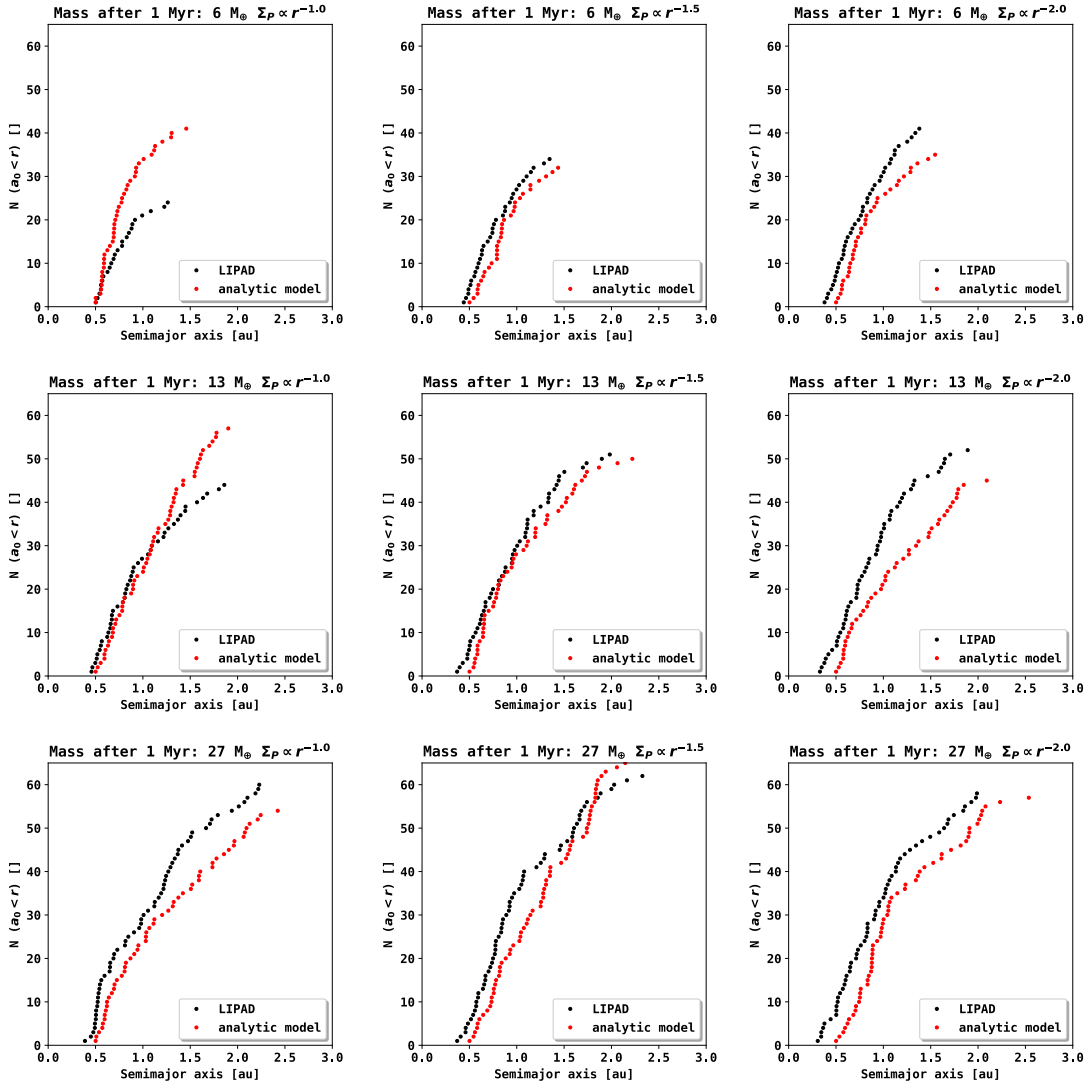


Figure 3.7: Cumulative number of embryos formed during the LIPAD runs from Fig. 3.2 to Fig 3.4 (black dots). The red dots show the cumulative number of embryos that would be placed according to the analytical model from Sect. 3.2.2.

0.5 au due to their dynamical interactions.

This spatial area of embryo formation is clearly defined by criterion I, see Fig. 3.2 to Fig. 3.4. The number of embryos within this area can be determined using criterion II by setting their orbital separations.

### 3.4.5 Orbital separation

Fig. 3.8 shows the time evolution of the average orbital separation of initial embryos for the LIPAD simulation and the analytical model, see Fig. 3.6. The mean orbital separation of all systems converges to a value around 10-15 $R_{Hill}$ after 200-400 ky. The orbital separation is a free parameter from criterion II of the analytical model that we chose to fit the numerical results from our N-body simulations. In combination with criterion I, this allows us to predict the number, spatial distribution, and formation time of planetary embryos for a specific planetesimal surface density evolution. The total number of embryos is given as the number of orbital separations (criterion II) within the possible area of embryo formation (criterion I). Their spatial distribution

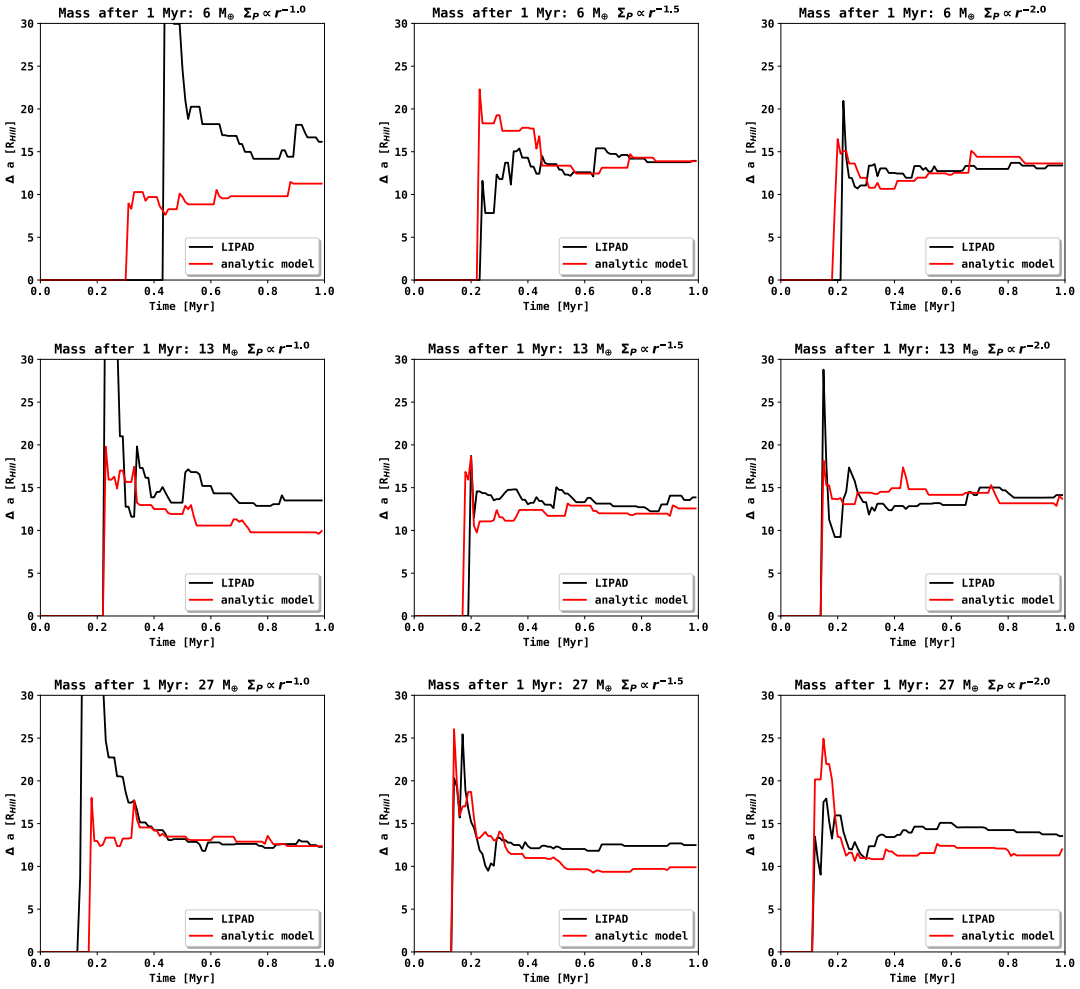


Figure 3.8: Mean orbital separation of the initial embryos from the LIPAD runs and the analytical model embryos over time. The input parameters for the analytical model are given as 17 $R_{Hill}$ with a randomization of 2.5 $R_{Hill}$.

is determined by their orbital separation, which is a function of the mutual Hill radii. In this way, the absolute orbital separation between embryos increases linearly with increasing distance to the star, leading to a logarithmic cumulative number of initial embryos (see Fig. 3.7).

Because of the low number of embryos for early times, the mutual distance can differ strongly between the analytical model and the LIPAD runs. This behavior however would also occur if we were to attempt to compare two LIPAD runs with similar initial conditions. This is due to the chaotic nature of the N-body evolution. We can show that for a larger number of embryos, the orbital separation in the analytical model shows the same behavior as in the N-body simulations.

### 3.4.6 Active number of embryos and mass in embryos

Fig. 3.9 shows the number of active embryos over time, the total mass that is given in these embryos, and the fraction of the total mass in embryos after 1 Myr ($M_{Emb}$) over the total mass in the system after 1 Myr ($M_D$). The number of active embryos after 1 Myr is between 30 and 40 embryos for eight out of our nine runs. Only the $6\,M_\oplus$ and $\Sigma_P \propto r^{-1.0}$ run contains fewer embryos ($N_{active} = 22$) after 1 Myr. While the total number of active embryos seems insensitive to the total planetesimal mass or the planetesimal surface density profile, the same is not true for the total mass that is in planetary embryos after one million years.

The total mass in embryos increases for steeper planetesimal surface density profiles and higher total masses after 1 Myr. The fraction of mass $M_{Emb}/M_{Disk}$ that is transformed into embryos increases for both higher masses and the slope of the planetesimal surface density. The number of embryos does not simply increase for more massive planetesimal disks in our runs because the embryos that form grow larger in more massive disks. They thereby increase their orbital separation to that of the other embryos again. While higher planetesimal disk masses allow for a larger zone in which embryo formation is possible (criterion I), the present embryos increase their orbital spacing due to their higher masses as well. In the case of 27 $M_\oplus$ in planetesimals after 1 Myr, the number of embryos decreases slightly ($N_{active} = 38$ for $\Sigma_P \propto r^{-1.0}$, $N_{active} = 36$ for $\Sigma_P \propto r^{-1.5}$, $N_{active} = 32$ for $\Sigma_P \propto r^{-2.0}$) for the steeper planetesimal surface density profiles, but their mass increases drastically ($M_{Emb} \approx 5\,\mathrm{M}_\oplus$ for $\Sigma_P \propto r^{-1.0}$ , $M_{Emb} \approx 10\,\mathrm{M}_\oplus$ for $\Sigma_P \propto r^{-1.5}$ , $M_{Emb} \approx 13\,\mathrm{M}_\oplus$ for $\Sigma_P \propto r^{-2.0}$).

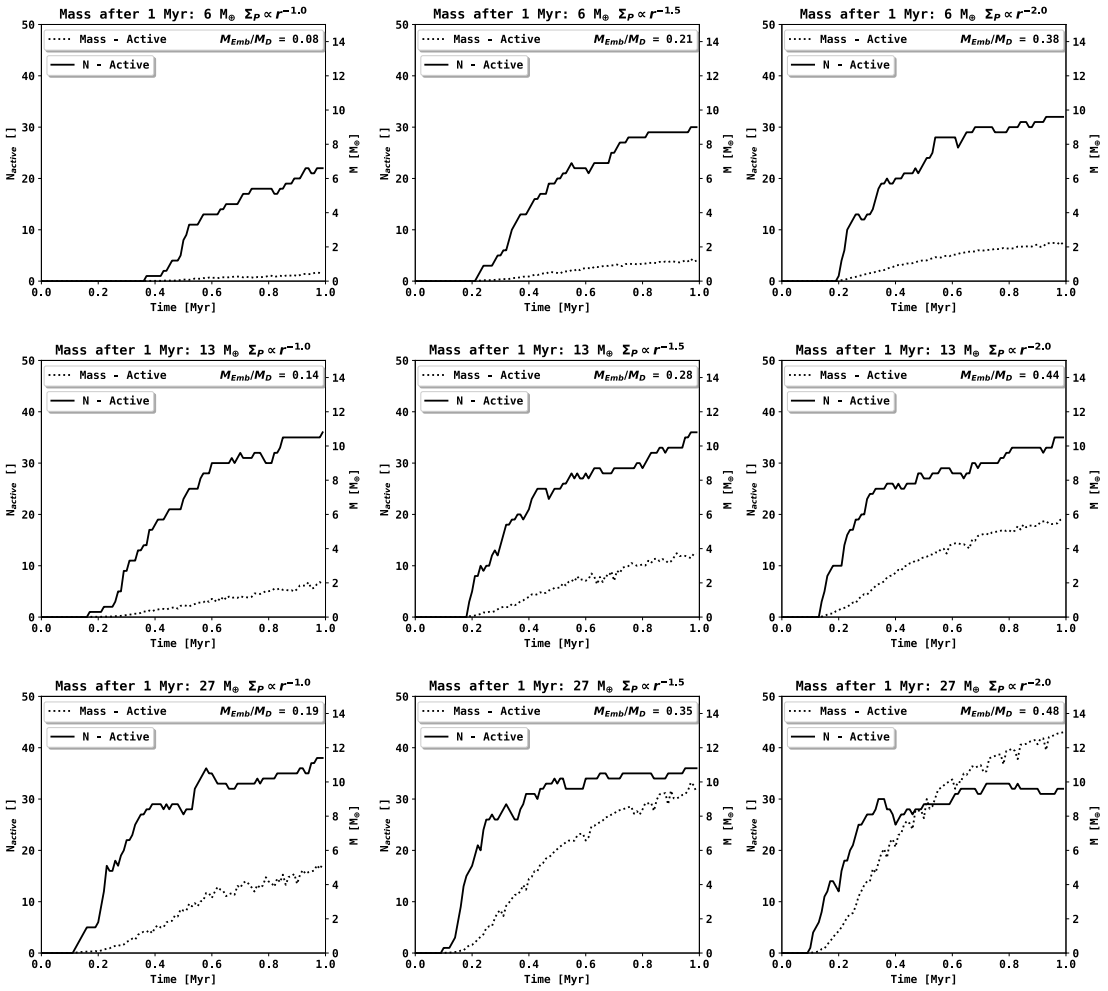


Figure 3.9: Active number of planetary embryos and mass in planetary embryos over time for the LIPAD runs from Fig. 3.2 to Fig. 3.4. We also show the fraction ($M_{Emb}/M_D$) of mass in embryos over the final planetesimal mass that entered the disk after 1 Myr.

## 3.5 Discussion

### 3.5.1 Embryo formation - LIPAD

Fig. 3.2 to Fig. 3.4 clearly show that embryo formation for every power-law planetesimal surface density profile occurs from the inside out. This is an expected result because the growth-timescales in the inner disk are shorter and the densities in planetesimals are correspondingly higher. Even though the individual moment and location at which an embryo forms (black dots) appears to be stochastic, there is a pattern to be found in the embryo formation of the system. The red curve that marks criterion I is well within the area of the initial embryos. The individual locations of the embryos, even though they follow the trend of the red line, appear chaotic. The exact location and time at which an object reaches the size of a planetary embryo appears stochastic due to the stochastic behavior of the N-body, but the analytic growth equations constrain the zone of their individual formation well.

Another effect that can be found is that embryos increase their orbital distance to other embryos when they grow in mass. This effect has previously been found and discussed by Kokubo and Ida [1998] and Kobayashi et al. [2011] when they studied the oligarchic growth of massive objects. In the general picture, initial embryos begin to form earliest at closer distance to the star.

Furthermore, the orbital separation of planetary embryos when expressed in terms of their Hill radii converges to a similar value in every setup we studied, as shown in Fig 3.8. This directly results in a cumulative number of embryos that scales logarithmic with distance, as shown in Fig. 3.7. The stochastic behavior of the orbital separation in Fig. 3.8 stems from the randomization, as explained in Sect. 3.2.2. With the stochasticity in our approach, the cumulative number of embryos in Fig. 3.7 would vary for the analytic and the N-body run. Overall, however, they agree very well. Additionally, the more embryos form, the more reliable the statistics. We see this as the reason for the better agreement within the setups that result in a higher number of embryos. As a comparison we show the cumulative number of embryos that would form with the analytic model, in which the orbital separation is always expressed in terms of the Hill radius of the previously placed embryos. The cumulative number of embryos and the number of active embryos does not vary sensitively with the initial parameters (total mass and planetesimal surface density slope). The total mass that is converted into embryos, however, does depend strongly on the planetesimal surface density slope and the total mass in planetesimals, as shown in Fig. 3.9. The number of active embryos even decreases slightly for higher disk masses and steeper planetesimal surface density profiles. As Fig. 3.2 to Fig. 3.4 show, the area in which planetary embryos form becomes larger for higher masses and steeper density profiles. Because their orbital separation increases for higher masses and because the mean orbital distance converges to the same number of Hill radii (Fig. 3.8), the total number of embryos within 1 Myr is not sensitive to different input parameters either.

### 3.5.2 Implications for pebble accretion

While the effect of pebble accretion on the formation of planetary embryos will be the main subject of our companion paper, we can already discuss some viable constraints here. It is notable to mention that the formation timescale of planetesimals is well within the formation timescales of the planetary embryos. This states that the formation of planetesimals continues to occur after planetary embryos have already formed from previously formed planetesimals. Because the growth rate of planetary embryos depends linearly on the local planetesimal surface density (Eq. 3.9), the local formation of planetesimals has to be taken into account to model the growth-timescales consistently. We conclude that because the formation of planetesimals requires a radial pebble flux, we can estimate first constraints on this pebble flux using our setup, and subsequently, we can estimate first constraints on the possibility of continuous pebble accretion.

| Total mass | $\Sigma_P$ profile | $T_0$ at 2 au | $T_0$ at 3 au | $T_0$ at 4 au |
|---|---|---|---|---|
| $6\,M_\oplus$ | $\Sigma_P \propto r^{-1.0}$ | 2.26 Myr | 5.06 Myr | 9.47 Myr |
| $6\,M_\oplus$ | $\Sigma_P \propto r^{-1.5}$ | 2.2 Myr | 5.76 Myr | >10 Myr |
| $6\,M_\oplus$ | $\Sigma_P \propto r^{-2.0}$ | 2.35 Myr | 7.16 Myr | >10 Myr |
| $13\,M_\oplus$ | $\Sigma_P \propto r^{-1.0}$ | 1.21 Myr | 2.63 Myr | 5.02 Myr |
| $13\,M_\oplus$ | $\Sigma_P \propto r^{-1.5}$ | 1.19 Myr | 3.02 Myr | 6.48 Myr |
| $13\,M_\oplus$ | $\Sigma_P \propto r^{-2.0}$ | 1.26 Myr | 3.77 Myr | 9.03 Myr |
| $27\,M_\oplus$ | $\Sigma_P \propto r^{-1.0}$ | 0.73 Myr | 1.45 Myr | 2.72 Myr |
| $27\,M_\oplus$ | $\Sigma_P \propto r^{-1.5}$ | 0.72 Myr | 1.65 Myr | 3.53 Myr |
| $27\,M_\oplus$ | $\Sigma_P \propto r^{-2.0}$ | 0.75 Myr | 2.05 Myr | 4.98 Myr |

Table 3.1: Analytic embryo formation model extrapolation until 10 Myr from the systems of Fig. 3.2 to Fig. 3.4.

Even though we did not take the accretion of pebbles onto planetesimals or planetary embryos into account in our simulations, we wish to highlight their importance in the general context of planetary growth, as has been displayed by several studies such as Ormel and Klahr [2010], Bitsch et al. [2015], and Ndugu et al. [2017]. The efficiency of pebble accretion directly depends on the local pebble flux at the location of an accreting body of sufficient mass. Becausee the formation of planetesimals $\Delta M_{disk}$ scales linearly with the local pebble flux, we can also derive from Fig. 3.1 that the pebble flux decreases drastically within the first $10^6$ years of the systems evolution. However, because we continue to form planetsimals well after the first embryos have formed, these embryos could grow by the remaining pebble flux that continues to form planetesimals as well. This indicates that the growth time scales of planetary embryos is a determining factor in defining the global efficiency of pebble accretion. A certain embryo size has to be reached at first to effectively accrete pebbles.

Another crucial effect on the pebble flux evolution is the formation of planetesimals itself because they form based on the disk evolution. The more planetesimals form, the earlier we also form planetary embryos that could accrete pebbles. However, the more planetesimals are formed, the lower the pebble flux because mass is transferred into planetesimals. Even though the exact evolution of the pebble flux differs for every disk, the results of our study can already be used to apply first constraints on the magnitude of the pebble flux based on the formation timescales of planetary embryos. Because $\sim 90\%$ of our planetesimals form within 400ky of our setup, we conclude that the magnitude of the pebble flux has decreased significantly before that time. Embryos that form after 400ky would therefore not be able to undergo significant pebble accretion in our model.

In our setup most embryos that form within 400 ky also form within 1 au. The formation of farther out embryos around 1.5-2.0 au occurs well after 400 ky. In conclusion, it is not possible for farther out planetary embryos to undergo pebble accretion in our setup. This statement holds true when we assume a power-law distribution for the planetesimal surface density such as the minimum mass solar nebula hypothesis, the dust profile of a viscous disk, or the pebble-flux-regulated planetesimal formation surface density profile. As a first estimate on the timescales necessary for an embryo to form at larger distances, we extrapolated our analytic model for 10 Myr. The times for an embryo to form at 2 au, 3 au, and 4 au are shown in table 3.1.

### 3.5.3 Architecture of planetary systems

Following our findings from Sect. 3.5.2, it is not too far-fetched to state that the architecture of planetary systems might very well be determined within the first few 100 ky of their formation in terms of pebble accretion. Our study assumed power-law density profiles for the planetesimal

surface density, and our results of inside-out planetary embryo formation are a direct consequence of this. If we were to assume deviation from the power-law profile due to local substructures in the the disk, for instance, around the ice line [Drążkowska and Alibert, 2017], this picture might change.

The early formation of planetary embryos around the ice line might lead to the formation of cold giant planets through pebble accretion. The formation of these planets can then have major consequences for the subsequent evolution of the inner system. Assuming that outer planetary embryos form early enough to undergo significant pebble accretion, they could alter the evolution of the inner system drastically because they would reduce the pebble flux that reaches the terrestrial planet region. The additional planetesimal formation itself will also have strong consequences for the interior pebble flux. An early decrease in the pebble flux would also lead to a decrease in the formation of planetesimals in the terrestrial planet region. This would again affect the formation of planetary embryos and planetary growth. It becomes clear that the formation of planetesimals, the formation of planetary embryos, and the evolution of the pebble flux are tightly connected within the first few 100 ky of a circumstellar disk.

Another scenario that might change the evolution of the system would be the stochastic formation of a planetesimal with an initial size much larger than 100 km [Johansen et al., 2007]. The formation of a significantly larger planetesimal in a reservoir of 100 km planetesimals and pebbles could reduce the timescales of planetary embryo formation significantly. This could lead to the presence of planetary embryos at much larger distances within the lifetime of the pebble flux.

### 3.5.4 Embryo formation: analytic model

The one-dimensional analytic parameterized approach agrees well with the sophisticated N-body simulations in terms of the formation timescales of a lunar-mass object and the total number of objects that reach this given size. In two out of our nine runs, the deviation of the total number of embryos is below 5 %, in four out of nine runs it is below 10 %, and in eight out of nine runs it is below 25 %. Only the $6M_{\oplus}$, $\Sigma_P \propto r^{-1.0}$ run deviates more strongly ($\approx 40\%$). The Hill criterion for the orbital separation of planetary embryos completely determines the number of planetary embryos without additional assumptions. Considering the time and location at which an object reaches the mass of a planetary embryo, we show that the analytic prescription represents the analytic planetesimal surface density evolution well (Sect. 3.4.3).

The N-body simulations require weeks (sometimes months) of computation time with the same planetesimal input, whereas the parameterized model takes mere seconds. While the N-body simulations clearly involve more complexity that allows for a more complete picture of the problem, the question of the manner, location and time at which many initial planetary embryos form is well reproduced with the analytic model. This makes the analytic approach well suited for other studies that aim for statistical properties in which computational time is a limiting factor, such as planet population synthesis.

Even though our study focused on an area from 0.5 au to 5 au, the analytical model should also hold true at farther locations and might be a valuable asset in considering planetary embryo formation in far out ring-like structures of circumstellar disks, as seen in ALMA observations. Other studies regarding planet formation through pebble accretion may use our findings to modify their initial conditions in terms of the available pebble flux, as explained in greater detail in Sect. 3.5.2.

## 3.6 Summary and outlook

We studied the spatial distribution and formation timescales of planetary embryos from an initial disk of gas and dust. For this purpose, we coupled a one-dimensional model for viscous disk evolution and planetesimal formation to the LIPAD code that studies the dynamical N-body evolution of the evolving planetesimal system. The size of an initial planetesimal was given as 100 km in diameter, and it grew dynamically through collisions with other planetesimals. We analyzed the first million years of nine different systems in which we varied the total mass in planetesimals and their surface density profile.

In combination with analytic estimates of growth rates of planetesimals based on their local surface density, we derived an analytical model for planetary embryo formation. Our model reproduces the spatial distribution and formation time of planetary embryos well. We used their orbital separation as a free parameter that can be fit to match the N-body simulations. The model can be used in further studies (e.g., global models of planet formation and population synthesis) that use a planetesimal surface density description to consistently model the spatial distribution and formation time of planetary embryos. The main findings of planetary embryo formation based on pebble flux regulated planetesimal formation are listed below

- Embryos form first in the innermost regions of planetesimal formation due to shorter growth time scales close to the star and higher planetesimal surface densities.
- The innermost embryos (<1 au) form well within the presence of an active pebble flux for most planetesimal disks, whereas the outer embryos(>2au) fail to do so in any disk we studied.
- Higher planetesimal disk masses or steeper planetesimal surface density profiles do not result in a higher number of active embryos, but in more massive embryos within a larger area.

We linked the formation timescale of planetesimal formation and the evolution of the radial pebble flux to the formation timescale of lunar-mass objects that formed by planetesimal collisions. In doing so, we determined crucial constraints for the possibility of pebble accretion as a planet formation process. These constraints need to be considered in studies that involve pebble accretion on planetary embryos because we showed that a planetary embryo and a pebble flux strongly depend on the radial distance of the embryo to the star.

It is shown that a power-law planetesimal surface density profile cannot build planetary embryos at larger distances within the timescale of a radial pebble flux. This consequence arises from the interplay of pebble-flux-regulated planetesimal formation and the timescales involved to form planetary embryos from 100 km sized bodies. The more planetesimals are formed, the earlier planetary embryos are formed, but the more planetesimals are formed, the lower the mass that remains in pebbles. Vice versa, when we decrease the formation of planetesimals to maintain a higher pebble flux, the growth time scales for planetary embryos increase as a result of lower planetesimal surface densities.

Future studies will include disk-consistent pebble accretion in the N-body simulation to study the effect of an active pebble flux on the formation of planetary embryos. Another study that will follow the approach we presented here will study the formation of embryos in far-out planetesimal rings that could result from pressure bumps during the disks evolution.

# 4 | Pebble accretion and embryo formation

This chapter resembles the work published in Voelkel et al. [2021b]. The title of the publication is "Linking planetary embryo formation to planetesimal formation II. The effect of pebble accretion in the terrestrial planet zone". I am the leading author of the manuscript. The document, including all figures and corresponding analysis have been conducted by me, taking into account the input of all listed co-authors. The simulations have been conducted by Rogerio Deienno and me, their analysis and discussion have been conducted by me. The embryo formation model presented has been developed and compared with the simulations by me. Rogerio Deienno, Katherine Kretke and Hubert Klahr supported the interpretation of the results with discussions.

The accretion of pebbles onto planetary cores has been widely studied in recent years and is found to be a highly effective mechanism for planetary growth. While most studies assume planetary cores as an initial condition in their simulation, the question of the manner, location, and time at which these cores form is often neglected. Voelkel et al. [2021b] studies the effect of pebble accretion during the formation phase and subsequent evolution of planetary embryos in the early stages of circumstellar disk evolution. In doing so, Voelkel et al. [2021b] aims to quantify the timescales and local dependence of planetary embryo formation based on the solid evolution of the disk. Voelkel et al. [2021b] connects a one-dimensional two-population model for solid evolution and pebble-flux-regulated planetesimal formation to the N-body code LIPAD. Voelkel et al. [2021b] focuses on the growth of planetesimals with an initial size of 100 km in diameter by planetesimal collisions and pebble accretion for the first one million years of a viscously evolving disk. Voelkel et al. [2021b] compares 18 different N-body simulations in which the total planetesimal mass after one million years, the surface density profile of the planetesimal disk, the radial pebble flux, and the possibility of pebble accretion are varied. Pebble accretion leads to the formation of fewer but substantially more massive embryos. The area of possible embryo formation is weakly affected by the accretion of pebbles, and the innermost embryos tend to form slightly earlier than in simulations in which pebble accretion is neglected. Pebble accretion strongly enhances the formation of super-Earths in the terrestrial planet region, but it does not enhance the formation of embryos at larger distances.

## 4.1 Introduction

The accretion of solids and eventually gas [Pollack et al., 1996] onto planetary cores is widely used as the standard scenario for planet formation. Most studies in the field of planet formation begin with an initial planetary core that grows by either planetesimal (Ida and Lin [2004], Mordasini et al. [2012a], Emsenhuber et al. [2020a], Emsenhuber et al. [2020b], Voelkel et al. [2020]) or pebble accretion (Bitsch et al. [2015], Ndugu et al. [2017], Lambrechts and Johansen [2012]). Recent work included the consistent formation [Lenz et al., 2019] and accretion of planetesimals onto planetary embryos into a global model of planet formation [Voelkel et al., 2020]. Despite the improvement, the presence of planetary embryos is still treated as an initial assumption. A fully consistent global model for planet formation however, would also have to form planetary embryos based on the previous evolution of the system. Studies that form planetary embryos from planetesimals usually neglect the formation of the planetesimals by assuming an initial distribution in the disk [Levison et al., 2015, Walsh and Levison, 2015, Carter et al., 2015, Clement et al., 2020]. We here present an expansion of our companion paper [Voelkel et al., 2021a], in which we investigated the formation of planetary embryos from a dynamically evolving planetesimal disk and derived a one-dimensional parameterized analytic model for planetary embryo formation. The effect of pebble accretion [Ormel and Klahr, 2010, Klahr and Bodenheimer, 2006] on the formation of planetary embryo formation is now added to the same framework in this study.

To motivate our work, we discuss the following aspects (often either neglected or not accounted for in detail by previous works). One aspect that is generally neglected in the study of pebble accretion is that the pebble flux in a disk is not a constant, but instead evolves through radial drift and decays over time. Because pebble accretion relies on the active pebble flux, the time and location at which a planetary embryo is introduced into the simulation is therefore imperative for the evolution of this embryo. The accretion of planetesimals onto planetary embryos, as well as planetesimal growth by collisions, is sensitive to the size of planetesimals, the local planetesimal surface density, and the orbital distance to the star. The evolution and growth of a planet thus strongly depends on its environment, but the cores themselves are also assumed to form from the smaller material in the disk. Modeling the formation of planetary embryos therefore requires an understanding of the local solid evolution of a circumstellar disk. To fully understand the local evolution, however, we need to understand the global evolution of the disk as well because solids can drift through the circumstellar disk from far-out regions. Modeling the formation of planetary embryos in the terrestrial planet region in a self-consistent disk therefore requires understanding the global formation of planetesimals and evolution of the pebble flux during the time of embryo formation. This study is an extension of our companion paper, Voelkel et al. [2021a], in which we studied the effect of the planetesimals surface density and disk mass on the formation of embryos. Our companion paper found that the formation of planetary embryos from 100 km planetesimals occurs from the inside out and that the orbital separation of initial embryos converges to $\approx 15 R_{Hill}$. Our finding confirmed the oligarchic growth nature of the embryo formation process (Kokubo and Ida [1998], Kobayashi et al. [2011], and Walsh and Levison [2019], to mention just a few).

One main result from Voelkel et al. [2021a] is that the total number of embryos does not simply increase by introducing more mass in the system. The embryos that exist grow larger, thus increasing their mutual orbital separation. Additionally, the formation area within 1 Myr increases for higher disk masses, which leads to a similar number of embryos after 1 Myr for our systems. The orbital separation leads to a cumulative number of embryos that increases logarithmic with distance. This behavior is not strongly affected by the planetesimal surface density profile.

Voelkel et al. [2021a] also introduced an analytic model that succeeded in reproducing the total

number, spatial distribution, and formation time of planetary embryos when given the same one-dimensional planetesimal surface density evolution.
In our companion paper, we find that the innermost embryos form while planetesimals are still forming as well. This instigates that an active pebble flux exists after the formation of the innermost embryos. The outer embryos form after the formation of planetesimals has mostly ceased. While the accretion of pebbles is not considered in our first study, their presence is promising for planetary growth.
In addition to our companion paper, we now introduce the accretion of pebbles onto planetesimals and planetary embryos. Studies regarding the evolution of a planetary system from planetesimals and pebbles in the LIPAD [Levison et al., 2012] code have been conducted by Kretke and Levison [2014]. In contrast to what has been studied in Kretke and Levison [2014], we introduce planetesimals over time based on their formation of a one-dimensional planetesimal formation model described in Sect. 4.2. Within this study we connect a global model for the evolution of a circumstellar disk that involves the formation and drift of pebbles, as well as the pebble-flux-regulated formation of planetesimals with N-body simulations. The N-body then tracks their subsequent growth and dynamical evolution. Using this framework, we study a wide range of parameters to investigate their individual contribution to the formation of planetary embryos and the evolution of planetary systems in the terrestrial planet region. In addition to the formation of planetesimals, we now introduce a radial pebble flux and the possibility of pebble accretion in our framework. The evolution of the pebble flux stems from the same disk evolution that also forms the planetesimals within the N-body simulation. Comparing our results from this study with our previous study, we present 18 different N-body simulations in which we vary the planetesimal surface density profile, the total mass in planetesimals, and the total pebble flux.
In Sect. 4.2 we summarize the theory behind our approach, and we explain the numerical setup in Sect. 4.3. Sect. 4.4 presents the results, which are discussed in Sect. 4.5. Sect. 4.6 summarizes our findings and gives an outlook to future work.

## 4.2 Pebbles, planetesimals, and embryos

The goal of this study is to comprehensively model the formation and early dynamical evolution of planetary embryos following an initial population of dust as it is converted into pebbles and planetesimals. We specifically focus on investigating how the accretion of pebbles affects this formation process. The framework that we chose to make this possible is split into two parallel subprocesses. We first compute the viscous evolution of a circumstellar gas disk including its solid evolution and planetesimal formation. The qualitative evolution of the solids serves as a proxy for planetesimal formation and the pebble flux to be included in the N-body simulations. In this way, the N-body simulation runs with the planetesimals and pebbles that have been formed using the one-dimensional approach while continuing to compute their growth through collision and accretion.
A detailed description of the pebble-flux-regulated planetesimal formation model and the two-population solid evolution model can be found in Lenz et al. [2019] and Birnstiel et al. [2012]. Our approach of coupling the one-dimensional planetesimal formation model to the N-body simulation in LIPAD [Levison et al., 2012], as well as a detailed description of the physical models, is described in our previous work [Voelkel et al., 2021a]. In the following we give a brief summary of the underlying physical principles.

### 4.2.1 Planetesimal formation and pebble evolution

Our framework uses the two-population solid evolution approach from Birnstiel et al. [2012] to compute the dust and pebble evolution of a viscously evolving circumstellar disk [Shakura

and Sunyaev, 1973] and the pebble-flux-regulated planetesimal formation model by Lenz et al. [2019]. This framework has recently been used to study the effect of planetesimal formation on the formation of planets [Voelkel et al., 2020] and was applied in our companion paper [Voelkel et al., 2021a].
The two-population model uses a parameterized mass relation between a small and a large population of solids in the disk, defined by their Stokes number. The small particles ($St \ll 1$) are coupled to the dynamic motion of the gas and can be seen as dust, while the larger particles ($St \sim 1$) are detached from the gas motion and can be seen as pebbles. The parameter that separates the two populations was derived by fitting the two-population approach to larger coagulation-based simulations of grain growth [Birnstiel et al., 2010]. Planetesimals then form proportional to the radial pebble flux [Lenz et al., 2019]. The planetesimal formation model assumes that particle traps can appear at any location in the disk and last for a given lifetime. The model assumes that a fraction of the radial pebble flux that drifts through a particle trap can be transformed into planetesimals. Planetesimals form with an initial size of 100 km in diameter [Klahr and Schreiber, 2020, Abod et al., 2019, Johansen et al., 2009] in our setup and in Lenz et al. [2019]. As an arising necessity, to form at least one planetesimal, a threshold mass has to be reached that is transformed from the pebble flux. The approach itself does not specify the underlying mechanism or instability (e.g., streaming instability or Kelvin-Helmholtz instability) that drives the formation of planetesimals, it is a model-independent framework that forms planetesimals based on the radial pebble flux.

### 4.2.2 Embryo formation

We define a planetary embryo as an object with at least one lunar mass ($M_e = 0.0123 M_\oplus$) in our study. Growing an embryo from 100 km sized planetesimals (with a bulk density of $\rho = 1 g/cm^3$) requires more than 5 orders of magnitude of growth. This would require hundreds of thousands of planetesimals to form a single embryo through collisions, making this problem computationally unfeasible for classical numerical integrators. Thus, in order to solve this problem, we used the code known as LIPAD (Lagrangian integrator for planetary accretion and dynamics, see Levison et al. [2012]). LIPAD is a Lagrangian code that uses the concept of tracer particles to follow the dynamical, collisional, and accretional evolution of a very large number of sub-kilometer and kilometer-sized planetesimals all the away until they become planets.
Collisional routines are employed to determine when collisions between tracers occur. In this event, following a probabilistic outcome based on a fragmentation law by Benz and Asphaug [1999], tracers can be assigned new physical radii. Therefore a distribution of tracers in LIPAD represents the size distribution of the evolving planetesimal population. The interaction among tracers results from statistical algorithms for viscous stirring, dynamical friction, and collisional damping.
Our study introduces planetesimal and pebble tracer particles and computes their growth by planetesimal collisions and pebble accretion. Tracer particles are represented by three quantities: mass, physical radius, and bulk density. These three quantities relate to each other as $n_{pl} = m_{tr}/[(4./3.)\rho r_{pl}^3]$. Here, $n_{pl}$ is the number of planetesimals represented by a single tracer particle, $m_{tr}$ is the tracer constant mass, $\rho$ its constant bulk density, and $r_{pl}$ the planetesimal size that the tracer represents. This implies that the number of planetesimals represented by a single tracer is larger for smaller planetesimals. It also implies that as planetesimals grow as a result of their collisional evolution and accretion, they are less represented by a single tracer. As a result, once a planetesimal grows to the point where a tracer will represent only one object (a lunar mass object in our case), this tracer becomes an embryo and is then treated as an individual N-body object in the simulation. These planetary embryos interact among themselves, as well as with tracers, through normal N-body routines [Duncan et al., 1998].

The promotion of a planetesimal tracer particle to a planetary embryo in LIPAD is what we define as the initial formation of a planetary embryo. We refer to Voelkel et al. [2021a] for a detailed description of the conversion of one-dimensional solid evolution outcomes into tracers, as well as to Levison et al. [2012]; Kretke and Levison [2014]; Walsh and Levison [2016]; Walsh and Levison [2019]; Deienno et al. [2019]: Deienno et al. [2020] for a series of previous applications of LIPAD.
LIPAD also contains a prescription of the gaseous nebula from Hayashi [1981]. This gas disk provides aerodynamic drag, eccentricity, and inclination damping on every object.

### 4.2.3 Pebble accretion

The fundamental difference to Voelkel et al. [2021a] of our study lies in the accretion of pebbles onto planetesimals and planetary embryos. In the following we briefly explain the concept of pebble accretion based on Ormel and Klahr [2010] and Lambrechts and Johansen [2012]. A detailed description of the implementation of pebble accretion in LIPAD can be found in Kretke and Levison [2014]. When we refer to pebble accretion, we talk about the accretion of particles onto bodies that is strongly enhanced by gas drag. For this to occur, several conditions need to be met. The stopping timescale of the particle that is to be accreted must be long compared to the timescale of deflection by the target's object gravity. More specifically, the timescale of the gravitational encounter must be shorter than four times the stopping time,

$$v_{rel}\frac{b^2}{GM_p} < 4t_s, \tag{4.1}$$

with $G$ as the gravitational constant and $t_s$ the stopping time. $v_{rel}$ is given as the relative velocity of the particle and the planetesimal or planetary embryo of mass $M_p$. The impact parameter $b^2$ can then be expressed as

$$b < \tilde{R}_C = \left(\frac{4GM_p t_s}{v_{rel}}\right)^{1/2}. \tag{4.2}$$

The second criterion states that the stopping time of the particle must be shorter than the time it takes for the particle to drift past the target. The impact parameter for the time at which a particle is deflected by 90° then gives

$$b = b_{90^\circ} = \frac{GM_p}{v_{rel}^2}. \tag{4.3}$$

In summary, the first criterion states that small dust cannot contribute to pebble accretion because it is too strongly coupled to the motion of the gas, while the second criterion illustrates why larger objects such as planetesimals do not benefit from gas drag. The critical crossing timescale can then be defined as

$$t_{s,*} = \frac{b_{90^\circ}}{v_{rel}} = \frac{GM_p}{v_{rel}^3}. \tag{4.4}$$

In the LIPAD simulation, pebbles radially drift inward. The decision whether a pebble can be accreted by an object is made if the particle is within the Hill radius of the object and under the condition that

$$b < R_C = \tilde{R}_C \exp\left[-\left(\frac{t_s}{4t_{s,*}}\right)^{\gamma}\right], \tag{4.5}$$

with $\gamma = 0.65$ [Ormel and Klahr, 2010]. Pebbles enter the N-body simulation in the form of pebble tracers [Kretke and Levison, 2014].

## 4.3 Simulation setup

The setup of our present study is an expansion of our previous work [Voelkel et al., 2021a] and is described there in greater detail, but for the purposes of this work, we briefly describe the model setup here. We computed the first 1 Myr of a viscously evolving disk including the two-population solid evolution and pebble-flux-regulated planetesimal formation model from Sect. 4.2. The mass rate of planetesimal formation was then given as input to the LIPAD N-body simulation in terms of a corresponding number of planetesimal tracers every 10 kyr. With our setup we studied the evolution of planetary embryo formation for 18 different systems in which we varied the total planetesimal disk mass after 1 Myr, the planetesimal surface density profile, and the total pebble flux. The total planetesimal masses after 1 Myr are given by $6\,M_\oplus$, $13\,M_\oplus$ , and $27\,M_\oplus$. The planetesimal surface density profile varied by $\Sigma_P \propto r^{-1.0}$, $\Sigma_P \propto r^{-1.5}$ , and $\Sigma_P \propto r^{-2.0}$. Our study individually compares systems in which pebble accretion is active to those in which it is ignored. In addition to our previously published work [Voelkel et al., 2021a], we introduced a radial pebble flux into the LIPAD simulation. Pebbles were placed outside the outer edge of our computational domain at 5 au. The total mass of the pebble flux over 1 Myr was varied by $57.7\,M_\oplus$ in the $6\,M_\oplus$ case, $115.8\,M_\oplus$ in the $13\,M_\oplus$ case, and $232.5\,M_\oplus$ in the $27\,M_\oplus$ case. The corresponding mass was introduced over 1 Myr into the simulation in the form of pebble tracers. Pebble tracers were then accreted by the planetesimal tracers and the embryos in the domain. The qualitative evolution of the pebble flux at 5 au was taken from our one-dimensional solid evolution model as well, similar to the formation of the planetesimal disk. LIPAD currently does not have the capability of transforming a flux of pebbles into planetesimals. The formation of planetesimals still stems from the one-dimensional disk evolution as in Voelkel et al. [2021a].
The change in disk mass, the disk formation rate, and the radial pebble flux at 5 au that were used in our setups is shown in Fig. 4.1. While simulations that evolve the systems for longer times (e.g., 100 Myr) are technically possible, we chose to focus on the first million years for several reasons. Not only is the longer computation very costly, but Fig. 4.1 also shows that the formation of planetesimals after 1 Myr in our setup has largely ceased. Another reason is that the interaction between larger planets and the gas disk (e.g., planetary migration) would need to be treated more carefully, as would the dispersal of the gas disk itself. The system after 1 Myr remains mostly dynamically cold. The reason is that the gas component of the disk does not decrease in our setup. Thus, aerodynamic damping in eccentricity plays an important role in our simulations. We understand that neglecting gas disk dispersal is not necessarily ideal (the amount of gas in the disk would likely decay with time). However, the gas is not expected to vanish within 1 Myr either, and even a small gas component could result in a substantial effect on the growing planets. Because of the large uncertainties involving gas-dispersal timescales and because we are mostly interested in determining where and when lunar-mass embryos would form (within a 1 Myr period), we therefore hold the differences regarding the gas-disk decay to be minor for our goals.

## 4.4 Numerical results

### 4.4.1 Embryo formation

In Fig. 4.2 to Fig. 4.4 we show the time, mass, and semimajor axis evolution of planetary embryo formation with the LIPAD code. The total mass after 1 Myr in planetesimals is given as $6M_\oplus$ (Fig. 4.2), $13M_\oplus$ (Fig. 4.3), and $27M_\oplus$ (Fig. 4.4). The simulations in which pebble accretion is not included (left panels) were taken from our previous work [Voelkel et al., 2021a] and serve as comparison in this study. The panels on the right always show the same system in which pebble accretion is included. The black dots can be interpreted as the initial formation of embryos. In addition to this, we define the term 'active' embryos. This term refers to all objects above embryo

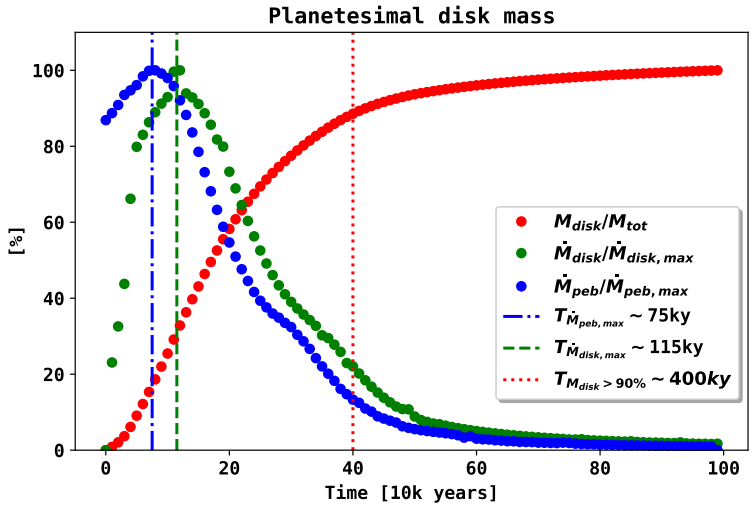


Figure 4.1: Percentage change of the planetesimal disk mass $\dot{M}_{disk}$ , the total disk mass $M_{disk}$ , and the radial pebble flux at 5 au. The disk mass (red dots) is normalized by the total disk mass after $10^6$ years. The green dots indicate the disk-mass increase every $10^4$ years ($\dot{M}_{disk}$), normalized by the maximum mass change ($\dot{M}_{disk,max}$). The blue dots indicate the pebble flux every $10^4$ years ($\dot{M}_{peb}$), normalized by the maximum pebble flux ($\dot{M}_{peb,max}$). We find that $\sim 90\%$ of planetesimals have formed within 400 kyr with a peak in the pebble flux at $\sim$ 75kyr and another in planetesimal formation at $\sim$ 115kyr.

mass at a given time. Every active embryo used to be an initial embryo, but not every initial embryo remains in the system because of mergers. The individual embryos are connected by a gray line for clarity. The red line refers to the analytical estimate after which embryo formation is possible from Voelkel et al. [2021a]

### 4.4.2 Embryo masses

Figure 4.5 shows the number of different embryo masses after 1 Myr for the systems from Fig. 4.2 to Fig. 4.4. The blue and orange histograms refer to simulations where we considered and neglected pebble accretion, respectively. Without pebble accretion, there is no embryo with a mass higher than 1 $M_\oplus$, whereas this is a very common outcome for the simulations in which pebble accretion is included. In every system, the highest mass is generally achieved when pebble accretion is included.
While the systems in which pebble accretion is neglected fail to build super-Earths with our input parameters, the formation of such planets becomes possible when pebble accretion is included. While the number of active embryos decreases when pebble accretion is included (see Fig. 4.6), their masses increase drastically.

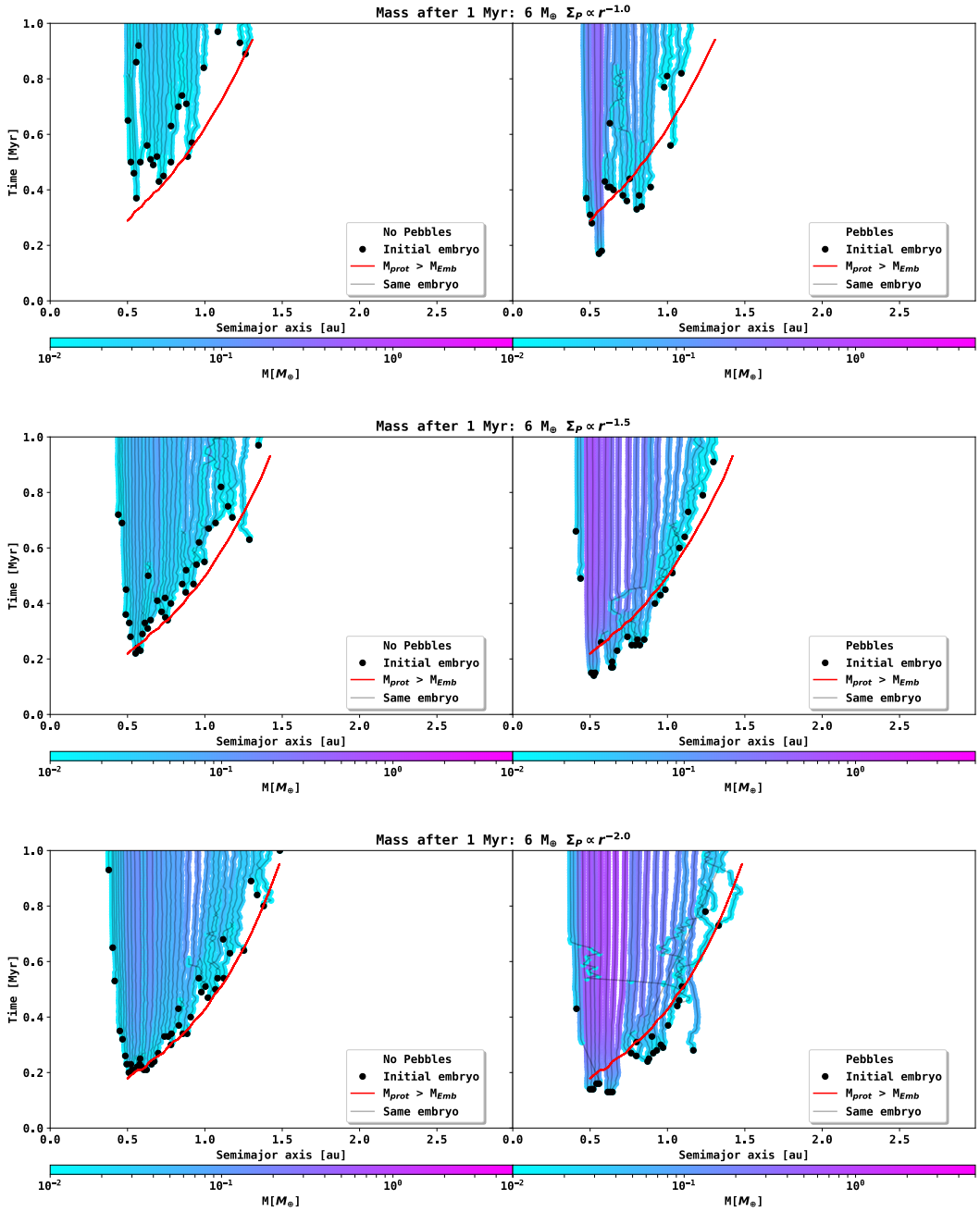


Figure 4.2: Time over semimajor-axis evolution of the N-body simulation in LIPAD. The time and location at which an object has first reached lunar mass is indicated by the black dots in the plot. The subsequent growth of the embryo is tracked and connected with the gray lines, and its mass is given by the color bar. The mass in planetesimals after 1 Myr is given by 6 $M_\oplus$ in these runs, the planetesimal surface density slope is varied ($\Sigma_P \propto r^{-1.0}$, $\Sigma_P \propto r^{-1.5}$ , and $\Sigma_P \propto r^{-2.0}$ ). The left panels show the system without pebble accretion. The right panels show the system in which pebble accretion is included. The red line indicates the time after which the analytic model presented in Voelkel et al. [2021a] states that embryo formation is possible.

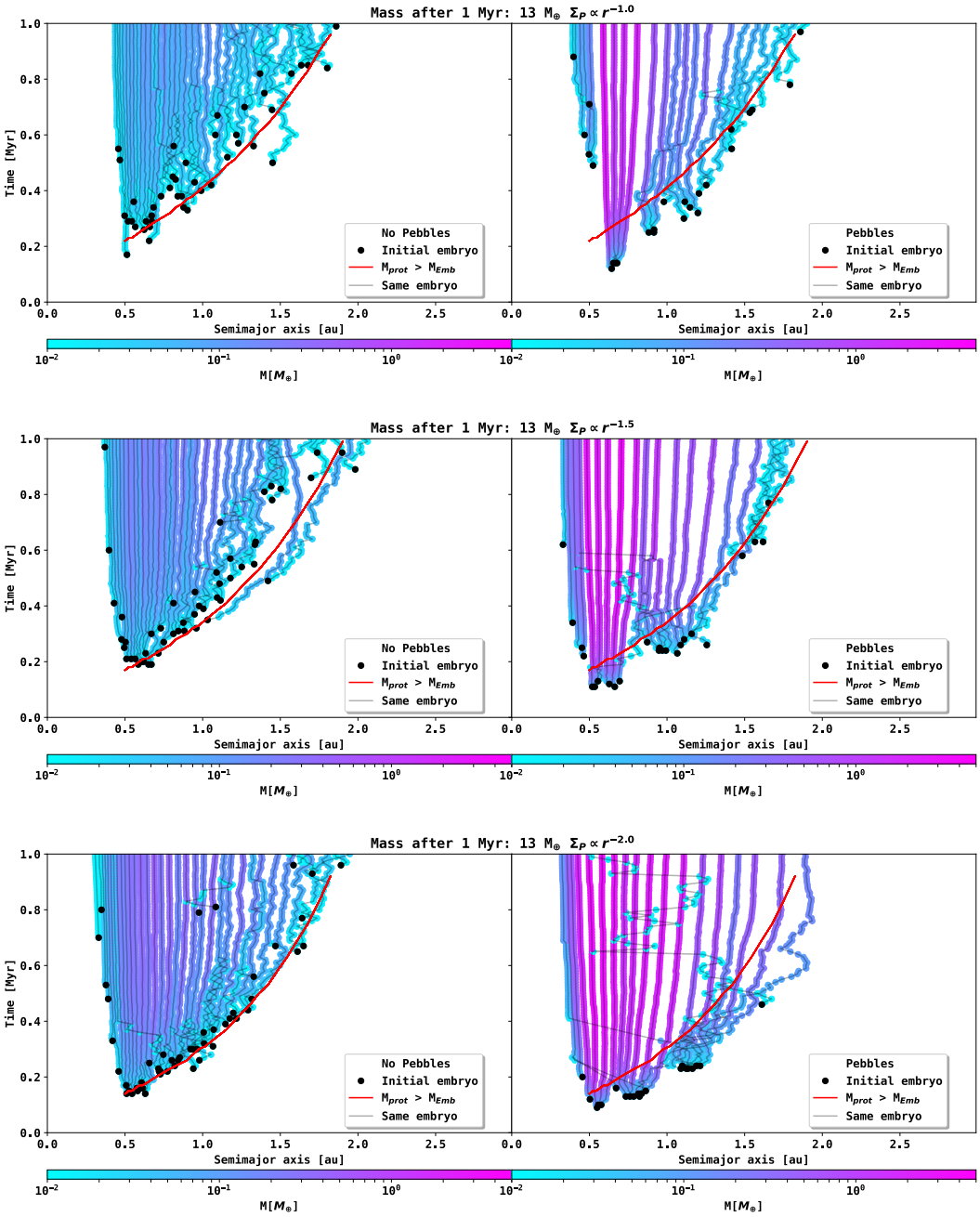


Figure 4.3: Time over semimajor-axis evolution of the N-body simulation in LIPAD. The time and location at which an object has first reached lunar mass is indicated by the black dots in the plot. The subsequent growth of the embryo is tracked and connected with the gray lines, and its mass is given by the color bar. The mass in planetesimals after 1 Myr is given by 13 $M_\oplus$ in these runs, the planetesimal surface density slope is varied ($\Sigma_P \propto r^{-1.0}$, $\Sigma_P \propto r^{-1.5}$ and , $\Sigma_P \propto r^{-2.0}$ ). The left panels show the system without pebble accretion. The right panels show the system in which pebble accretion is included. The red line indicates the time after which the analytic model presented in Voelkel et al. [2021a] states that embryo formation is possible.

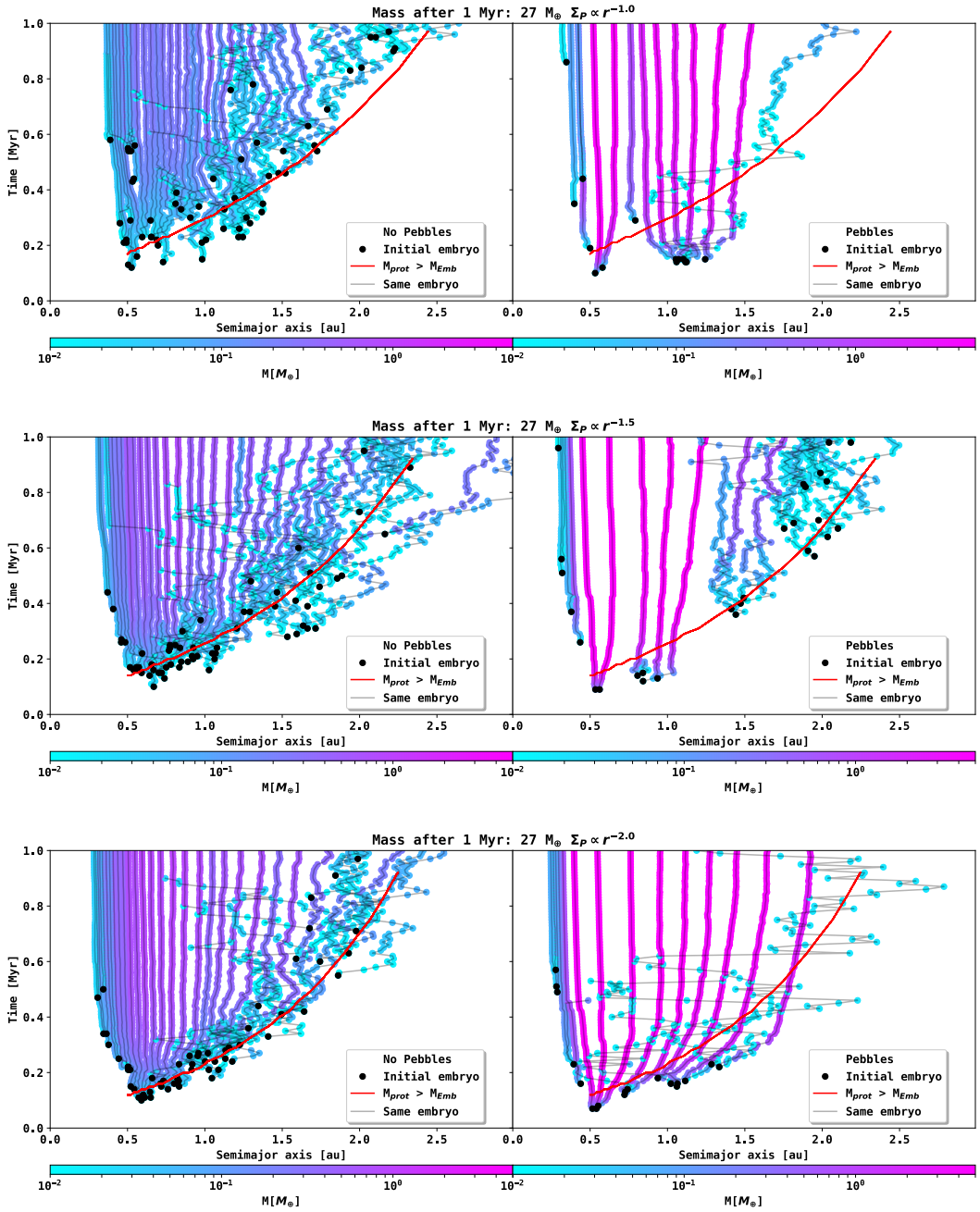


Figure 4.4: Time over semimajor-axis evolution of the N-body simulation in LIPAD. The time and location at which an object has first reached lunar mass is indicated by the black dots in the plot. The subsequent growth of the embryo is tracked and connected with the grey lines, and its mass is given by the colorbar. The mass in planetesimals after 1 Myr is given by 27 $M_\oplus$ in these runs, the planetesimal surface density slope is varied ($\Sigma_P \propto r^{-1.0}$, $\Sigma_P \propto r^{-1.5}$ , and $\Sigma_P \propto r^{-2.0}$ ). The left panels show the system without pebble accretion. The right panels show the system in which pebble accretion is included. The red line indicates the time after which the analytic model presented in Voelkel et al. [2021a] states that embryo formation is possible.

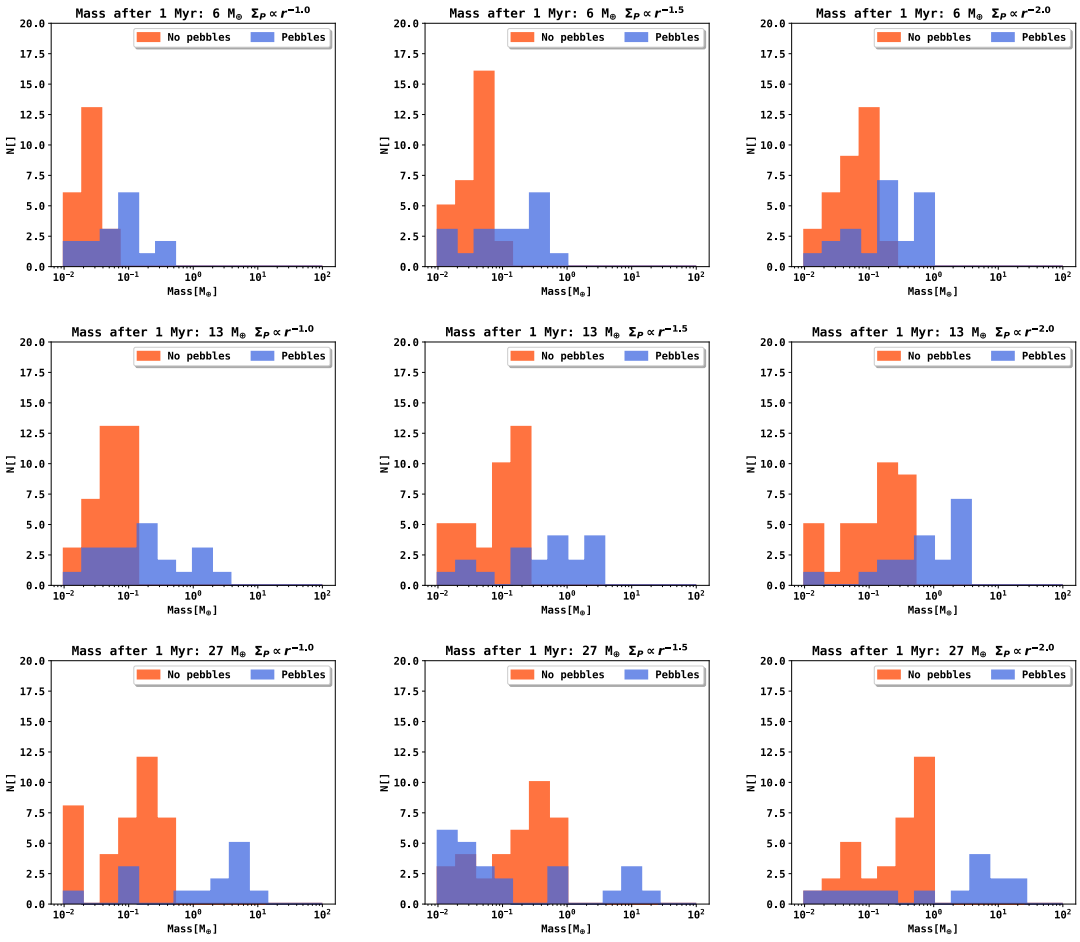


Figure 4.5: Embryo masses after 1 Myr for the different parameters from Fig. 4.2 to Fig. 4.4. The orange histograms show the systems in which pebble accretion is neglected, and the blue histograms show the systems in which pebble accretion is enabled.

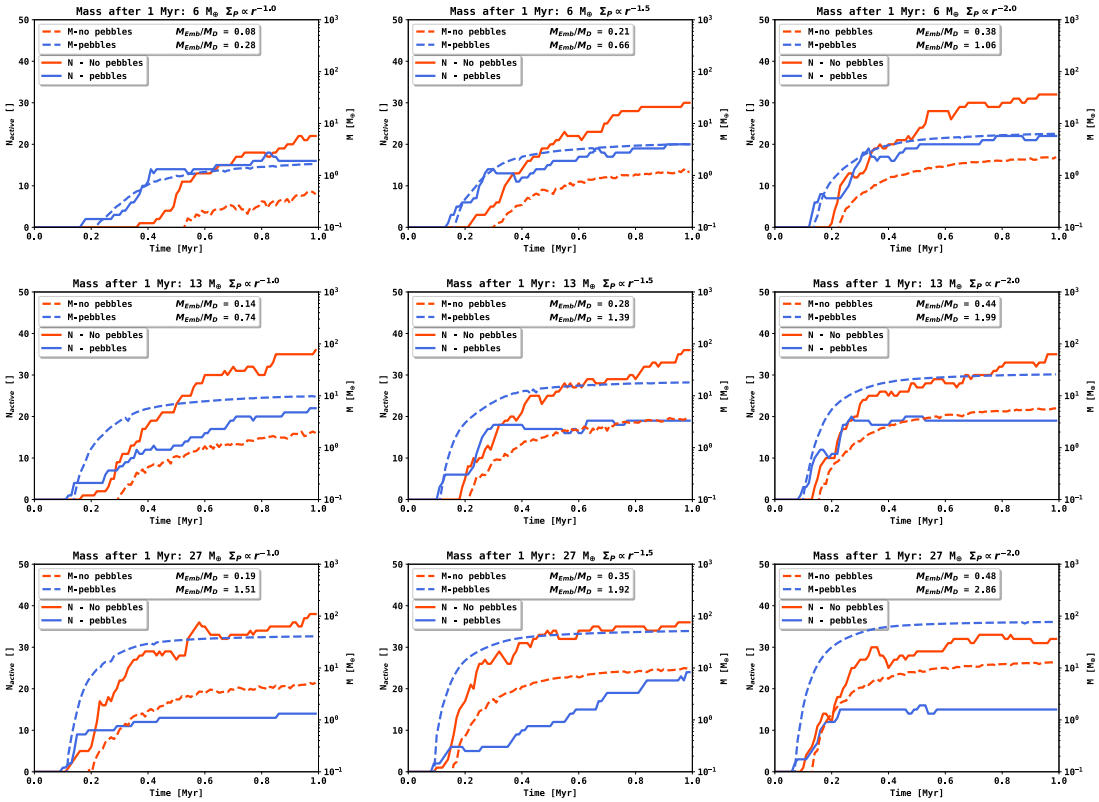


Figure 4.6: Number of active embryos (solid line) and total mass in embryos (dashed line) over time for the systems from Fig. 4.2 to Fig. 4.4. The orange curves refer to the systems in which pebble accretion is disabled, whereas the blue lines refer to the systems in which pebble accretion is enabled. We also give the fraction of embryo mass over the total mass that entered the planetesimal disk after 1 Myr ($M_{Emb}/M_D$).

### 4.4.3 Active number and total mass

Figure 4.6 shows the total number of embryos and the total mass that is in embryos over time for the setups from Fig. 4.2 to Fig. 4.4. We also give the fraction of total embryo mass $M_{Emb}$ over the mass that was given to the planetesimal disk after 1 Myr ($M_D$) for each setup. The first embryos always form in the systems in which pebble accretion is enabled. However, the number of active embryos during the simulation is almost a factor of 2 below the number of embryos in the systems without pebble accretion. The mass in embryos differs even more strongly than the active number of embryos for the corresponding systems. The fraction $M_{Emb}/M_D$ consistently increases for higher total masses and steeper $\Sigma_P$-profiles, respectively. In the systems in which pebble accretion is included, it can exceed unity. This means that the mass in planetary embryos can be higher than the mass that is transformed into planetesimals through pebble accretion.

### 4.4.4 Orbital separation

In Fig. 4.7 we compare the mean orbital separation of embryos over time for the systems from Fig. 4.2 - Fig. 4.4. The orbital separation is expressed in units of the embryos Hill radii. The mean orbital separation after 1 Myr converges to $\approx 10 R_{hill}$ for each setup. The simulations in which pebble accretion is included show a smoother and more stable behavior over time than the systems in which pebble accretion is neglected. The explanation of these differences lies in the fact that the first embryos can start growing farther apart from each other in the runs that only consider planetesimal accretion. Therefore numerous embryos are needed in order to converge

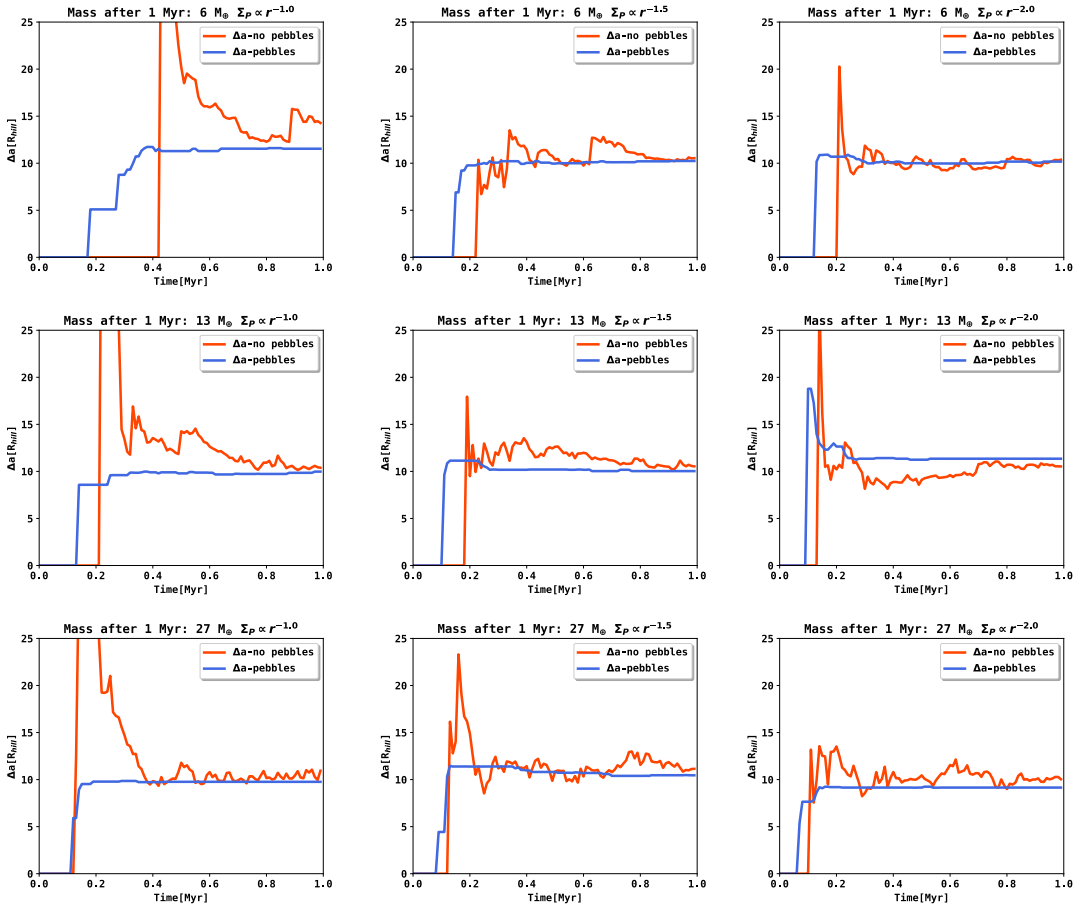


Figure 4.7: Orbital separation of active embryos over time from the systems from Fig. 4.2 - Fig. 4.4. The orange curves refer to the systems in which pebble accretion is disabled, and the blue curves refer to the systems in which pebble accretion is enabled. The distance is expressed in units of the embryos Hill radii.

for a characteristic orbital Hill spacing.
When pebble accretion is considered, embryos initially tend to grow closer to each other. Connecting the orbital separation from Fig. 4.7 with the embryo masses from Fig. 4.5 and the time semimajor-axis evolution from Fig. 4.2 to Fig. 4.4, we can see that the absolute physical distance between embryos increases largely because of their mass increase and therefore their increasing Hill radius.
The dynamical separation of embryos when expressed in Hill radii does not change, but their physical separation as a consequence does. The possible area of embryo formation, on the other hand, does not enlarge if pebble accretion is included (see Fig. 4.2 to Fig. 4.4). Because the orbital separation increases, the number of active embryos within the possible area of embryo formation decreases. This is a consequence of their rapid growth by pebble accretion.

### 4.4.5 Cumulative distribution

As we showed in Fig. 4.6, the total number of active embryos in the simulation decreases strongly when pebble accretion is included. In Fig. 4.8 we show the cumulative number of initial embryos for the systems from Fig. 4.2 to Fig. 4.4. We also highlight where the innermost and outermost embryos form within 1 Myr for each setup via vertical dotted lines with corresponding colors. In terms of the initial formation of embryos, the outermost embryo forms farther out in the

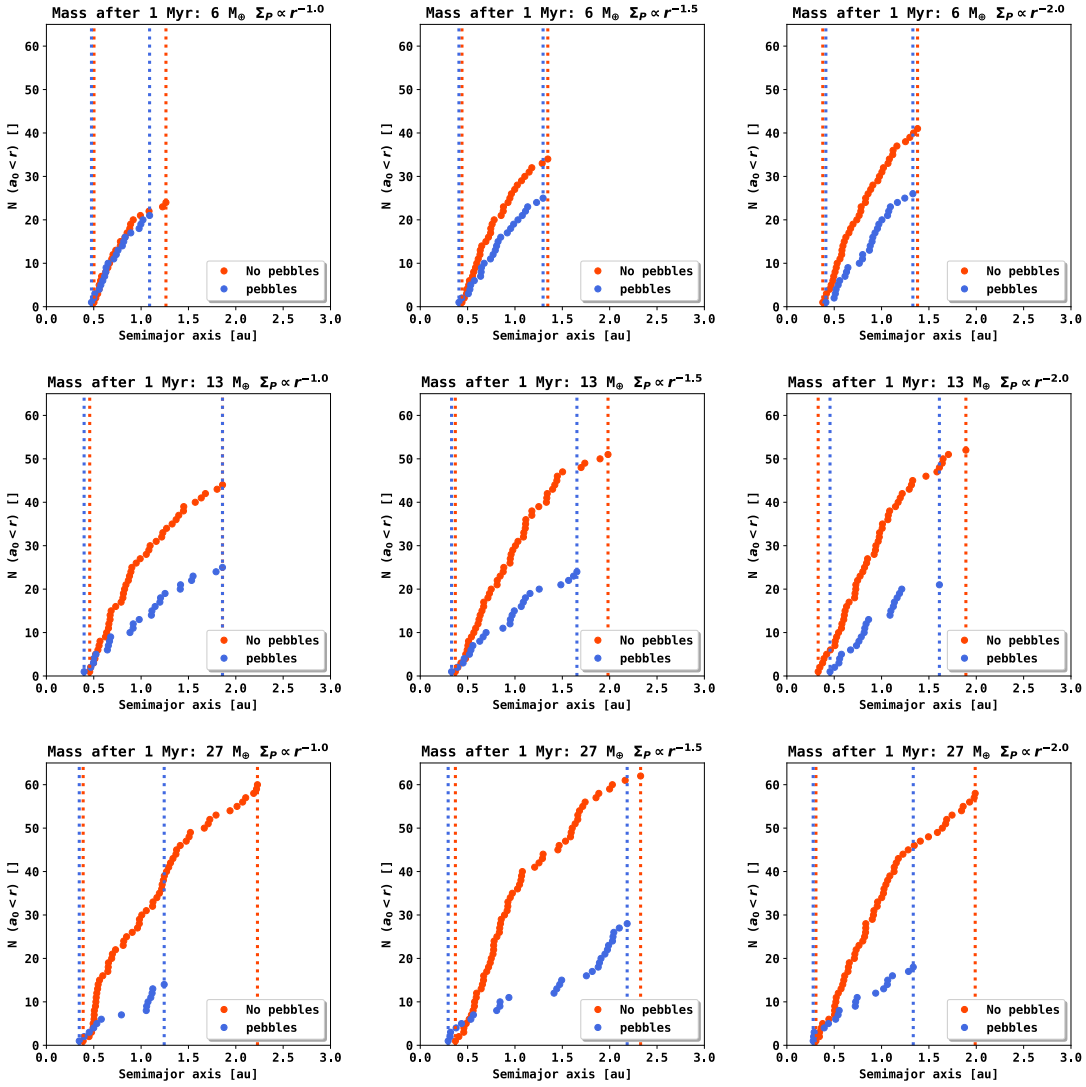


Figure 4.8: Cumulative number of initial embryos after 1 Myr for the systems from Fig. 4.2 to Fig. 4.4. The orange dots refer to the systems in which pebble accretion is disabled, and the blue dots refer to the systems in which pebble accretion is enabled.

system in which pebble accretion is neglected. For the formation of the innermost embryo, pebble accretion shows no dominant effect. Because the orbital separation is still the same in terms of the embryos Hill radii, which scales linearly with the distance to the star, we find the same logarithmic distribution of cumulative embryos, but with a lower total number than in the simulations without pebble accretion.

## 4.5 Discussion

### 4.5.1 Effect of pebble accretion

We showed that an active pebble flux has major consequences on the evolution of the planetary systems within the first 1 Myr. The accretion of pebbles leads to the formation of a lower number of substantially more massive embryos within a smaller semimajor-axis interval of embryo formation. The physical spacing between embryos increases because of their higher masses in the pebble accretion runs. Their orbital separation when expressed in Hill radii remains unaffected

and converges to $\approx 10\,R_{Hill}$ in both cases. Embryos that form at larger distances (>1.5 au) well after $T_{M_{disk}>90\%}$ remain with low masses because they fail to undergo significant pebble accretion. This behavior has been predicted in our first study, which neglected the accretion of pebbles, but suggested that the disk formation rate is a valid constraint for pebble accretion because it depends on pebble flux. We find that the outer edge of embryo formation moves slightly inwards when the accretion of pebbles is considered. No formation of embryos occurs at larger heliocentric distances within the lifetime of the pebble flux. The necessary size for significant pebble accretion is not reached at larger distances within the lifetime of our pebble flux.
The formation of the first embryo occurs earlier in the inner region when pebble accretion is considered. The embryos that form first finally have the highest masses after 1 Myr. The accretion of pebbles plays a major role once embryos have formed. Their effect on the local formation time, while noticeable, plays a subordinate role. In general, the accretion of pebbles strongly favors the formation of super-Earths in the terrestrial planet region, but it does not enhance planetary embryo formation at larger distances.

### 4.5.2 Consequences for the analytic embryo formation model

In our companion study [Voelkel et al., 2021a] we introduced an analytic model that succeeded to reproduce the results of the local formation time, the spatial distribution, and the total number of initial embryos in N-body simulations without pebble accretion. In brief, the formation of embryos in the analytic model is based on two criteria. Criterion I refers to the necessary local growth time. Criterion II determines the orbital separation to other embryos. The model uses a parameterized approach to compute the local growth timescales of planetesimals based on the local planetesimal surface density evolution. Embryos are placed if the analytic growth surpassed the mass of a planetary embryo and the orbital separation to the other already existing embryos is above an input parameter.
As discussed in Sect. 4.5.1, the effect of pebble accretion is largely found in the mass of the embryos, not in their initial formation time. Criterion I of the embryo formation model therefore still yields the correct results (even though we find slight deviations in the inner regions).
The number of embryos and their spatial distribution are determined by criterion II. Under the assumption that the already placed embryos grow by pebble accretion and their Hill radii increase, respectively, the physical spacing between the embryos thus enlarges. As a consequence, the total number of embryos decreases because the semimajor-axis interval of embryo formation does not increase (criterion I). The analytic model for embryo formation from Voelkel et al. [2021a] is therefore still valid in a framework that includes pebble accretion. Implementing the analytic model into a global model for planet formation that includes planetesimal formation and pebble accretion is the subject of future studies.

## 4.6 Summary and outlook

We studied the effect of pebble accretion and planetesimal formation on the formation of planetary embryos in the terrestrial planet region. For this purpose, we connected a one-dimensional model for pebble-flux-regulated planetesimal formation and solid evolution with the N-body code LIPAD. Thus we studied the growth and fragmentation of planetesimals with an initial size of 100 km in diameter within the first million years of a viscously evolving circumstellar disk. In this paper we compared 18 different N-body simulations in which we varied the total mass in planetesimals, the radial pebble flux, and the planetesimal surface density profile. Building on the efforts of our previous study [Voelkel et al., 2021a], we included a radial pebble flux and the accretion of pebbles during the formation of planetary embryos. The main effects on embryo formation by pebble accretion in the terrestrial planet region are summarized below

- Pebble accretion is highly favorable for the formation of super-Earths.
- When compared with planetesimal accretion alone, the total number of embryos decreases strongly when pebble accretion is considered, while the individual embryos grow significantly more massive.
- Embryos that form early in the inner regions of the disk grow rapidly by pebble accretion, whereas the outer embryos that form later fail to do so.
- The outer edge of planetary embryo formation is not increased when pebble accretion is included. Our work indicates that it is not possible to form planetary embryos at larger distances (>2 au) within the lifetime of a radial pebble flux for our assumptions.

Our findings from the first part of our study are still valid: the formation of planetary embryos first occurs in the innermost regions and then proceeds to larger distances. The number of embryos is given as the number of orbital distances within their possible formation zone. Because embryos grow more massive when pebble accretion is included, we find that the number of embryos decreases. The area in which they form, however, is not increased by pebble accretion because pebble accretion only becomes an effective growth mechanism for sizes far larger than 100 km. By the time the outer objects have grown to larger sizes by planetesimal collisions, the pebble flux has largely ceased. Even though the first embryos form earlier in the inner parts of the disk for the simulations in which pebbles are accreted, this trend does not continue to larger distances. The conundrum of distant embryo formation within the lifetime of a radial pebble flux as found in [Voelkel et al., 2021a] remains. A possible solution to this issue might be locally enhanced substructures in the planetesimal surface density profile at larger distances or the formation of planetesimals that initially form large enough for pebble accretion. Future work may include the formation of planetary embryos in distant local substructures, such as in pressure bumps and around the water-ice line [Drążkowska and Alibert, 2017].

# 5 | On the multiple generations of planetary embryos

This chapter resembles the work submitted in Voelkel et al. [submitted to A&A]. The preliminary title of the publication is "On the multiple generations of planetary embryo formation". I am the leading author of the manuscript. The document, including all figures and corresponding analysis have been conducted by me, taking into account the input of all listed co-authors. The simulations, their analysis and discussion have been conducted by me. The implementation of the additional code has been supported by Alexandre Emsenhuber with discussions. Hubert Klahr and Christoph Mordasini supported the interpretation of the results with discussions.

Global models of planet formation tend to begin with an initial set of planetary embryos for the sake simplicity. While this approach gives valuable insights on the evolution of the initial embryos, the initial distribution itself is a bold assumption. Limiting oneself to an initial distribution may neglect essential physics that precedes, or follows said initial distribution. Voelkel et al. [submitted to A&A] investigates the effect of dynamic planetary embryo formation on the formation of planetary systems. The presented framework begins with an initial disk of gas, dust and pebbles. The disk evolution, the formation of planetesimals and the formation of planetary embryos is modeled consistently. Embryos then grow by pebble, planetesimal and eventually gas accretion. Planet disk interactions and N-body dynamics with other simultaneously growing embryos is included in the framework. Voelkel et al. [submitted to A&A] shows that the formation of planets can occur in multiple consecutive phases. Earlier generations grow massive by pebble accretion but are subject to fast type I migration and thus accretion to the star. The later generations of embryos that form grow to much smaller masses by planetesimal accretion, as the amount of pebbles in the disk has vanished. The formation history of planetary systems may be far more complex than an initial distribution of embryos could reflect. The dynamic formation of planetary embryos needs to be considered in global models of planet formation to allow for a complete picture of the systems evolution.

## 5.1 Introduction

### 5.1.1 Motivation

Latest observational constraints on grain growth in young protostellar disks via thermal dust emission [Harsono et al., 2018] imply that the formation of planets may begin in the earliest embedded phases in the life of young stars. The idea that previous generations of gas giant planets may have been accreted by the host star as a result of inward migration has already been introduced by [Lin and Papaloizou, 1986]. This hypothesis states that the final system of planets that can be observed around a star may only reflect a small subset of the planets that initially formed. The possibility of a previous protogiant planet in the solar system is mentioned as well, however not the existence of previous super Earths or other terrestrial mass planets. The number of planets that form and survive during the lifetime of a circumstellar disk is unknown. Only the minimum number of survived planets per system is a lower constraint, as it is given as the number of exoplanet detections. While this number often lacks completeness due to the low detectability of low mass planets in certain systems, it completely lacks the information on the previous history of the system. Already discussed is also that planet bearing stars might be polluted and show higher metalicities [Gonzalez, 1997, Murray and Chaboyer, 2002]. It is thus possible that the currently observed population of planets merely reflects a small fraction of the planets that initially formed. While the research conducted on how individual planets grow and evolve, based on an initially placed embryo continues to flourish, the initial formation of the used embryo is typically an initial assumption. As recently shown in Schlecker et al. [2021], this initial embryo location is the initial condition with the highest predictive power on the the outcome of a planet. The question on how many embryos form and how many of those survive however cannot be neglected if one attempts to study the formation of planets in a consistent fashion. Essential to this is a model that predicts the number of planetary embryos from the previously evolved system and tracks their combined evolution until the dispersal of the circumstellar disk. This study will present a self consistent global model of planet formation and disk evolution that allows for such a study. The presented model enables us to investigate the number of planets that form and evolve within a circumstellar disk over its entire lifetime. We find that the formation history of planetary systems is far more complex than an initial distribution of planetary embryos could reflect.

### 5.1.2 Global models of planet formation

To clarify the terminology we wish to give a brief overview on current models of planet formation, focusing on their differences, similarities and limitations. One similarity that all planet formation models bring with themselves is that the approach aims to combine multiple physical processes in a common framework. This results from the complexity of the problem, as the formation of planets cannot be described in an isolated manner. Not only ranges the process from a dust grain to a gas giant over numerous orders of magnitude in mass, it also needs to be embedded in the global evolution of a circumstellar disk. In addition to the evolution of the disk itself , interactions with other simultaneously growing planets can influence planet formation. Planet-planet interaction, as well as planet-disk interactions can decide the fate of a planet during its formation and/or later evolutionary stages.

Current global models of planet formation focus either on a specific time in planet formation, a specific accretion mechanism (pebble accretion or planetesimal accretion), or a specific location in the disk. Models that have been introduced by Ida and Lin [2004], Alibert et al. [2005], Mordasini et al. [2012] and Emsenhuber et al. [2020a] focus on the accretion of planetesimals on initially placed planetary cores. Even though the size of these planetesimals is its own ongoing field of research, here we refer to planetesimals as objects in the size range from 600 m in diameter [Emsenhuber et al., 2020a] to 100 km in diameter Voelkel et al. [2020]. Their size plays a major role in the accretion mechanism, as more massive objects are less likely to be accreted and the

stirring by a protoplanet increases their eccentricities and inclinations. Even at sizes of several hundred meters to km however, the gas disk can significantly damp the planetesimals dynamical states and make them a highly efficient mechanism for protoplanetary growth [Emsenhuber et al., 2020a]. The accretion of smaller particles for which gas drag can cause the object to even spiral onto the accreted protoplanet is called pebble accretion [Ormel and Klahr, 2010]. Planet formation models that are built around the accretion of pebbles onto initially placed planetary embryos have been introduced in [Bitsch et al., 2015, Ndugu et al., 2017, Brügger et al., 2020]. The aforementioned planet formation models either focus on the accretion of planetesimals or the accretion of pebbles. Hybrid accretion models have recently been introduced by e.g. Alibert et al. [2018] or Guilera et al. [2020]. A major drawback of these models however, as well as models that study pebble or planetesimal accretion in an isolated fashion is the initial placement of planetary embryos. This initial assumptions skips the earliest phase of the circumstellar disk evolution in which the planetesimals form that later accumulate to planetary embryos. As results from Bitsch et al. [2015] show, the location and the time when an embryo is placed plays a dominant role in the subsequent evolution. Recent work presented in Voelkel et al. [2021a] and Voelkel et al. [2021b] studies the formation of planetary embryos from planetesimals that form from an evolving pebble disk. They find that more distant embryos (>2-3 au) form after the pebble flux has largely vanished. While the accretion of pebbles on planetesimals and planetary embryos is included in [Voelkel et al., 2021b], only the innermost planetary embryos can benefit from pebble accretion, as the outer embryos fail to form during the lifetime of the pebble flux.
Recent work by Guilera et al. [2020] studied the formation of giant planets around pressure bumps. They combined a global disk evolution model containing gas, dust and pebble dynamics with the formation of planetesimals due to streaming instability behind the pressure bumps. The embryo was placed once the mass in planetesimals is equivalent of the mass of a planetary embryo. They also used a hybrid accretion model that combines pebble and planetesimal accretion, as well as a global disk evolution model. While in their extensive model they did not use the embryo as an initial assumption, the embryo was placed in a specific location, which was subject to an initial assumption as well. The formation time of the embryo in their work is given by the time it takes until a lunar mass of 100 km planetesimals has formed around their pressure bump. While this is a first constraint on the initial placement time, it does not account for planetesimal growth by planetesimal collisions, which can take significantly longer than it takes to form the 100 km planetesimals themselves. Additionally, their placed embryo was the only embryo in the system, which neglects planet planet interactions. While this model attempts to model all stages of the single planet in the system (beginning from dust and pebbles to a final gas giant) using a global disk evolution model, the planet formation studied remains local, as the location and the number of planets in the system remains fixed.
A planet formation model based on planetesimal accretion that forms planetesimals consistent with the radial evolution of dust and pebbles is also presented in Voelkel et al. [2020]. This approach connected a two population model for dust and pebble dynamics [Birnstiel et al., 2012] with the pebble flux regulated model for planetesimal formation from Lenz et al. [2019]. The evolution of dust, pebbles and planetesimals was merged with the planet formation model from Emsenhuber et al. [2020a] to study the impact of different planetesimal distributions on planet formation. While planetesimals formed consistently with the disks evolution, pebble accretion was neglected and planetary embryos remained an initial assumption. The formation model of Emsenhuber et al. [2020a] however is capable of also tracking the growth and N-body dynamics/interactions of up to 100 planetary embryos. A model that forms planetary embryos based on the local planetesimal surface density evolution is presented and discussed in Voelkel et al. [2021a] and Voelkel et al. [2021b]. To bridge the gap between disk evolution and the accretion of pebbles and planetesimals onto planetary embryos, we decided to implement the

embryo formation model from Voelkel et al. [2021a] into the planet formation model described in [Voelkel et al., 2020] and model the accretion of both pebbles and planetesimals.
We wish to highlight here that the planet formation model presented in this work combines the currently known accretion mechanisms (pebble accretion, planetesimal accretion, gas accretion) during the entire lifetime of the circumstellar disk, that includes the formation of planetary embryos, as well as late stage gas accretion. The number, as well as the formation time and location of planetary embryos are no longer an assumption, but the result of the analytic embryo formation model from Voelkel et al. [2021a]. This stands in contrast to the models of Emsenhuber et al. [2020b] where a fixed number of embryos (1,20,50,100) is inserted at t=0 throughout the disk uniformly in log). In the following we will discuss the individual stages of the planet formation model used in this study. A detailed description of the different stages of planet formation that are covered in the model that is presented in this paper are described in Sect. 5.2.

## 5.2 Our global model of planet formation

In the following we will discuss the different stages of planet formation that are covered in our global formation model. As a reminder, the computation of the disk evolution, the accretion of material, the formation of embryos and planetary migration are computed simultaneously. The existence of a planet changes the pebble flux due to pebble accretion. The formation of planetesimals (as it is regulated by the pebble flux) changes accordingly and thus the formation of other planetary embryos is affected as well.

### 5.2.1 Disk evolution model

A detailed description on the implementation of the gas and solid disk evolution model used in our planet formation framework can be found in Voelkel et al. [2020], here we will discuss the underlying fundamentals. We use a one dimensional disk evolution model that tracks the evolution of gas, dust, pebbles and planetesimals. The viscously evolving gas disk [Lüst, 1952, Lynden-Bell and Pringle, 1974] uses an $\alpha$-prescription for turbulence [Shakura and Sunyaev, 1973] and includes internal and external photoevaporation [Picogna et al., 2019] . Coupled to the evolution of the gas disk is the two population solid evolution by Birnstiel et al. [2012]. This model solves an advection diffusion equation of a combined solid density. Depending on whether the particles at a given radial location can be considered in the drift or in the fragmentation limit of growth, a fixed mass relation is applied. This relation splits the solid density into two populations. Depending on the individual Stokes number of the particles, these populations can be considered as dust (St$<<1$) or pebbles (St$\geq 1$) respectively.
The formation of planetesimals in our framework is regulated by the local radial pebble flux. The model we use has been introduced by Lenz et al. [2019] and it does not specify which physical mechanism (e.g. Kelvin Helmholtz instability or streaming instability) drives the formation of planetesimals. Its underlying assumption is that planetesimals form in trapping zones that can appear at any location of the disk. These trapping zones appear for a given lifetime and with a radial separation of $d(r)$. In Lenz et al. [2019] planetesimals form proportional to the radial pebble flux and the formation rate of planetesimals is given as

$$\dot{\Sigma}_p(r) = \frac{\varepsilon}{d(r)} \frac{\dot{M}_{peb}(r)}{2\pi r} \tag{5.1}$$

with $\Sigma_P(r)$ as the local planetesimal surface density at a heliocentric distance $r$ and $\dot{M}_{peb}(r)$ as the local radial pebble flux. $\varepsilon$ describes the amount of the pebble flux that is transformed into planetesimals over the trap distance $d(r)$. The distance of pebble traps is given as 5 gas pressure scale heights in our approach. Planetesimals are assumed to be in the oligarchic regime [Ida

and Makino, 1993, Thommes et al., 2003, Chambers, 2006]. They are described in a fluid type fashion using a surface density $\Sigma_P$ with eccentricity and inclination. For their dynamical state we use the approach from Fortier et al. [2013]. Planetesimals are stirred by the embryos, as well as by each other and damped by the gas disk. This stirring by the protoplanet follows Guilera et al. [2010] while the planetesimal planetesimal stirring follows Ohtsuki et al. [2002]. The damping of planetesimals follow Inaba et al. [2001] in the quadratic regime, Adachi et al. [1976] and Rafikov [2004] in the Stokes and Epstein regime. The size at which planetesimals form is given as 100 km in diameter. While the size of planetesimals is an ongoing field of research, we choose a size of 100 km in diameter, as observational constraints from the solar systems infer [Bottke Jr et al., 2005, Walsh et al., 2017, Delbo' et al., 2017] and what numerical simulations suggest [Schäfer et al., 2017, Klahr and Schreiber, 2020]. Other work suggests smaller sizes, in the range of several 100 m to kilometres in diameter [Arimatsu et al., 2019, Schlichting et al., 2013, Weidenschilling, 2011, Zheng et al., 2017].

### 5.2.2 Planetesimals to planetary embryos

Planetesimals are described as a one dimensional surface density ($\Sigma_p$), analogous to gas, dust and pebbles. While we do not track the N-body evolution of this large number of planetesimals, we track the dynamical N-body evolution of up to 100 planetary embryos. These embryos are introduced over time into the simulation, consistent with the evolution of the planetesimal surface density and its dynamical state. The embryo formation model that we use has been introduced by Voelkel et al. [2021a] and will be briefly described in the following.
Once planetesimals begin to form, we track their growth by integrating the local mass growth rate of a planetesimal in the oligarchic regime within a swarm of planetesimals [Lissauer, 1993]

$$\frac{dM_p(r,t)}{dt} = \frac{\sqrt{3}}{2}\Sigma_P(r,t)\cdot\Omega(r)\pi {r_b}^2\left(1+\frac{v_{\rm esc}^2(M_p,r_b)}{v_\infty^2(r,t)}\right) \tag{5.2}$$

with $M_p(r,t)$ as the mass of the largest object at a heliocentric distance $r$ at a time $t$. $\Sigma_P(r,t)$ is given as the local planetesimal surface density, $\Omega(r)$ as the orbital Kepler frequency, $r_b$ the radius of the largest object, $v_{\rm esc}$ as the escape velocity of $M_p$ at its surface and $v_\infty$ as the dispersion velocity of planetesimals, which we give as $v_\infty = e(r)\cdot\Omega(r)$ with $e(r)$ as the planetesimals eccentricity. $M_p$ is initially set to the mass of a 100 km planetesimal with a solid density of $\rho_s = 1.0\,\mathrm{g/cm^3}$

$$M_p(r,t_0) = M_{100\,km} \tag{5.3}$$

Once $M_p$ locally surpasses the mass of a planetary embryo, which in our case is given as a lunar mass ($M_{emb} = 0.0123\mathrm{M}_\oplus$), a new N-body object is introduced into the simulation and $M_p$ is reset to $M_p(r,t) = M_{100\,km}$ within 15 Hill radii of the placed embryo. An additional constraint from Voelkel et al. [2021a] is that an embryo cannot form within $15\mathrm{R}_{Hill}$ of any other embryo in the system. The orbital separation of planetary embryos in the oligarchic growth regime has already been found and confirmed in Kokubo and Ida [1998], Kobayashi et al. [2011], Walsh and Levison [2019] and serves as a good constraint on the number of planetary embryos within a given spatial distribution. While the model has been derived without including the effect of pebble accretion, the effect of pebble accretion on embryo formation has been studied in Voelkel et al. [2021b] in a similar framework, including pebble accretion. It is shown that the accretion of pebbles largely affects the mass growth rate of planetary embryos with masses >0.01 $\mathrm{M}_\oplus$ and thus their physical spacing to each other. When expressed in the embryos Hill radii however, the orbital separations remain similar to what has been found in Voelkel et al. [2021a], Kokubo and Ida [1998], Kobayashi et al. [2011], Walsh and Levison [2019]. Pebble accretion only begins to be an

effective accretion mechanism at masses much larger than that of a 100km planetesimal. The initial planetesimal growth from 100 km to a lunar mass object therefore remains dominated by planetesimal collisions. The initial formation time of a lunar mass object is therefore only weakly influenced by pebble accretion [Voelkel et al., 2021b]. Its subsequent growth however begins to be dominated by pebble accretion. Including the embryo formation model from Voelkel et al. [2021a] into our planet formation framework therefore ensures that the total number of embryos in the system, their formation time and their spatial distribution is consistent with the evolution of the planetesimal surface density and its dynamical state.

### 5.2.3 Embryos and beyond

Once a planetary embryo has formed according to Sect. 5.2.2 it is subject to several simultaneously occurring processes. Its mass growth is given by the accretion of pebbles, planetesimals and gas [Pollack et al., 1996]. To avoid confusion, there is no physical difference in our model between a planetary embryo and a planet. The terminology of an embryo only refers to the object at its initial lunar mass of $0.0123\,M_{\oplus}$. It is then treated as a single N-body object and will be referred to as planet in the following. Every planet that formed in our model was initially introduced to the systems as a lunar mass embryo based on the model described in Sec. 5.2.2. During its growth, the planet is subject to planetary migration and the dynamical interaction with other planets in the system. Planets can be scattered out of the systems, as well as merge with other simultaneously forming planets.
As mentioned, planetesimals are considered to be in the oligarchic regime. They are accreted by embryos and evolve their eccentricity and inclination by self stirring, by the interaction with the embryo and by the damping of the gas disk (see Sec. 5.2.1). Next to the accretion of planetesimals, we included the accretion of pebbles from the disk, based on the prescription of Ormel [2017]. The accretion of pebbles is considered until the planet reaches its local pebble isolation mass [Lambrechts et al., 2014]. Once planets are large enough to accrete gas from their surrounding, the 1D structure of the gas envelope is retrieved by solving the internal structure equations [Bodenheimer and Pollack, 1986]. The accretion of solids affects the accretion of gas during the initial phase via accretional heating [Pollack et al., 1996, Lee and Chiang, 2015, Alibert et al., 2018]. As seen in Voelkel et al. [2020], this effect can suppress runaway gas accretion for high planetesimal surface densities, as runaway gas accretion can only occur if the accretion rate of gas surpasses the accretion rate of planetesimals [Pollack et al., 1996] .
As planets that are embedded in the gas disk grow, they can undergo type I and type II migration. Type I migration is treated as described in Coleman and Nelson [2014], type II migration as in Dittkrist et al. [2014] and to distinguish between them we use the prescription by Crida et al. [2006] for gap opening. As discussed in Coleman and Nelson [2014], the formation of strong corotation torques can also lead to type I outward migration within our framework.

The entire framework is described in great detail in Emsenhuber et al. [2020a], whereas here we only give a brief overview over the included physics. Strictly speaking, Emsenhuber et al. [2020a] refers to a model for planet population synthesis, that contains a planet formation model at its heart. In this sense Emsenhuber et al. [2020a] is an updated version of Mordasini [2018], in which a model for planet formation [Alibert et al., 2005, 2013] and planet evolution [Mordasini et al., 2012] is combined to carry out a planet population synthesis approach, as in Mordasini et al. [2009]. As we will not carry out a population synthesis in this study, but investigate a single system, we will not make use of the population synthesis capabilities of our used framework. However we wish to mention here, that the entire framework presented in this paper is capable of conducting the same population synthesis studies as presented in e.g. Emsenhuber et al. [2020b] or Schlecker et al. [2021], as our additional physical models (pebble and dust dynamics, pebble accretion, planetesimal formation and planetary embryo formation) do not require high

computational costs.

## 5.3 Numerical setup and initial conditions

We focus on a set of disk parameters that has been introduced in Lenz et al. [2020] (see Table 5.1). Their attempt was to constrain the parameters of the solar nebula by conducting a large parameter study. The parameters found resulted in what Lenz et al. [2020] refer to as the "most appealing solar nebula" (MASN). The distribution of planetesimals that resulted from the aforementioned parameters did best in constraining the solar nebula, based on the distribution of planets and asteroids in the solar system today.

| Symbol | Value | Meaning |
|---|---|---|
| $M_{disk}$ | $0.1\,M_\odot$ | Total mass of the gas disk |
| $a_{in}$ | 0.03 au | Inner disk radius |
| $a_{out}$ | 20 au | Exponential cutoff radius |
| $\gamma$ | 1.0 | initial $\Sigma_g$ profile ($\Sigma_g \propto r^{-\gamma}$) |
| $d_g$ | $1.34 \times 10^{-2}$ | Dust-to-gas ratio |
| $\alpha$ | $3.0 \times 10^{-4}$ | Turbulence parameter |
| $L_x$ | $3.0 \times 10^{29}$ ergs/s | X-ray luminosity |
| $v_{frag}$ | 200 cm/s | Fragmentation velocity |
| $\varepsilon$ | 0.05 | $\Sigma_P$ formation efficiency |
| $d$ | 5 h | $\Sigma_P$ trap distance |
| $\tau_f$ | 1600 $t_{orbit}$ | $\Sigma_P$ trap lifetime |
| $\rho_s$ | 1.0 g/cm$^3$ | $\Sigma_P$ solid density |

Table 5.1: Disk and planetesimal formation parameters used in our study. The set of parameters stems from the most appealing solar nebula, as described in Lenz et al. [2020]. The planetesimal trap distance $d$ is set to 5 gas pressure scale heights.

## 5.4 Simulation results

We investigate the effect of dynamic embryo formation on the formation of a planetary system. While this extensive model allows for a multitude of effects to investigate in greater detail, our study focuses on the composition, mass and semimajor axis evolution of the resulting planetary system (Sec. 5.4.1), the number of active and formed planets over time (Sec. 5.4.2), the evolution of the disk surface densities and masses (Sec. 5.4.3), the evolution of the solid mass components (Sec. 5.4.4) and the final system of planets (Sec. 5.4.5).

### 5.4.1 Planetary system evolution

Fig. 5.1 shows the mass, pebble mass fraction and semi-major axis over time of all planets during the lifetime of the gas disk. Fig. 5.2 shows the mass and semimajor axis distribution of the system, including their growth tracks and the initial formation time of the corresponding planetary embryo. Fig. 5.3 shows the evolution of the corresponding planet masses. In Fig. 5.1, within the first 350 kyr, we find that several embryos form within 1 au and grow dominantely by pebble accretion, as given by the color of the dots. As it can be seen in Fig. 5.3, the most massive planet reaches up to 20 $M_\oplus$. These early formed planets experience strong type I migration and eventually end at the inner edge of the gas disk. As more planets migrate to the inner edge, the innermost planets are accreted by the host star, as shown by the triangular markers in Fig. 5.2. The same evolution is underwent by the next set of planets that forms after 350 kyr. Within the first 1 Myr, we see that several new embryos form in the terrestrial planet zone. Initially dominated by pebble accretion, those super Earth mass planets first experience outward migration due to positive corotation torques [Coleman and Nelson, 2014], followed by inward migration before halting at the inner edge of the gas disk again. Those planets form within 1.2 au but temporarily reach a semimajor axis of 2-3 au. Within the first 3.5 Myr, we see that one planet does not migrate to the inner edge of the disk within the first 1 Myr, but over a significantly longer timescale. As it can be seen by the pebble mass fraction evolution of the outermost planet at 1 Myr, it was initially dominated by pebble accretion. Over the course of the next 2.5 Myr, its pebble mass fraction strongly decreases due to ongoing planetesimal accretion. During that phase, a set of sub Earth mass planets has formed in the area around 1 au. After the outer super Earth goes into another phase of type I inward migration, it pushes the sub Earth mass planets to the inner edge of the gas disk as well, eventually clearing the terrestrial planet zone of planets. After the last super Earth has migrated to the inner edge of the gas disk at 3.5 Myr, a large set of sub Earth mass planets emerges over the next 13 Myr. Those planets stay at smaller masses than their super Earth predecessors for the lifetime of the gas disk and consequentially experience significantly slower type I migration. As it can be seen in Fig. 5.3, the most massive planet of the remaining system has formed at 350 kyr as part of the second generation of embryo formation and no planet from the first generation of embryo formation survived until the dispersal of the gas disk.

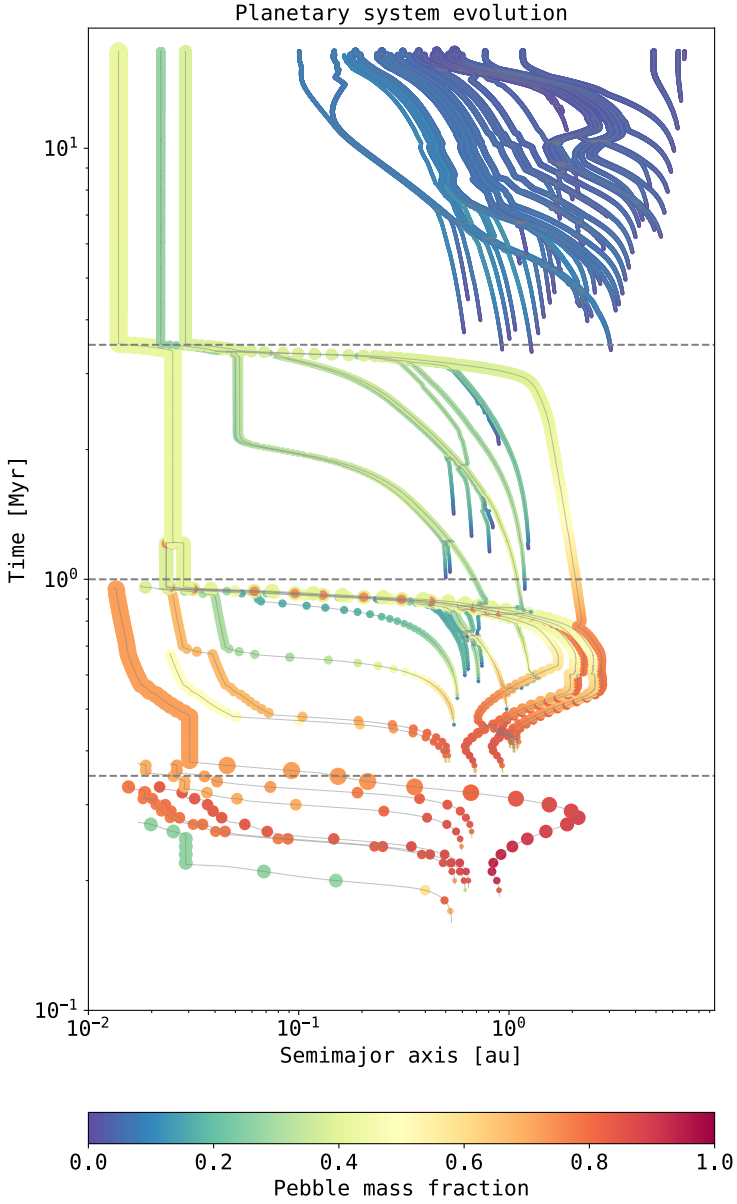


Figure 5.1: Semimajor axis over time evolution for the planetary system. The evolution of a planet is linked via the grey line and the size of the dots indicate the mass of the planets every 10 ky. The color of the planets show their pebble mass fraction $M_{peb}/M_P$. The horizontal lines are drawn at 350 kyr, 1 Myr and 3.5 Myr and show the moments at which most currently active planets are accreted by the host star or were subject to mergers. Thus we find four distinct generations of planets.

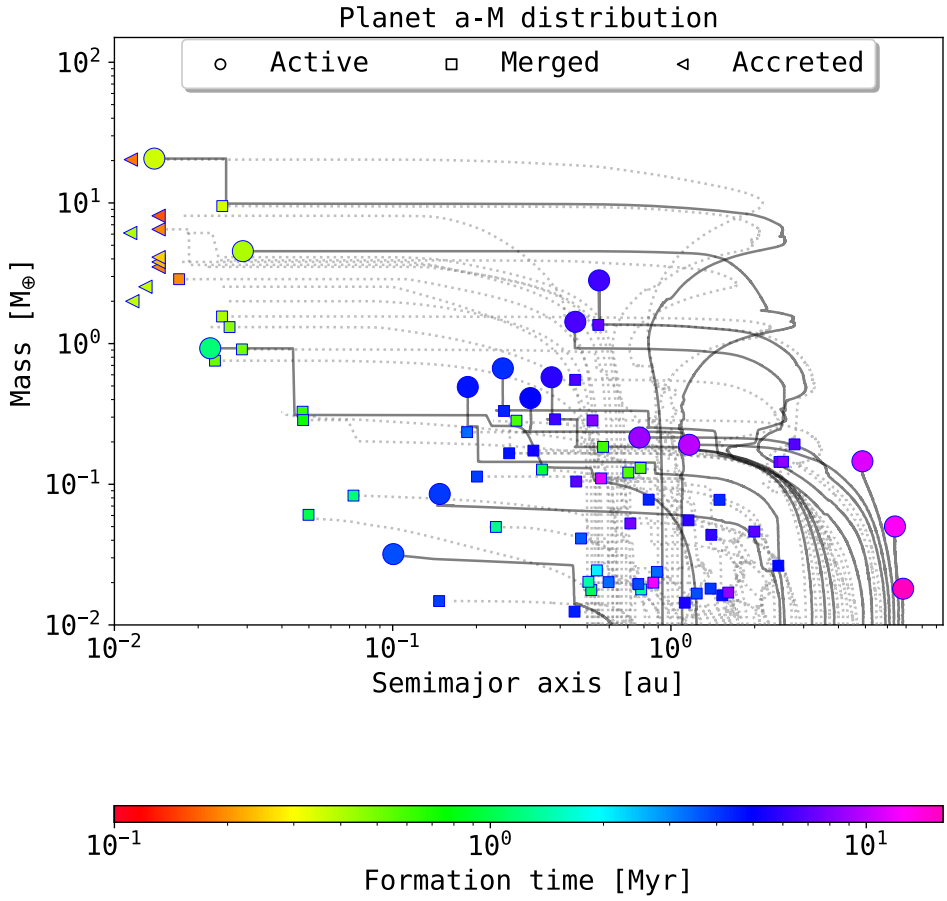


Figure 5.2: Mass and semimajor axis distribution of the entire planetary system until the dispersal of the gas disk. The large circle markers indicate planets that remain active until the end of the simulation. Planets that were accreted by the host star are shown as triangles and planets that merged via collisions with other planets are indicated as squares. The track of the planets is shown as the solid grey line for active planets and dotted grey lines for accreted or merged planets. The color of the final marker indicates the initial formation time of the corresponding planetary embryo.

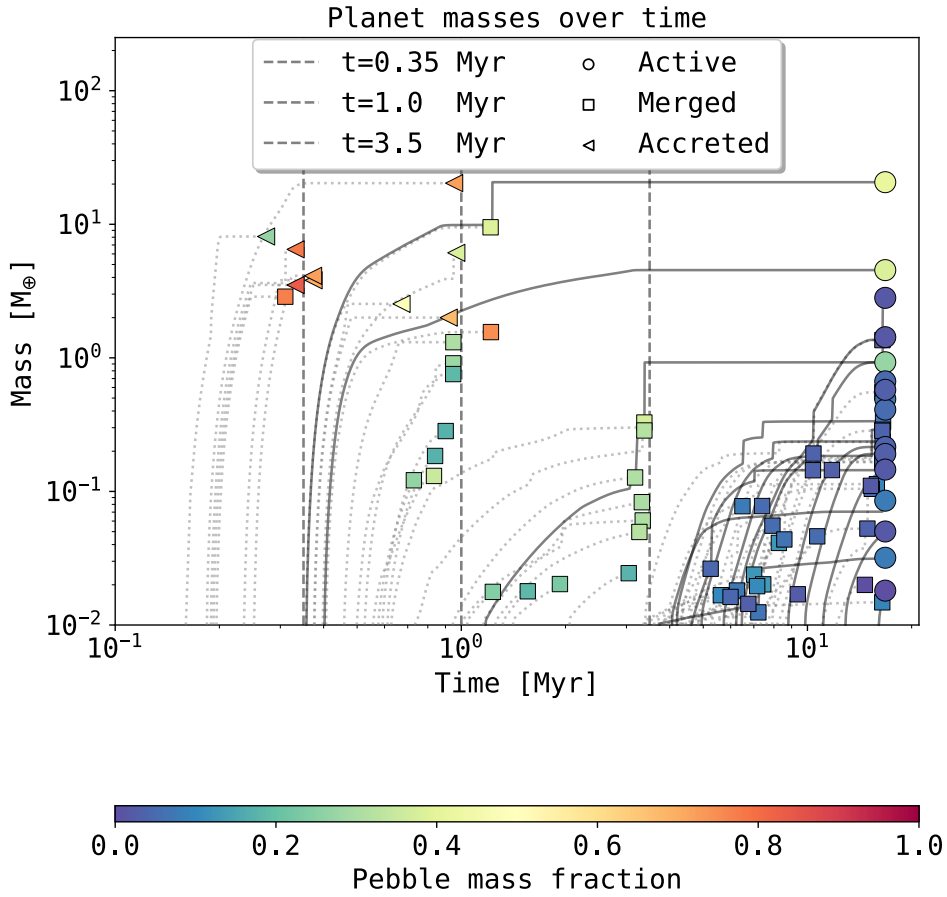


Figure 5.3: Planet mass over time. The vertical lines are drawn at 350 kyr, 1 Myr and 3.5 Myr and show the moments at which most currently active planets are accreted by the host star or were subject to mergers. The vertical steps are caused by giant impacts that result in planet mergers. The large circle markers indicate planets that remain active until the end of the simulation. Planets that were accreted by the host star are shown as triangles and planets that merged via collisions with other planets are indicated as squares. The track of the planets is shown as the solid grey line for active planets and dotted grey lines for accreted or merged planets. The color of the final marker indicates the pebble mass fraction of the corresponding planet.

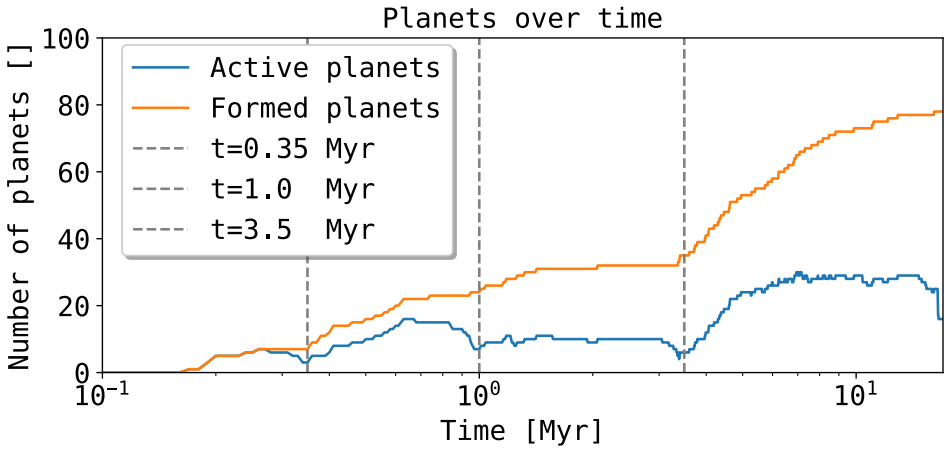


Figure 5.4: Number of planets over time. The blue line shows the number of currently active planets in the system, while the orange line shows the total number of planets that have formed. The vertical lines are drawn at 350 kyr, 1 Myr and 3.5 Myr and show the moments at which most currently active planets are accreted by the host star or were subject to mergers.

### 5.4.2 Number of planets over time

In Fig. 5.4 we show the total number of active planets and the cumulative number of planets that formed during the lifetime of the gas disk. As the number of formed planets continuously increases, the number of active planets shows three significant moments of decrease. The first decrease can be found at 350 ky, the second at 1 Myr and the third at 3.5 Myr. The local minima of active planets in the disk are indicated by the vertical lines. The total number of planets that formed during the lifetime of the disk is given as 78, whereas the total number of active planets after the lifetime of the disk is given as 16. The largest number of planets formed in the last generation after 3.5 Myr. While the number of formed planets keeps increasing after 5 Myrs, the number of active planets after that time remains almost constant at $\sim$30 due to giant impacts and mergers. In the latest stages after 16Myr, the number of active planets drops to 16, as planets continue to collide and merge, but no more embryos are forming.

### 5.4.3 Disk evolution

Fig. 5.5 and Fig. 5.6 show the surface densities and planetesimal eccentricity of the circumstellar disk at 0.35 Myr, 1 Myr, 3.5 Myr and 16.8 Myr. The semimajor axes of the active planets in the system are displayed as dashed vertical lines. Fig. 5.5 and Fig. 5.6 also show the disk component masses at the various snapshots. The very long gas disk lifetime of this setup is due to the large initial gas disk mass ($0.1\,M_\odot$) in combination with the small $\alpha = 3 \times 10^{-4}$. As discussed in Lenz et al. [2019], a higher photoevaporation rate would not greatly influence the formation of planetesimals, as most planetesimals form within the first Myr of the systems evolution. In order to stay consistent with Lenz et al. [2019] we thus chose to use the same parameters. A higher photoevaporation rate to induce a shorter disk lifetime would however not affect the initial Myrs of the systems evolution. Within the first 1 Myr, the mass of the pebble and dust disk drops from an initial value of 450.93 $M_\oplus$ to only 5.92 $M_\oplus$. The mass of the planetesimal disk after 1 Myr is given as 73.61 $M_\oplus$. The largest fraction of the dust and pebble disk is accreted by the host star due to continuous inward drift. The inner region of the circumstellar disk is largely depleted of planetesimals when the gas disk has vanished. After 16.8 Myr, we still find 67.59 $M_\oplus$ of planetesimals in the entire disk, most of which between 5 au and 10 au. As it can be seen in any snapshot in which planets are present, the eccentricity of planetesimals greatly increases at the location of active planets. Once the planets have migrated however, the planetesimals eccentricity is again reduced via damping by the gas disk.

Fig. 5.7 shows the fraction of the planetesimal disk and the combined dust and pebble disk mass over the gas disk mass within 1 au, 2.5 au and 5 au during the lifetime of the gas disk. As known from Lenz et al. [2019], the planetesimal surface density profile is steeper than the surface density profile of the gas disk, due to the influx of pebbles from distant regions of the disk. As a consequence we find that in the early phase of the evolution, the disk mass fraction of planetesimal mass over gas mass within a smaller region shows the highest value. After 200 ky we find that the fraction of planetesimal mass over gas mass within 1 au is >1.5%, whereas the fraction of planetesimal mass over gas mass within 5 au only reaches 0.5% at that time. If it was not for the formation of planetary embryos, we would expect this trend to continue during the lifetime of the disk. After the formation of planetary embryos however, the planetesimal disk mass within 1 au strongly varies as a consequence of planetesimal accretion and continuous planetesimal formation. As can be seen in Fig. 5.5 and Fig. 5.6, the planetesimal disk within 1 au experiences the most depletion due to planets, as most embryos within 1 Myr form within 1.5 au. The sharp increase in the mass fraction at later times is due to the depletion of the gas disk as a consequence of photoevaporation and accretion to the host star. The mass of the combined dust and pebble disk vastly exceeds the mass of the planetesimal disk for the first 350 kyr within 5 au, 2.5 au and 1 au. As the planets that form within the first 350kyr also formed within 2.5 au, their mass growth is dominated by pebble accretion. Between 350 kyr and 1 Myr, the planetesimal disk mass exceeds the combined dust and pebble disk mass for every shown radius. As the total solid disk mass begins to be dominated by planetesimals, the accretion of pebbles is no longer the dominant mechanism of growth. Planets that form in the second generation begin to reduce their pebble mass fraction, due to the depletion of the pebble reservoir.

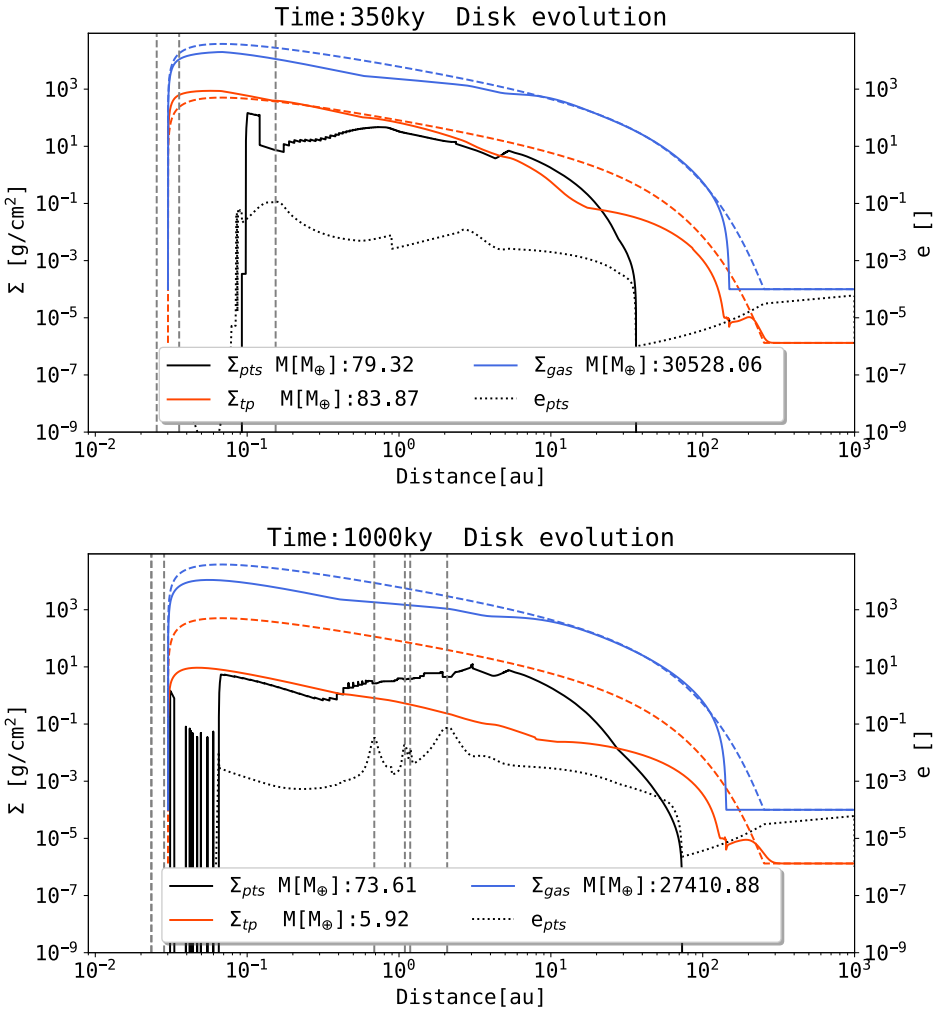


Figure 5.5: Surface density and planetesimal eccentricity evolution of the circumstellar disk. We show the gas surface density (blue), planetesimal surface density (black) and the combined dust and pebble surface density (orange) at t = 350 ky and t=1 Myr. The initial corresponding density is shown as the dashed line. The initial mass of the gas disk is given as $M(\Sigma_g) = 34102.64\,M_\oplus$, the initial solid mass in dust and pebbles is given as $M(\Sigma_{tp}) = 450.93\,M_\oplus$ and the initial planetesimal disk mass is given as $M(\Sigma_{tp}) = 0\,M_\oplus$. The location of an active planet is indicated via dashed vertical lines. The planetesimal eccentricity is given as the dotted line respectively.

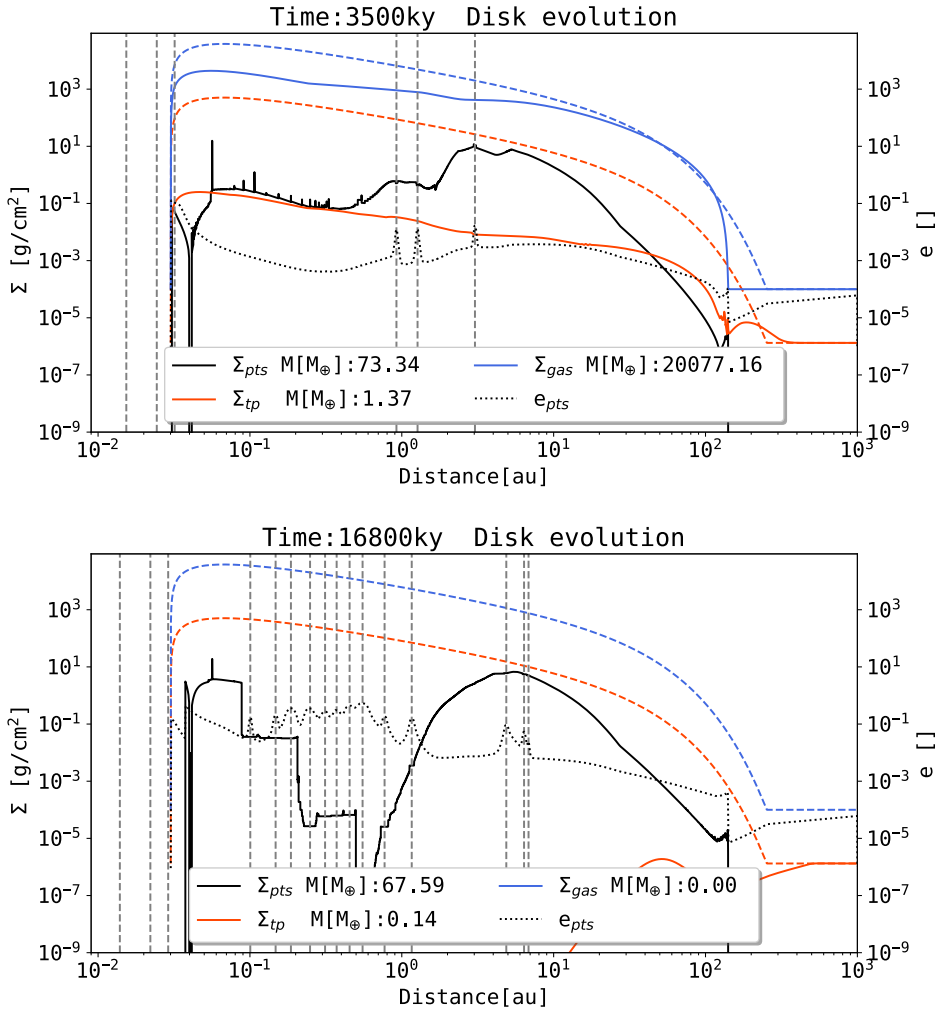


Figure 5.6: Surface density and planetesimal eccentricity evolution of the circumstellar disk. We show the gas surface density (blue), planetesimal surface density (black) and the combined dust and pebble surface density (orange) at t=3.5 Myr and t=16.8 Myr. The initial corresponding density is shown as the dashed line. The initial mass of the gas disk is given as $\mathrm{M}(\Sigma_g) = 34102.64\,\mathrm{M}_\oplus$, the initial solid mass in dust and pebbles is given as $\mathrm{M}(\Sigma_{tp}) = 450.93\,\mathrm{M}_\oplus$ and the initial planetesimal disk mass is given as $\mathrm{M}(\Sigma_{tp}) = 0\,\mathrm{M}_\oplus$. The location of an active planet is indicated via dashed vertical lines. The planetesimal eccentricity is given as the dotted line respectively.

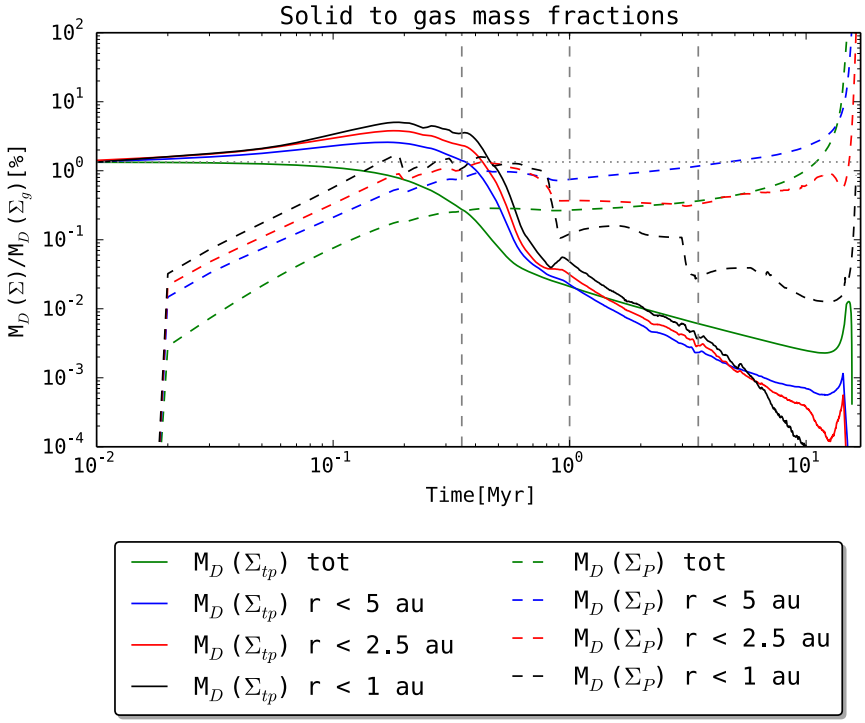


Figure 5.7: Fraction of the planetesimal disk mass ($M_D(\Sigma_P)$) and combined dust and pebble disk mass ($M_D(\Sigma_{tp})$) over the gas disk mass ($M_D(\Sigma_g)$) within 1 au, 2.5 au and 5 au over time in percent. The grey dotted line indicates the global initial dust to gas ratio $d_g$=1.34%. The dashed vertical lines are drawn at 350 kyr, 1 Myr and 3.5 Myr and show the moments at which most currently active planets are accreted by the host star or were subject to mergers.

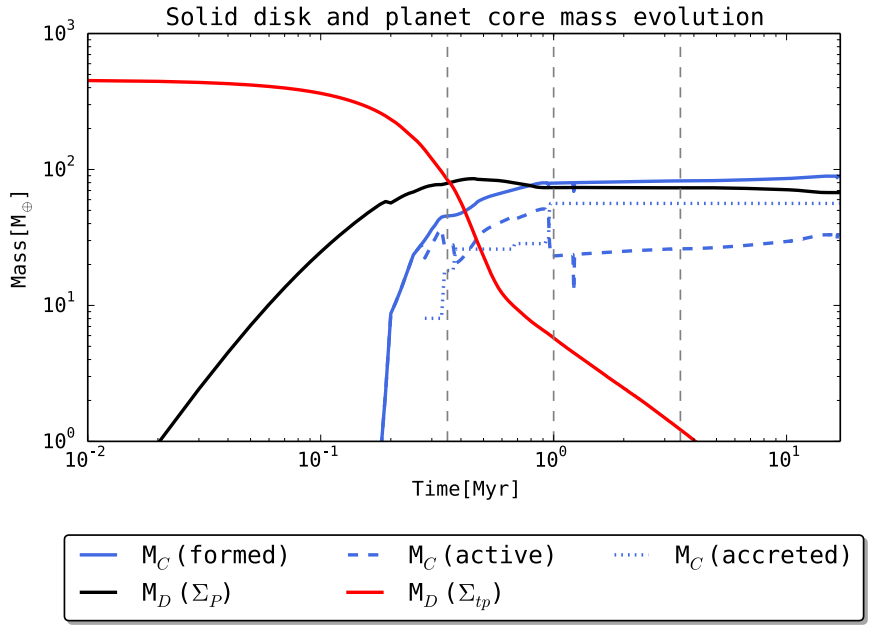


Figure 5.8: Solid mass evolution during the lifetime of the gas disk. We show the total pebble and dust disk mass ($M_D(\Sigma_{tp})$), the total planetesimal disk mass ($M_D(\Sigma_P)$), the mass in active planetary cores ($M_C$(active)), the mass of all formed planetary cores ($M_C$(formed)) and and the mass of planetary cores that have been accreted by the host star ($M_C$(accreted)). The dashed vertical lines are drawn at 350 kyr, 1 Myr and 3.5 Myr and show the moments at which most currently active planets are accreted by the host star or were subject to mergers.

### 5.4.4 Solid mass evolution

Fig. 5.8 shows the evolution of the different solid mass components of the system in Fig. 5.1. This includes the total pebble and dust disk mass, the total planetesimal disk mass, the mass in all active planetary cores, the mass in all formed planetary cores and the mass of all planetary cores that were accreted by the host star. We find that the mass of cores which were accreted by the host star is larger than the remaining mass in active cores at the end of the gas disks lifetime. The mass of the planetesimal disk surpasses the mass of the dust and pebble disk after ∼350 kyrs. The mass of active planetary cores never surpasses the mass of the planetesimal disk, the mass of all cores that have formed however surpasses the mass of the planetesimal disk within 1 Myrs. The planetesimal disk mass reaches its highest value after ∼ 450 kyrs and then decreases. This is due to low planetesimal formation as a result of the largely depleted pebble and dust disk and planetesimal accretion onto planetary cores.

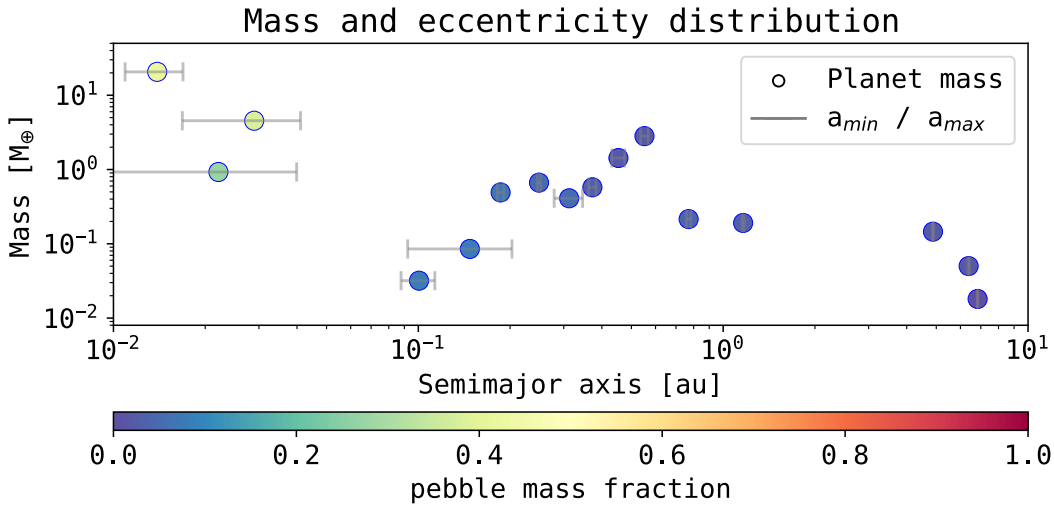


Figure 5.9: Mass and semimajor axis distribution of the planetary system after the gas disk has dispersed. The perihel and aphel of the planet as caused by its eccentricity is displayed via the error bars. The color shows the planets pebble mass fraction.

### 5.4.5 Final planetary system

Fig. 5.9 shows the mass, semimajor axis and eccentricity of the final system at 16.8 Myr. The colormap indicates the pebble mass fraction of the individual planet. We find that the sub earth mass planets in the terrestrial planet zone are dominantly composed of planetesimals and the inner super earths show a composition that stems from both pebbles and planetesimals. There is a clear dichotomy to be found between the close in super-Earths and the planets outside of 0.1 au. The close in planets show significantly higher eccentricities than than the planetesimal composed planets in the terrestrial planet zone. Most planets outside 0.1 au share very low eccentricities.
Fig. 5.10 shows the pebble mass fraction over the planet mass for the final system after 16.8 Myr. The colormap indicates the formation time of the corresponding embryo. The highest mass planets also contain the highest pebble mass fraction and the earliest formation time. The planets that formed at a later stage of the disk evolution remain at small masses and their pebble mass fraction remains below 10 %

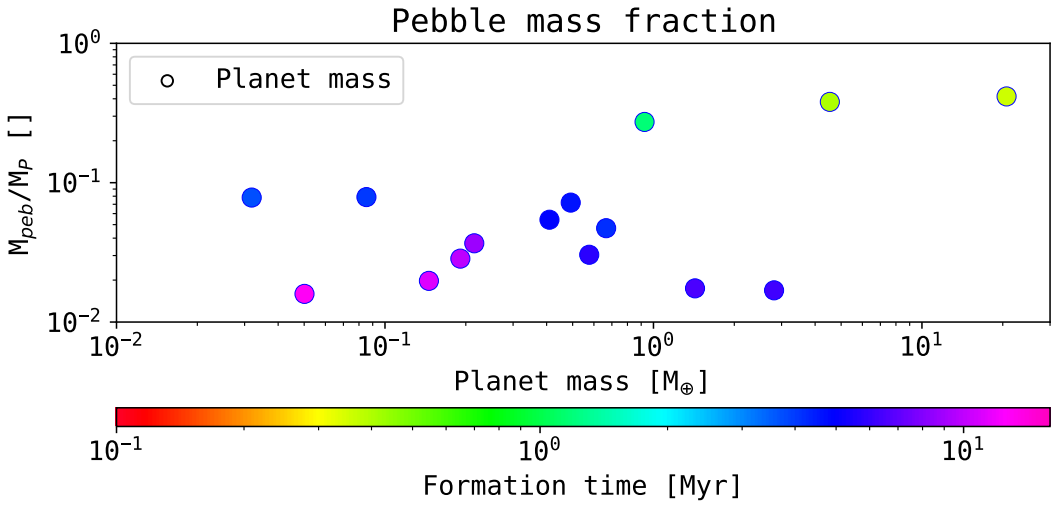


Figure 5.10: Mass and pebble mass fraction of the planetary system after the gas disk has dispersed. The color shows the formation time of the planets.

## 5.5 Discussion

### 5.5.1 The formation of multiple generations of planets

As a result of the embryo formation model, the first embryos form only in the inner region of the disk, in which they are subject to effective pebble accretion. Embryos then rapidly grow in mass and migrate to the inner edge of the disk. Since the formation of planetary embryos depends both on the planetesimal surface density and the heliocentric distance, embryos at larger distances (>10 au) do not form within the lifetime of the gas disk.

As the formation of embryos in our used model does not occur within a given orbital separation to other embryos/planets, we find no embryo formation once the terrestrial planet region is populated by simultaneously growing planets. Further out embryo formation can not take place within that time, as planetesimals could not grow to a lunar mass as a consequence of larger growth time scales with orbital distances, as well as lower corresponding planetesimal surface densities. Once the super Earth mass planets have migrated to the inner edge of the gas disk and were accreted by the star, the inner region of the disk is free from planets and embryo formation from the remaining planetesimals occurs. Since there is still a larger amount of gas by the time the first super Earth planets migrated inwards, eccentricity damping of the remaining planetesimals occurs. These planetesimals were excited by the super Earth mass planets that rapidly grew to $>10\,M_\oplus$. The embryo growth rate depends on the dispersion velocity (see Eq. 5.2), which again is given as $v_\infty = e(r) \cdot \Omega(r)$ in our framework. An increase in the eccentricity thus reduces the growth of planetary embryos. Eccentricity damping by the gas however leads again to shorter embryo growth time scales, as eccentricity damping reduces the dispersion velocity.

In our model we thus find multiple generations of planets. The first generation of planets that forms in the terrestrial planet zone grows rapidly by pebble accretion followed by rapid inward migration and subsequent accretion onto the star. Then follows a second generation with a similar fate as the first generation. The second generation of embryos also forms within the lifetime of the pebble flux. This generation grows to super earth masses via pebble accretion as well and is then subject to migration. As the pebble flux vanishes over time, the next generation cannot grow as massive as the previous ones and its migration speed is thus largely reduced. We find a set of sub earth mass planets growing by planetesimal accretion from 1 Myrs to 3.5 Myrs. Those

planets however are also pushed to the host star eventually, as a more massive planet from the previous generation migrates inward as well. After the last pebble based super Earth has migrated to the inner edge of the disk after 3.5 Myrs, the terrestrial planet zone is free from planets once again and eccentricity damping enables the last generation to form. Until the end of the gas disk lifetime at c.a. 16.8 Myrs, planetary embryos can form up to a distance of 7 au. The last generation grows dominantly by planetsimal accretion and remains largely at sub-Earth masses. The last generation of planets does not experience strong type I migration because of their low masses. A clearing of planets in the terrestrial planet zone as with previous generations therefore does not occur. We find that for as long as we have an active pebble flux, pebble accretion on embryos and fast type I migration clear the terrestrial zone from planets and eccentricity damping of planetesimals enables the next generation of embryos to form.
The planets composition in terms of whether their mass stems from pebble or planetesimal accretion reflects this picture. The early generations of planets are mostly composed of pebbles, whereas the lower mass later generations of planets is dominantly formed by planetesimal accretion. The close in super Earth mass planets in the final system are composed both of pebbles and planetesimals. They stem from the second generation of planet formation during which the pebble flux largely vanished. While the most massive remaining planet initially grew mostly by pebble accretion as well, a large fraction of its mass stems from planetesimals as it continues to accrete planetesimals after the pebble flux has vanished. We also find that the highest number of planets forms in the latest generation, since type I migration no longer forces planets to the inner edge of the disk and their small masses allow for a smaller orbital spacing.

### 5.5.2 Embryo formation and migration

The model for embryo formation that is used in this study has been derived using N-body simulations including planetesimal formation [Voelkel et al., 2021a] and has been compared to simulations that also include the effect of pebble accretion [Voelkel et al., 2021b]. Both of these studies did not show multiple generations of planetary embryo formation within 1 Myrs. Even though several setups in [Voelkel et al., 2021b] showed the rapid growth of super Earth mass planets in the terrestrial planet zone, these super Earth mass planets did not migrate inwards, as planetary migration due to planet disk interaction was not included. The formation of a next generation was therefore suppressed due to the presence of the super Earth mass planets in the terrestrial region. Including planetary migration in the more sophisticated N-body simulations, that contain both the formation of planetesimals and the accretion of pebbles, should form multiple generations of embryos within 1 Myr as well. Such a study would support and underline the findings of this paper and will be conducted in future work.

### 5.5.3 Long term evolution

We chose to end our simulation after the dispersal of the gas disk because our focus lies on the dynamic embryo formation of the first Myrs. However we still wish to briefly discuss the long term evolution of the system. After the gas disk has vanished we find 16 active planets in the system and 68.59 $M_\oplus$ in planetesimals. Three of those planets are very close in (a«0.1 au) with masses of $\geq$1$M_\oplus$ and eccentric orbits. Those (super) Earth mass planets are likely to be accreted by the host star due to tidal interactions. The remaining system would then consist of the 13 planetesimal composed planets and the remaining 68.59 $M_\oplus$ of planetesimals. The remaining planetesimal disk mass greatly exceeds that of the 13 planetesimal composed planets, a long term integration of the system should therefore also include the remaining planetesimals and their potential embryo formation to make a concise statement on the final system after several hundred Myrs. Without the damping effect of the gas disk however, the higher eccentricities of the planetesimals would reduce planetesimal accretion and embryo formation due to higher

dispersion velocities.

### 5.5.4 On the architecture of the solar system

We wish to discuss our simulations in consideration to the initial setup of the Grand Tack model [Walsh et al., 2011]. In the solar system, we find two gas giant planets at distances of 5-10 au, followed by two ice giants at 19-30 au. The inner region is populated with four smaller terrestrial planets. As our model suggests, the last generation resembles a large set of Earth mass and sub Earth mass terrestrial embryos that are believed to form the four terrestrial planets in the Grand Tack model. The profound difference between the Grand Tack and our formation model is that the sub Earth mass terrestrial embryos did not form as a second or third generation in the Grand Tack scenario. Instead, they were merely the first generation of embryos and the reason why they did not grow to super Earth mass planets due to pebble accretion is due to Jupiter shielding the pebble flux. In contrary to the Grand Tack, our simulation suggests that a first generation of super Earth mass planets (eventually accreted by the host star) may have populated the terrestrial planet region during the first stages of the solar systems evolution.

As the solar system contains gas giants, which we do not form within our framework, this hypothesis is subject to further investigation. The non-formation of Jupiter in the model presented raises several profound challenges. The formation of planetary embryos is the result of planetesimals growth. This results in the very late formation of an embryo at larger distances (>5 Myr at 5 au). By that time, the flux of pebbles has vanished and the growth of a Jupiter core would extend the lifetime of the gas disk. The early formation of a core at a larger distance to form Jupiter would either require a single initially much larger planetesimal to form or a local overdensity in planetesimals to reduce the formation time. Such an overdensity of planetesimals is discussed to be the result of a pressure bump in the gas disk [Guilera et al., 2020]. This pressure bump however would also have major implications on the evolution of the inner system. Whether or not we also find multiple generations of terrestrial planets when a pressure bump is included will be part of future work.

Another possible way to form giant planets, which would require the treatment of additional physics, would be further outward migration due to orbital resonances. If two planets are captured in mean motion resonance they may form a gap in the gas disk [Walsh et al., 2011]. In case the inner planet is the more massive one, this gap can cause outward migration of both planets. Effectively this might cause the formation of giant planets outside the initial orbit of their embryos formation. As gap opening in the disk is currently not included in our model, we can not observe this process within our simulation.

## 5.6 Summary and Outlook

In this paper we investigate the effect of dynamic planetary embryo formation during the lifetime of the gaseous disk. To pave the way for our approach we present a self consistent global model of planet formation that begins with an initial circumstellar disk of gas, dust and pebbles. The model presented viscously evolves the gas disk and uses a two population approach to model the evolution of dust and pebbles. Planetesimals form based on the radial pebble flux and planetary embryos are introduced based on the evolution of the planetesimal surface density and their dynamical state. The eccentricities and inclinations of planetesimals are increased by nearby planetary embryos and self stirring. Simultaneously, eccentricity and inclination damping by the evolving gas disk is considered. Once planetary embryos have formed, they can grow by pebble, planetesimal and gas accretion. Planets follow N-body dynamics with other planets and are subject to planet disk interactions, such as planetary migration. The number of embryos in the system, their initial location and formation time, are no longer an initial assumption, but the

result of the disks evolution. Our main findings can be summarized as followed:

- We find distinct generations of planets forming in the terrestrial planet region within the lifetime of the gas disk. Earlier generations grow dominantly by pebble accretion and are largely accreted by the host star due to migration. Later generations are composed largely of planetesimals, as those planets form after the pebble flux has mostly vanished.
- We find close in super Earth mass planets composed of both pebbles and planetesimals and mostly planetesimal composed sub Earth mass planets in the terrestrial region. A mostly pebble composed first generation of embryos did not survive the gaseous disk, as they were accreted by the host star. The formation of super-Earths and mini Neptunes is a likely outcome for the early generations of planet formation.
- The majority of planetary embryos that form do not outlive the gas disk disk. Out of the 78 embryos that formed in total, only 16 remained after the disk has vanished. The rest is victim to either accretion to the star or mergers.

These findings mark the onset of a large variety of possibilities for the presented planet formation and disk evolution model. While the parameter space that we studied in this paper focused on one set of disk parameters, our model can be used in a framework of planet population synthesis as well. Additionally it can be used to study individual features of single systems in a more detailed fashion like e.g. the formation of planets in primordial rings due to pressure bump. Next to our presented planet formation model, we will study the possibility of multiple generations of embryo formation using large scale N-body simulations. As multiple generations appear to already form within the first 1 Myr, a sophisticated N-body study, similar to Voelkel et al. [2021b] is computationally feasible and should confirm our findings. The underlying hypothesis of most planet formation models states, that the final planets are the end-product from the initially placed bodies. This hypothesis is heavily challenged by our results. Dynamic planetary embryo formation shows the possibility of multiple distinct phases of planet formation. This promises to have a fundamental effect on the formation history and composition of planets both in the solar system and exoplanet systems. It therefore needs to be accounted for in future studies.
Even though we claim to start with a nebula that was designed to create the solar system [Lenz et al., 2020], our simulations did not lead to planetary systems that resemble our solar system. Three effects can be responsible for this: a statistical effect of the N-body solver, our systematic initial condition and/or missing physics. The statistical effect could be tested by performing numerous similar simulations and check whether this leads to a more solar system like state for a number of outcomes. MCMC simulations can then be used to further constrain the potential initial conditions that formed the solar system, like e.g. disk mass, size, profile etc. But most likely the missing physics, even without improving the turbulence model, the viscous evolution of the disk or the dust growth physics, can be crucial for not forming the solar system. A major drawback in our framework are the tidal forces acting on the disk, which are not implemented yet. Gap formation with pebble trapping or resonant outward migration of planet pairs as in the Grand Tack model can therefore not occur. This missing process however could have produced a more solar system like outcome for the chosen initial conditions.

# 6 | Summary, Discussion and Outlook

## 6.1 Summary

My thesis establishes the first global self-consistent model of planet formation that does not rely on far reaching assumptions regarding initial planetary embryos or planetesimals. The combined framework presented in Chapter 5 is the first GPFM that consistently links the evolution of an initial circumstellar disk of gas and dust during its entire lifetime with a final set of planets. The total number of embryos and as such the number of final planets are no longer an assumption, but the result of consistent physical modeling. The presented GPFM is to date the only one that can predict the total number of forming planets and their final properties given only initial disk parameters. The individual stages of development are shown in 4 consecutive publications, each of which building on the results of the previous.

For the evolution of the dust and pebbles in the disk I use state of the art two population modeling. The formation of planetesimals and their size are based on most recent prescriptions. Their formation is regulated by the pebble flux and as such links the formation of 100 km in diameter planetesimals with the evolution of the disk. Inward drifting pebbles result in a steep surface density profile of planetesimals. Highly condensed zones of planetesimals in the inner disk are the outcome. This alone can cause the formation of giant planets in the inner region of the disk without invoking pebble accretion. This result marks a turning point in the debate around the efficiency of large planetesimal accretion for planetary growth.

Combining the disk model from Voelkel et al. [2020] with high resolution N-body simulations using the LIPAD code, I present a semi analytic model for planetary embryo formation. Their formation time is the result of planetesimal growth via collisions. The total number of embryos is constrained by the orbital separation of massive objects in the oligarchic growth regime. I successfully link the formation of single planetary embryos with the planetesimal surface density evolution of the disk. The presented model for embryo formation can be easily included in other global planet formation models that use a planetesimal surface density prescription. This step effectively removes the single largest blind sport in global planet formation modeling to date.

Next to the previously implemented accretion of planetesimals, I include the accretion of the evolving pebble flux on planetary embryos. The presented GPFM combines the three main growth mechanisms (planetesimal accretion, pebble accretion and gas accretion) during the entire disk lifetime. This allows for a detailed study on the individual efficiency of pebble and planetesimal accretion within the same common framework. As the accretion of pebbles reduces the pebble flux, the formation of planetesimals is reduced and thus affected as well. This allows for a unique way to globally study the back reaction of planet formation on the evolution of the solid disk. Embryos, pebbles and planetesimals all stem from the same initial solid content, given by the initial metalicity. The presented GPFM is the first to make a self-consistent statement on how much initial dust mass is transformed into pebbles, planetesimals and planets. This infers revolutionary insights on the effect of growing planets on observable quantities like the lifetime

of the dust and pebble disk.

Finally, I show that a disk consistent treatment of embryo formation leads to the formation of multiple distinct generations of planets. The generation in which an embryo forms has far reaching implications on its final properties. The question whether a planet is formed dominantly via pebble or planetesimal accretion can be answered by the generation in which it formed. Early generations of embryos easily grow to super Earth masses via pebble accretion. Their survival probability due to efficient type I migration, however, is very low. Accretion onto the host star is a common fate for many early generation embryos. Later embryo generations grow dominantly via the accretion of planetesimals, as the pebble reservoir is depleted. These results reveal unknown complexity within the formation history of planets, which future work in the field will need to account for.

### 6.1.1 Dust, pebbles and planetesimals

In Chapter 2 [Voelkel et al., 2020], I implement a model for pebble flux regulated planetesimal formation [Lenz et al., 2019] and a two population model for dust and pebble evolution [Birnstiel et al., 2012] into the GPFM presented in Emsenhuber et al. [2020a]. The inward drifting pebbles result in a steeper planetesimal surface density profile ($\Sigma_P \propto r^{-2.1}$) than the minimum mass solar nebula hypothesis ($\Sigma_P \propto r^{-1.5}$) or the profile of a viscous gas disk ($\Sigma_P \propto r^{-0.9}$). Using single embryo planet population synthesis, the planet populations that formed for those different initial planetesimal surface density slopes and the dynamically forming planetesimals are compared. The main results of planetesimal formation for single embryo planet population synthesis are listed below [Voelkel et al., 2020]

- The accretion of large planetesimals with a size of 100 km is a highly efficient mechanism of planetary growth in the inner region of a circumstellar disk.
- Pebble flux regulated planetesimal formation results in highly condensed regions of planetesimals in the inner region of a circumstellar disk. This effect enables the formation of gas giant planets.
- The studied setup fails to form cold giant planets. The reason lies within orbital migration and accretional heating of planetary cores, not in core growth timescales that exceed the lifetime of the gas disk
- The number of planets above $10\,M_E$ increases by 89% and the number of planets above $20\,M_E$ increases by 345% if one assumes the pebble flux regulated planetesimals formation in comparison to the MMSN hypothesis.

The implementation of planetesimal formation and the two population model for dust and pebble evolution brings a variety of technical advantages. The main advantages are listed below.

- As pebbles evolve dynamically in the disk, their accretion onto planetary embryos can be included.
- Instead of requiring a far reaching assumption like the steep MMSN profile for the planetesimals, we can start our simulations with a shallow gas surface density profile consistent with observations of disks around young stars.
- Connecting the timescales of planetesimal formation with the evolution of the disk, we can include the dynamic formation of planetary embryos.

These improvements will set the foundation for the other developments that are shown in this thesis.

### 6.1.2 Linking planetary embryo formation to planetesimal formation I

In Chapter 3 [Voelkel et al., 2021a], I study the formation of planetary embryos via planetesimal collisions from initially 100 km diameter planetesimals by connecting a one dimensional model for planetesimal formation with the N-body Code LIPAD. Nine simulations in which the surface density slope and total planetesimal mass is varied are shown. An analytic model for the formation of planetary embryos based on the evolution of the planetesimal surface density is introduced. The main findings of planetary embryo formation based on pebble flux regulated planetesimal formation are listed below [Voelkel et al., 2021a]

- The first embryos form in the innermost region of the disk. This result is expected due to high planetesimal surface densities and shorter orbital timescales.
- The first embryos form well within the lifetime of the pebble flux and within 1 au for the studied disks. Embryos that form outside 2 au form after the pebble flux has vanished.
- The number of active embryos does not increase for higher disk masses or steeper planetesimal surface density profiles. The area of embryo formation and their corresponding masses, however, do enlarge for higher disk masses and steeper surface density profiles.

I show that a power-law planetesimal surface density profile cannot build planetary embryos at larger distances within the timescale of a radial pebble flux. This consequence arises from the interplay of pebble-flux-regulated planetesimal formation and the timescales involved in forming planetary embryos from 100 km sized bodies. The more planetesimals are formed, the earlier planetary embryos are formed, but the more planetesimals are formed, the lower the mass that remains in pebbles. Vice versa, if the formation of planetesimals is reduced to maintain a higher pebble flux, the growth time scales for planetary embryos increase as a result of lower planetesimal surface densities.

The one dimensional model for planetary embryo formation presented in this work does well in reproducing the formation timescale, spatial distribution and total number of planetary embryos for a given planetesimal surface density evolution. Most importantly within the scope of this thesis, it marks the paradigm shift from a surface density prescription of planetesimals to a fixed set of individual planetary embryos. As this aspect has not been treated disk consistently in any other GPFM , it marks the single largest blind spot in self-consistent planet formation modeling.

### 6.1.3 Linking planetary embryo formation to planetesimal formation II

In Chapter 4 [Voelkel et al., 2021b], I study the effect of pebble accretion during the formation phase of planetary embryos. The work succeeds Chapter 3 [Voelkel et al., 2021a] by adding the effect of pebble accretion next to planetesimal accretion during the formation stage of planetesimals and planetary embryos. The main effects on embryo formation by pebble accretion in the terrestrial planet region are summarized below [Voelkel et al., 2021b]

- The formation of super Earths is strongly enhanced via pebble accretion.
- Individual embryos grow substantially more massive if pebble accretion if included. The total number of embryos, however, strongly decreases.
- Only the embryos that form early and thus in the inner region of the disk can benefit from pebble accretion.
- Embryos do not form at larger distances if pebble accretion is included. Forming a planetary embryo at larger distances within the lifetime of the pebble flux is not possible for our assumptions.

The efficiency of pebble accretion on distant embryos is challenged in this study, as the timescales for embryo formation at larger distances may exceed the lifetime of the pebble flux for a power law surface density profile of planetesimals. More refined substructures, like e.g. rings in disks may prolong the lifetime of the pebble flux and/or decrease the embryo formation timescales due to locally enhanced zones of planetesimal formation.

### 6.1.4 On the multiple generations of planetary embryos

In Chapter 5 [Voelkel et al., submitted to A&A], I merge the embryo formation model presented in Chapter 3 [Voelkel et al., 2021a] into the GPFM presented in Chapter 2 [Voelkel et al., 2020] and include the effect of pebble accretion next to planetesimal accretion for planetary growth. The presented framework is the first to self-consistently model the formation of planets from an initial circumstellar disk of gas and dust during its entire lifetime without invoking far reaching assumptions on initially placed planetary embryos or planetesimals. The number of embryos in the system, their initial location and formation time, are no longer an initial assumption, but the result of the disks evolution. The main findings are listed below [Voelkel et al., submitted to A&A]

- It is shown that planets form in distinct generations during the lifetime of the gas disk. The first generation is subject to accretion on the host star after type I migration and massive growth via pebble accretion. The later generations form after the pebble flux has vanished and grow largely via planetesimals.
- The most massive planets in the final system are composed of pebbles and planetesimals and stem from the second generation. The formation of super Earths and mini-Neptunes is a likely outcome of this phase. The last generation that forms remains largely at sub-Earth masses and is dominantly composed of planetesimals.
- 78 embryos form during the lifetime of the disk, but only 16 planets are found in the final system. The rest is either subject to accretion on the host star, or subject to mergers.

The presented GPFM marks the final development stage presented in this thesis. It successfully links the surface density prescription of the disk evolution with a distinct set of planetary embryos and tracks their subsequent growth via solid (pebble and planetesimal) and gas accretion. Furthermore, the framework is computationally feasible to be used in planet population synthesis studies as presented in Emsenhuber et al. [2020b].

## 6.2 Discussion

The presented framework and its results have far reaching implications on several ongoing debates within planet formation. Among others the efficiency of large planetesimal accretion in itself and its efficiency in regard to the accretion of pebbles.

#### On the sizes of planetesimals

The recent years have been subject to numerous studies regarding the efficiency of large planetesimal accretion, such as Johansen and Bitsch [2019]. They often result in a negative statement on forming giant planets using large planetesimals. In order to stay consistent with the large planetesimal sizes that stem from numerical simulations [Klahr and Schreiber, 2020] or observations from the asteroid belt [Bottke Jr et al., 2005, Walsh et al., 2017, Delbo' et al., 2017], the accretion of pebbles has revealed itself to be a thankful circumvention to explain the formation of massive planets. The inward drifting pebbles can be efficiently accreted by planetary embryos and numerous studies around this scenario have been conducted (e.g. Ormel and Klahr [2010], Bitsch et al. [2015], Ndugu et al. [2017]). If one however considers that the formation of planetesimals follows the evolution of the inward drifting pebble flux, the surface density profile of planetesimals becomes much steeper than initially assumed. Lenz et al. [2019] shows that the resulting planetesimal surface density can be as steep as $\Sigma_P \propto r^{-2.1}$, instead of the previously assumed. $\Sigma_P \propto r^{1.5}$ (MMSN) or $\Sigma \propto r^{-0.9}$(viscous disk). In the Voelkel et al. [2020] I show that this surface density profile change alone can result in the formation of giant planets using only 100 km in diameter planetesimals. The statement on the inefficiency of large planetesimal accretion is thus heavily challenged. The formation of giant planets does not require the accretion of pebbles and it does not require planetesimal sizes that would be inconsistent with observations.

#### Pebble vs. planetesimal accretion for planetary growth

Among the most valuable findings within this thesis is the in-detail comparison between pebble and planetesimal accretion in Chapter 5. Previous models mainly focused on one of the two in an isolated fashion. I show that the answer to the question on which mechanism is the more dominant lies in the formation of the embryo. More precisely in the generation in which it formed. Early generations of embryos can grow massively via pebble accretion. They can form within the lifetime of the pebble reservoir and grow to massive sizes. On the other side, their survival probability is low because of type I migration and stellar accretion. No planet that formed in the first generation of Chapter 5 survived until the end of the gas disk. While pebble accretion is efficient for rapidly growing massive planets, their survival is not granted. Later generations form after the pebble flux has vanished and as such grow more dominantly via planetesimal accretion. Most surviving planets found in Chapter 5 formed dominantly via the accretion of planetesimals and remain at sub-Earth masses. Most super Earth mass planets that formed dominantly via pebble accretion are subject to accretion on the host star. The most massive planets of the final system formed via pebble accretion and planetesimal accretion alike. Now let's ask the question, how did most of the planets form that we can see today? The question about which mechanism determines the formation of a planet is answered by the formation of the planetary embryo.

#### On pebble polluted terrestrial planets

Models that are based on the accretion of pebbles often struggle to form low mass terrestrial planets. The high efficiency of pebble accretion favors the formation of massive super Earths. A shielding from the incoming pebble flux to remain at low masses is required (like e.g. a giant planet). I propose an alternative scenario in which low mass terrestrial planets can form without any shielding effect. Embryos that form after the pebble reservoir is depleted grow to lower masses by accreting the remaining planetesimals. The solution to overly efficient planetary growth via pebble accretion in the terrestrial planet region may lie within the consistent formation of planetary embryos.

#### On the overproduction of planets

As found in Mulders et al. [2019], the synthetic population presented in Emsenhuber et al. [2020b] shows increased planet occurrence rates when compared to the Kepler survey. Emsenhuber et al. [2020b] shows five populations which either use 1, 10, 20, 50 or 100 planetary embryos as initial conditions. All disks studied in each of the sub populations use the same number of planetary embryos. The number of embryos that a disk can form depends however on the disks evolution. The assumption of a fixed number of initial embryos for each disk is highly inconsistent and most likely leads to incorrect results when it comes to the total number of planets. The newly presented GPFM constrains the number of embryos via the evolution of the disk. Additionally as seen in Chapter 5, the accretion of pebbles can be a highly destructive force in planet formation. No planet that formed in the first generation survived until the end of the gas disk due to fast type I migration. As Emsenhuber et al. [2020b] did not include the accretion of pebbles, the survival rate of planets may have been overestimated. Including the accretion of pebbles and consistent embryo formation promises to have a significant effect on the total number of planets.

#### Additional observables

Instead of merely increasing the complexity of planet formation models, we need to find additional ways to verify them with observational quantities. I connect the evolution of a dust and pebble disk into the arguably most complex global planet formation model to date. This model can be used for planet population synthesis studies as in Emsenhuber et al. [2020b]. My advancements equip the newly built GPFM to not only be verified via planetary properties, but via disk evolution properties as well. This allows for a completely new type of disk population synthesis study. The previous GPFM used observable disk properties as input and planet properties as output. The newly implemented self-consistent dust and pebble evolution includes back reaction of the emerging planets. This allows for comparing the entire model of planet formation and disk evolution with observations. Studies regarding the evolution of dust and pebbles often conclude very short lifetimes for the dust and pebble disk Birnstiel et al. [2010]. Such studies however do not include the back reaction of planets on the evolving dust and pebble disk. The effect of planet formation on the the lifetime of the dust and pebble disk can only be studied in a framework that includes both. The resulting disk lifetimes can then be verified via latest observational results regarding circumstellar disks.

## 6.3 Outlook

The newly obtained GPFM and the insights generated in its first application offer a variety of new possibilities for future studies. Due to the computational feasibility of the presented framework it can be used in a planet population synthesis study, similar to Emsenhuber et al. [2020b]. Such a study allows for an investigation on the effect of the newly included physical models, such as the accretion of pebbles and the formation of planetary embryos on planet formation. Next to the GPFM , the embryo formation model itself can be incorporated into other frameworks of planet formation that involve a planetesimal surface density prescription to allow for a more consistent treatment. In the following I will give an overview over future projects that either involve the continuous improvement of the presented GPFM , its application, or independent research regarding the obtained results.

#### The formation of more distant planets

The embryo formation model was introduced using power law surface density profiles of planetesimals and therefore did not form embryos at larger distances within the lifetime of the pebble flux or the gas disk in our study. Explaining the formation of more distant planets will be subject to future work. Possible solutions could be the inclusion of a primordial planetesimal size function that allows for the initial formation of larger than 100 km planetesimals. This would effectively reduce the embryo formation timescale. Forming a large set of smaller planetesesimals than 100 km in diameter can also decrease the embryo formation time due to more efficient accretion of smaller planetesimals. Another solution for the formation of distant planets without changing the size of initially formed planetesimals revolves around potential substructure in the disk, like e.g. distant rings [Dullemond et al., 2018]. Assuming that the rings are the result of disk dynamics without the initial presence of a giant planet, a pressure bump in the disk may cause a ring of solid material to form. Due to highly condensed zones of solid material, the formation of planetesimals and consequentially the formation of a planetary embryo may be greatly enhanced.

One future project regarding the improvement of the presented GPFM thus involves the implementation of a planetesimal size function and the implementation of disk substructures within the disk evolution model. This includes a more complex prescription of turbulence within the evolution of the one dimensional gas surface density.

#### The effect of turbulence in disks on planet formation

The presented GPFM in Voelkel et al. [submitted to A&A] allows for a global study on the effect of disk turbulence on planet formation. Such a study can be conducted in a self-consistent manner by introducing e.g. a variable $\alpha$-turbulence parameter. For now, a simple constant $\alpha$-parameter is used, as introduced in Shakura and Sunyaev [1973]. A more complex prescription and its resulting effect on planet formation is however within the capability of the presented GPFM . As the formation of planetary embryos is linked to the formation of planetesimals, which again is linked to the evolution of dust and pebbles, a change in the gas disk evolution promises to have an immediate effect on the formation of planetary embryos. Such a study and its results are currently work in progress by the author.

Next to the inclusion of a more complex turbulence prescription, the inclusion of pressure bumps caused by planets at their pebble isolation mass Lambrechts et al. [2014] will be subject to future work. The back reaction of massive planets on the evolution of the disk and the corresponding effect on the formation of other planets promises to be an exciting field to study in a globally self-consistent manner.

#### Multiple generations of embryos

As shown on Voelkel et al. [submitted to A&A], we find multiple distinct phases of planetary embryo formation in the inner disk, even within the first 1 Myrs of the disks evolution. Investigating this effect in greater detail will be subject to future studies. The high resolution LIPAD N-body studies presented in Voelkel et al. [2021a] and Voelkel et al. [2021b] did not show the formation of multiple generations of planetary embryos within the terrestrial planet region within the first 1 Myrs of the systems evolution. As these studies did not include planetary migration, embryos that form do not migrate to the inner edge of the gas disk, as observed in Voelkel et al. [submitted to A&A]. Consequentially the formation of the next generation of planetary embryos is suppressed. Including the effect of type I planetary migration into a setup similar to the one presented in Voelkel et al. [2021b] should therefore validate the effect of multiple generations of planetary embryos. Such a study and its results are currently work in progress by the author.

#### The chemical composition of exoplanet atmospheres

Next to the formation of more distant planets, the presented GPFM can be used to obtain viable constraints on the composition of the resulting exoplanets and linking them to their formation history. Due to future observational capabilities, the composition of exoplanet atmospheres can be an additional observable quantity to verify our models. The formation history of the planet is expected to be vital to its composition. The formation of planetary embryos therefore needs to be accounted for consistently with the (chemical) evolution of the disk. Including a more complex chemical model for the disk, the planets cores and their atmospheres can equip the synthetic population with essential observable quantities.

The previously implemented compositional model did not track the evolution of an inward drifting pebble flux. The composition was based on the location of the initially placed planetesimals. A new model that tracks the composition of the evolving dust, pebbles and resulting planetesimals needs to be included into the GPFM to allow for a precise treatment on the compositional evolution of the dust and pebbles.

#### Planet formation around low mass stars

Future work will revolve around suiting the presented GPFM for planet population synthesis around low mass stars (e.g. M-dwarfs). The currently used dust and pebble evolution has been derived for solar type stars. Assessing its accuracy and potentially adapting it to be fit for other stellar types is subject to ongoing research. Investigating the formation of planets around non solar type stars will be a highly promising field of research.

#### Constraining the solar nebula and the formation history of its planets

Next to its appliance for planet population synthesis and exoplanet research, the presented GPFM can also be used for studying the solar system. Studies that aim to constrain the initial solar nebula as in Lenz et al. [2020] did not include the formation of planets during the formation of planetsimals. The formation of planets however occurs simultaneously to the formation of planetesimals. Their back reaction on the evolution of the disk therefore needs to be considered. The solar system delivers the most accurate constraints on a final planetary system that we know. Besides the planets themselves, the asteroid belt, the Kuiper belt and the Oort cloud deliver crucial constraints on the final distribution of planetesimals. Future projects will revolve around reproducing essential features of the solar system using the self-consistent framework by conducting an MCMC type study. They can give viable constraints on the initial state of the solar nebula and valuable insights on the formation history of its planets, including our own Earth. Understanding its peculiar composition is a key issue for understanding the formation of life.

# List of my own publications

## Published

VOELKEL, O., R. DEIENNO, K. KRETKE, AND H. KLAHR (2021): "Linking planetary embryo formation to planetesimal formation-II. The effect of pebble accretion in the terrestrial planet zone," *Astronomy & Astrophysics*, 645, A132.

VOELKEL, O., R. DEIENNO, K. KRETKE, AND H. KLAHR (2021): "Linking planetary embryo formation to planetesimal formation-I. The effect of the planetesimal surface density in the terrestrial planet zone," *Astronomy & Astrophysics*, 645, A131.

VOELKEL, O., H. KLAHR, C. MORDASINI, A. EMSENHUBER, AND C. LENZ (2020): "Effect of pebble flux-regulated planetesimal formation on giant planet formation," *Astronomy & Astrophysics*, 642, A75.

## Submitted

VOELKEL, O., H. KLAHR, AND C. MORDASINI (submitted to A&A): "On the multiple generations of planetary embryo formation," *Astronomy & Astrophysics*.

# Bibliography


Charles P Abod, Jacob B Simon, Rixin Li, Philip J Armitage, Andrew N Youdin, and Katherine A Kretke. The mass and size distribution of planetesimals formed by the streaming instability. ii. the effect of the radial gas pressure gradient. *The Astrophysical Journal*, 883(2):192, 2019.

Isao Adachi, Chushiro Hayashi, and Kiyoshi Nakazawa. The gas drag effect on the elliptic motion of a solid body in the primordial solar nebula. *Progress of Theoretical Physics*, 56(6): 1756–1771, 1976.

Fred C Adams, Gregory Laughlin, and Genevieve JM Graves. Red dwarfs and the end of the main sequence. In *Revista Mexicana de Astronomia y Astrofisica Conference Series*, volume 22, pages 46–49, 2004.

Matthew Alessi, Ralph E Pudritz, and Alex J Cridland. On the formation and chemical composition of super earths. *Monthly Notices of the Royal Astronomical Society*, 464(1):428–452, 2017.

Yann Alibert, Christoph Mordasini, Willy Benz, and Christophe Winisdoerffer. Models of giant planet formation with migration and disc evolution. *A&A*, 434(1):343–353, 2005.

Yann Alibert, Frédéric Carron, Andrea Fortier, Samuel Pfyffer, Willy Benz, Christoph Mordasini, and David Swoboda. Theoretical models of planetary system formation: mass vs. semi-major axis. *A&A*, 558:A109, 2013.

Yann Alibert, Julia Venturini, Ravit Helled, Sareh Ataiee, Remo Burn, Luc Senecal, Willy Benz, Lucio Mayer, Christoph Mordasini, Sascha P Quanz, et al. The formation of jupiter by hybrid pebble–planetesimal accretion. *Nature astronomy*, 2(11):873–877, 2018.

Sean M. Andrews, D. J. Wilner, A. M. Hughes, Chunhua Qi, and C. P. Dullemond. Protoplanetary disk structures in ophiuchus. ii. extension to fainter sources. *ApJ*, 723(2):1241–1254, Oct 2010. ISSN 1538-4357. doi: 10.1088/0004-637x/723/2/1241. URL http://dx.doi.org/10.1088/0004-637X/723/2/1241.

Sean M Andrews, Jane Huang, Laura M Pérez, Andrea Isella, Cornelis P Dullemond, Nicolás T Kurtovic, Viviana V Guzmán, John M Carpenter, David J Wilner, Shangjia Zhang, et al. The disk substructures at high angular resolution project (dsharp). i. motivation, sample, calibration, and overview. *The Astrophysical Journal Letters*, 869(2):L41, 2018.

M Ansdell, JP Williams, L Trapman, SE van Terwisga, S Facchini, CF Manara, N van der Marel, A Miotello, Marco Tazzari, M Hogerheijde, et al. Alma survey of lupus protoplanetary disks. ii. gas disk radii. *The Astrophysical Journal*, 859(1):21, 2018.

Ko Arimatsu, Koji Tsumura, Fumihiko Usui, Yoshiharu Shinnaka, Kohei Ichikawa, Takafumi Ootsubo, Takayuki Kotani, Takehiko Wada, Koichi Nagase, and Junichi Watanabe. A kilometre-sized kuiper belt object discovered by stellar occultation using amateur telescopes. *Nature Astronomy*, 3(4):301–306, 2019.

Isabelle Baraffe, Derek Homeier, France Allard, and Gilles Chabrier. New evolutionary models for pre-main sequence and main sequence low-mass stars down to the hydrogen-burning limit. *Astronomy & Astrophysics*, 577:A42, 2015.

C. Baruteau, A. Crida, S. J. Paardekooper, F. Masset, J. Guilet, B. Bitsch, R. Nelson, W. Kley, and J. Papaloizou. Planet-Disk Interactions and Early Evolution of Planetary Systems. In Henrik Beuther, Ralf S. Klessen, Cornelis P. Dullemond, and Thomas Henning, editors, *Protostars and Planets VI*, page 667, January 2014. doi: 10.2458/azu_uapress_9780816531240-ch029.

W. Benz, S. Ida, Y. Alibert, D. Lin, and C. Mordasini. Planet Population Synthesis. In Henrik Beuther, Ralf S. Klessen, Cornelis P. Dullemond, and Thomas Henning, editors, *Protostars and Planets VI*, page 691, January 2014. doi: 10.2458/azu_uapress_9780816531240-ch030.

Willy Benz and Erik Asphaug. Catastrophic disruptions revisited. *arXiv preprint astro-ph/9907117*, 1999.

Carlos A Bertulani. *Nuclei in the Cosmos*. World Scientific, 2013.

Hans Albrecht Bethe and Charles Lewis Critchfield. The formation of deuterons by proton combination. *Physical Review*, 54(4):248, 1938.

T. Birnstiel, C. P. Dullemond, and F. Brauer. Gas- and dust evolution in protoplanetary disks. *Astronomy and Astrophysics*, 513:A79, Apr 2010. ISSN 1432-0746. doi: 10.1051/0004-6361/200913731. URL http://dx.doi.org/10.1051/0004-6361/200913731.

T Birnstiel, H Klahr, and B Ercolano. A simple model for the evolution of the dust population in protoplanetary disks. *A&A*, 539:A148, 2012.

Tilman Birnstiel and Sean M Andrews. On the outer edges of protoplanetary dust disks. *The Astrophysical Journal*, 780(2):153, 2013.

Bertram Bitsch and Wilhelm Kley. Orbital evolution of eccentric planets in radiative discs. *Astronomy & Astrophysics*, 523:A30, 2010.

Bertram Bitsch and Wilhelm Kley. Evolution of inclined planets in three-dimensional radiative discs. *Astronomy & Astrophysics*, 530:A41, 2011.

Bertram Bitsch, Michiel Lambrechts, and Anders Johansen. The growth of planets by pebble accretion in evolving protoplanetary discs. *A&A*, 582:A112, 2015.

Bertram Bitsch, Andre Izidoro, Anders Johansen, Sean N Raymond, Alessandro Morbidelli, Michiel Lambrechts, and Seth A Jacobson. Formation of planetary systems by pebble accretion and migration: Growth of gas giants. *Astronomy & Astrophysics*, 623:A88, 2019.

P. Bodenheimer and J. B. Pollack. Calculations of the accretion and evolution of giant planets: The effects of solid cores. *Icarus*, 67(3):391–408, September 1986. doi: 10.1016/0019-1035(86)90122-3.

P. Bodenheimer, O. Hubickyj, and J. J. Lissauer. Models of the in Situ Formation of Detected Extrasolar Giant Planets. *Icarus*, 143:2–14, January 2000. doi: 10.1006/icar.1999.6246.

Alan P Boss. Giant planet formation by gravitational instability. *Science*, 276(5320):1836–1839, 1997.

William F Bottke Jr, Daniel D Durda, David Nesvornỳ, Robert Jedicke, Alessandro Morbidelli, David Vokrouhlickỳ, and Harold F Levison. Linking the collisional history of the main asteroid belt to its dynamical excitation and depletion. *Icarus*, 179(1):63–94, 2005.

Christopher H Broeg and Willy Benz. Giant planet formation: episodic impacts versus gradual core growth. *Astronomy & Astrophysics*, 538:A90, 2012.

Natacha Brügger, Yann Alibert, Sareh Ataiee, and Willy Benz. Metallicity effect and planet mass function in pebble-based planet formation models. *A&A*, 619:A174, 2018.

Natacha Brügger, Remo Burn, Gavin Coleman, Yann Alibert, and Willy Benz. Pebbles versus planetesimals: the outcomes of population synthesis models. *arXiv preprint arXiv:2006.04121*, 2020.

Remo Burn, Martin Schlecker, Christoph Mordasini, Alexandre Emsenhuber, Yann Alibert, Thomas Henning, Hubert Klahr, and Willy Benz. The new generation planetary population synthesis (ngpps). iv. planetary systems around low-mass stars. *arXiv preprint arXiv:2105.04596*, 2021.

Philip J Carter, Zoë M Leinhardt, Tim Elliott, Michael J Walter, and Sarah T Stewart. Compositional evolution during rocky protoplanet accretion. *The Astrophysical Journal*, 813(1):72, 2015.

John Chambers. A semi-analytic model for oligarchic growth. *Icarus*, 180(2):496–513, 2006.

John E Chambers. A hybrid symplectic integrator that permits close encounters between massive bodies. *Monthly Notices of the Royal Astronomical Society*, 304(4):793–799, 1999.

CJ Clarke, A Gendrin, and M Sotomayor. The dispersal of circumstellar discs: the role of the ultraviolet switch. *Monthly Notices of the Royal Astronomical Society*, 328(2):485–491, 2001.

Matthew S. Clement, Nathan A. Kaib, and John E. Chambers. Embryo Formation with GPU Acceleration: Reevaluating the Initial Conditions for Terrestrial Accretion. *The Planetary Science Journal*, 1(1):18, June 2020. doi: 10.3847/PSJ/ab91aa.

Matthew S Clement, Nathan A Kaib, and John E Chambers. Embryo formation with gpu acceleration: reevaluating the initial conditions for terrestrial accretion. *The Planetary Science Journal*, 1(1):18, 2020.

Gavin AL Coleman and Richard P Nelson. On the formation of planetary systems via oligarchic growth in thermally evolving viscous discs. *Monthly Notices of the Royal Astronomical Society*, 445(1):479–499, 2014.

A. Crida, A. Morbidelli, and F. Masset. On the width and shape of gaps in protoplanetary disks. *Icarus*, 181:587–604, April 2006. doi: 10.1016/j.icarus.2005.10.007.

Jeffrey N. Cuzzi, Robert C. Hogan, and William F. Bottke. Towards initial mass functions for asteroids and Kuiper Belt Objects. *Icarus*, 208:518–538, August 2010. doi: 10.1016/j.icarus.2010.03.005.

Rogerio Deienno, Kevin J Walsh, Katherine A Kretke, and Harold F Levison. Energy dissipation in large collisions—no change in planet formation outcomes. *The Astrophysical Journal*, 876 (2):103, 2019.

Rogerio Deienno, Kevin J Walsh, Harold F Levison, and Katherine A Kretke. Collisional evolution of meter-to kilometer-sized planetesimals in mean motion resonances: Implications for inward planet shepherding. *The Astrophysical Journal*, 890(2):170, 2020.

Marco Delbo', Kevin Walsh, Bryce Bolin, Chrysa Avdellidou, and Alessandro Morbidelli. Identification of a primordial asteroid family constrains the original planetesimal population. *Science*, 357:1026–1029, September 2017. doi: 10.1126/science.aam6036.

K.-M. Dittkrist, C. Mordasini, H. Klahr, Y. Alibert, and T. Henning. Impacts of planet migration models on planetary populations. Effects of saturation, cooling and stellar irradiation. *A&A*, 567:A121, July 2014. doi: 10.1051/0004-6361/201322506.

K. Dittrich, H. Klahr, and A. Johansen. Gravoturbulent Planetesimal Formation: The Positive Effect of Long-lived Zonal Flows. *ApJ*, 763:117, February 2013. doi: 10.1088/0004-637X/763/2/117.

J. Drążkowska and Y. Alibert. Planetesimal formation starts at the snow line. *A&A*, 608:A92, December 2017. doi: 10.1051/0004-6361/201731491.

J. Drążkowska and Y. Alibert. Planetesimal formation starts at the snow line. *A&A*, 608:A92, Dec 2017. ISSN 1432-0746. doi: 10.1051/0004-6361/201731491. URL http://dx.doi.org/10.1051/0004-6361/201731491.

Cornelis P Dullemond, Tilman Birnstiel, Jane Huang, Nicolás T Kurtovic, Sean M Andrews, Viviana V Guzmán, Laura M Pérez, Andrea Isella, Zhaohuan Zhu, Myriam Benisty, et al. The disk substructures at high angular resolution project (dsharp). vi. dust trapping in thin-ringed protoplanetary disks. *The Astrophysical Journal Letters*, 869(2):L46, 2018.

Martin J Duncan, Harold F Levison, and Man Hoi Lee. A multiple time step symplectic algorithm for integrating close encounters. *The Astronomical Journal*, 116(4):2067, 1998.

Alexandre Emsenhuber, Christoph Mordasini, Remo Burn, Yann Alibert, Willy Benz, and Erik Asphaug. The new generation planetary population synthesis (ngpps). i. bern global model of planet formation and evolution, model tests, and emerging planetary systems. *arXiv preprint arXiv:2007.05561*, 2020a.

Alexandre Emsenhuber, Christoph Mordasini, Remo Burn, Yann Alibert, Willy Benz, and Erik Asphaug. The new generation planetary population synthesis (ngpps). ii. planetary population of solar-like stars and overview of statistical results. *arXiv preprint arXiv:2007.05562*, 2020b.

A. Fortier, Y. Alibert, F. Carron, W. Benz, and K. M. Dittkrist. Planet formation models: the interplay with the planetesimal disc. *A&A*, 549:A44, January 2013. doi: 10.1051/0004-6361/201220241.

Andrea Fortier, Omar Gustavo Benvenuto, and Adrian Brunini. Oligarchic planetesimal accretion and giant planet formation. *Astronomy & Astrophysics*, 473(1):311–322, 2007.

Laure Fouchet, Yann Alibert, Christoph Mordasini, and Willy Benz. Effects of disk irradiation on planet population synthesis. *Astronomy & Astrophysics*, 540:A107, 2012.

Peter Goldreich and Scott Tremaine. The excitation of density waves at the lindblad and corotation resonances by an external potential. *Astrophysical Journal*, 233(3):857–871, 1979.

Guillermo Gonzalez. The stellar metallicity—giant planet connection. *Monthly Notices of the Royal Astronomical Society*, 285(2):403–412, 1997.

Octavio M Guilera, Adrián Brunini, and Omar Gustavo Benvenuto. Consequences of the simultaneous formation of giant planets by the core accretion mechanism. *Astronomy & Astrophysics*, 521:A50, 2010.

OM Guilera, Zs Sándor, MP Ronco, J Venturini, and MM Bertolami. Giant planet formation at the pressure maxima of protoplanetary disks ii. a hybrid accretion scenario. *arXiv preprint arXiv:2005.10868*, 2020.

Daniel Harsono, Per Bjerkeli, Matthijs HD van der Wiel, Jon P Ramsey, Luke T Maud, Lars E Kristensen, and Jes K Jørgensen. Evidence for the start of planet formation in a young circumstellar disk. *Nature Astronomy*, 2(8):646–651, 2018.

Thomas Hartlep and Jeffrey N. Cuzzi. Cascade Model for Planetesimal Formation by Turbulent Clustering. *arXiv e-prints*, art. arXiv:2002.06321, February 2020.

Chushiro Hayashi. Structure of the Solar Nebula, Growth and Decay of Magnetic Fields and Effects of Magnetic and Turbulent Viscosities on the Nebula. *Progress of Theoretical Physics Supplement*, 70:35–53, 01 1981. ISSN 0375-9687. doi: 10.1143/PTPS.70.35. URL https://doi.org/10.1143/PTPS.70.35.

Shigeru Ida and Doug NC Lin. Toward a deterministic model of planetary formation. i. a desert in the mass and semimajor axis distributions of extrasolar planets. *ApJ*, 604(1):388, 2004.

Shigeru Ida and Junichiro Makino. Scattering of Planetesimals by a Protoplanet: Slowing Down of Runaway Growth. *Icarus*, 106(1):210–227, November 1993. doi: 10.1006/icar.1993.1167.

Satoshi Inaba, Hidekazu Tanaka, Kiyoshi Nakazawa, George W Wetherill, and Eiichiro Kokubo. High-accuracy statistical simulation of planetary accretion: Ii. comparison with n-body simulation. *Icarus*, 149(1):235–250, 2001.

André Izidoro, Bertram Bitsch, Sean N Raymond, Anders Johansen, Alessandro Morbidelli, Michiel Lambrechts, and Seth A Jacobson. Formation of planetary systems by pebble accretion and migration: Hot super-earth systems from breaking compact resonant chains. *arXiv preprint arXiv:1902.08772*, 2019.

James Hopwood Jeans. I. the stability of a spherical nebula. *Philosophical Transactions of the Royal Society of London. Series A, Containing Papers of a Mathematical or Physical Character*, 199(312-320):1–53, 1902.

S. Jin, C. Mordasini, V. Parmentier, R. van Boekel, T. Henning, and J. Ji. Planetary Population Synthesis Coupled with Atmospheric Escape: A Statistical View of Evaporation. *ApJ*, 795:65, November 2014. doi: 10.1088/0004-637X/795/1/65.

Sheng Jin, Christoph Mordasini, Vivien Parmentier, Roy Van Boekel, Thomas Henning, and Jianghui Ji. Planetary population synthesis coupled with atmospheric escape: a statistical view of evaporation. *The Astrophysical Journal*, 795(1):65, 2014.

A. Johansen, J. S. Oishi, M.-M. Mac Low, H. Klahr, T. Henning, and A. Youdin. Rapid planetesimal formation in turbulent circumstellar disks. *Nature*, 448:1022–1025, August 2007. doi: 10.1038/nature06086.

A. Johansen, A. Youdin, and M.-M. Mac Low. Particle Clumping and Planetesimal Formation Depend Strongly on Metallicity. *ApJ*, 704:L75–L79, October 2009. doi: 10.1088/0004-637X/704/2/L75.

A. Johansen, H. Klahr, and T. Henning. High-resolution simulations of planetesimal formation in turbulent protoplanetary discs. *A&A*, 529:A62, May 2011. doi: 10.1051/0004-6361/201015979.

Anders Johansen and Bertram Bitsch. Exploring the conditions for forming cold gas giants through planetesimal accretion. *A&A*, 631:A70, November 2019. doi: 10.1051/0004-6361/201936351.

Anders Johansen, Jeffrey S Oishi, Mordecai-Mark Mac Low, Hubert Klahr, Thomas Henning, and Andrew Youdin. Rapid planetesimal formation in turbulent circumstellar disks. *Nature*, 448(7157):1022–1025, 2007.

Anders Johansen, Hubert Klahr, and Th Henning. High-resolution simulations of planetesimal formation in turbulent protoplanetary discs. *Astronomy & Astrophysics*, 529:A62, 2011.

Anders Johansen, Andrew N Youdin, and Yoram Lithwick. Adding particle collisions to the formation of asteroids and kuiper belt objects via streaming instabilities. *Astronomy & Astrophysics*, 537:A125, 2012.

Anders Johansen, Shigeru Ida, and Ramon Brasser. How planetary growth outperforms migration. *Astronomy & Astrophysics*, 622:A202, 2019.

Immanuel Kant. Allgemeine naturgeschichte und theorie des himmels [universal natural history and theory of the heavens]. *Trans. by Ian Johnston. Arlington, VA: Richer Resources*, 1755.

Hubert Klahr and Peter Bodenheimer. Formation of Giant Planets by Concurrent Accretion of Solids and Gas inside an Anticyclonic Vortex. *ApJ*, 639(1):432–440, March 2006. doi: 10.1086/498928.

Hubert Klahr and Andreas Schreiber. Turbulence sets the length scale for planetesimal formation: Local 2D simulations of streaming instability and planetesimal formation. *arXiv e-prints*, art. arXiv:2007.10696, July 2020.

Hiroshi Kobayashi, Hidekazu Tanaka, and Alexander V. Krivov. PLANETARY CORE FORMATION WITH COLLISIONAL FRAGMENTATION AND ATMOSPHERE TO FORM GAS GIANT PLANETS. *The Astrophysical Journal*, 738(1):35, aug 2011. doi: 10.1088/0004-637x/738/1/35. URL https://doi.org/10.1088%2F0004-637x%2F738%2F1%2F35.

Eiichiro Kokubo and Shigeru Ida. On runaway growth of planetesimals. *Icarus*, 123(1):180–191, 1996.

Eiichiro Kokubo and Shigeru Ida. Oligarchic growth of protoplanets. *Icarus*, 131(1):171–178, 1998.

KA Kretke and HF Levison. Challenges in forming the solar system's giant planet cores via pebble accretion. *The Astronomical Journal*, 148(6):109, 2014.

ANNE-MARIE Lagrange, DANA E Backman, and PAWEL Artymowicz. Planetary material around main-sequence stars. *Protostars and planets IV*, 639, 2000.

Michiel Lambrechts and Anders Johansen. Rapid growth of gas-giant cores by pebble accretion. *A&A*, 544:A32, 2012.

Michiel Lambrechts, Anders Johansen, and Alessandro Morbidelli. Separating gas-giant and ice-giant planets by halting pebble accretion. *Astronomy & Astrophysics*, 572:A35, 2014.

E. J. Lee and E. Chiang. To Cool is to Accrete: Analytic Scalings for Nebular Accretion of Planetary Atmospheres. *ApJ*, 811:41, September 2015. doi: 10.1088/0004-637X/811/1/41.

Christian T. Lenz, Hubert Klahr, and Tilman Birnstiel. Planetesimal population synthesis: Pebble flux-regulated planetesimal formation. *ApJ*, 874(1):36, mar 2019. doi: 10.3847/1538-4357/ab05d9. URL https://doi.org/10.3847%2F1538-4357%2Fab05d9.

Christian T Lenz, Hubert Klahr, Tilman Birnstiel, Katherine Kretke, and Sebastian Stammler. Constraining the parameter space for the solar nebula-the effect of disk properties on planetesimal formation. *Astronomy & Astrophysics*, 640:A61, 2020.

Harold F Levison, Martin J Duncan, and Edward Thommes. A lagrangian integrator for planetary accretion and dynamics (lipad). *The Astronomical Journal*, 144(4):119, 2012.

Harold F Levison, Katherine A Kretke, and Martin J Duncan. Growing the gas-giant planets by the gradual accumulation of pebbles. *Nature*, 524(7565):322, 2015.

Douglas NC Lin and John Papaloizou. On the tidal interaction between protoplanets and the protoplanetary disk. iii-orbital migration of protoplanets. *The Astrophysical Journal*, 309: 846–857, 1986.

Jack J Lissauer. Timescales for planetary accretion and the structure of the protoplanetary disk. *Icarus*, 69(2):249–265, 1987.

Jack J Lissauer. Planet formation. *Annual review of astronomy and astrophysics*, 31(1):129–172, 1993.

R. Lüst. Die Entwicklung einer um einen Zentralkörper rotierenden Gasmasse. I. Lösungen der hydrodynamischen Gleichungen mit turbulenter Reibung. *Zeitschrift Naturforschung Teil A*, 7 (1):87–98, January 1952. doi: 10.1515/zna-1952-0118.

D. Lynden-Bell and J. E. Pringle. The evolution of viscous discs and the origin of the nebular variables. *MNRAS*, 168:603–637, September 1974. doi: 10.1093/mnras/168.3.603.

Wladimir Lyra, Natalie Raettig, and Hubert Klahr. Pebble-trapping Backreaction Does Not Destroy Vortices. *Research Notes of the American Astronomical Society*, 2(4):195, October 2018. doi: 10.3847/2515-5172/aaeac9.

Carlo Felice Maria Manara. *The physics of the accretion process in the formation and evolution of Young Stellar Objects*. PhD thesis, lmu, 2014.

Pierre Simon marquis de Laplace. *Elementary illustrations of the Celestial mechanics of Laplace: part the first, comprehending the first book*. J. Murray, 1821.

Isamu Matsuyama, Doug Johnstone, and Lee Hartmann. Viscous diffusion and photoevaporation of stellar disks. *The Astrophysical Journal*, 582(2):893, 2003.

Michel Mayor and Didier Queloz. A jupiter-mass companion to a solar-type star. *Nature*, 378 (6555):355–359, 1995.

Lokesh Mishra, Yann Alibert, Adrien Leleu, Alexandre Emsenhuber, Christoph Mordasini, Remo Burn, Stéphane Udry, and Willy Benz. The new generation planetary population synthesis (ngpps). vi. introducing kobe: Kepler observes bern exoplanets. theoretical perspectives on the architecture of planetary systems: Peas in a pod. *arXiv preprint arXiv:2105.12745*, 2021.

Hiroshi Mizuno. Formation of the giant planets. *Progress of Theoretical Physics*, 64(2):544–557, 1980.

Paul Mollière and Christoph Mordasini. Deuterium burning in objects forming via the core accretion scenario-brown dwarfs or planets? *Astronomy & Astrophysics*, 547:A105, 2012.

Alessandro Morbidelli, William F Bottke, David Nesvornỳ, and Harold F Levison. Asteroids were born big. *Icarus*, 204(2):558–573, 2009.

C. Mordasini, Y. Alibert, H. Klahr, and T. Henning. Characterization of exoplanets from their formation. I. Models of combined planet formation and evolution. *A&A*, 547:A111, November 2012. doi: 10.1051/0004-6361/201118457.

C Mordasini, Yann Alibert, Willy Benz, H Klahr, and Th Henning. Extrasolar planet population synthesis-iv. correlations with disk metallicity, mass, and lifetime. *A&A*, 541:A97, 2012a.

C Mordasini, Yann Alibert, C Georgy, K-M Dittkrist, H Klahr, and T Henning. Characterization of exoplanets from their formation-ii. the planetary mass-radius relationship. *Astronomy & Astrophysics*, 547:A112, 2012b.

C. Mordasini, P. Mollière, K. M. Dittkrist, S. Jin, and Y. Alibert. Global models of planet formation and evolution. *International Journal of Astrobiology*, 14(2):201–232, April 2015. doi: 10.1017/S1473550414000263.

Christoph Mordasini. Planetary Population Synthesis. In Hans J. Deeg and Juan Antonio Belmonte, editors, *Handbook of Exoplanets*, page 143. Springer Living Reference Work, 2018. ISBN 978-3-319-30648-3. doi: 10.1007/978-3-319-55333-7_143.

Christoph Mordasini, Yann Alibert, and Willy Benz. Extrasolar planet population synthesis-i. method, formation tracks, and mass-distance distribution. *A&A*, 501(3):1139–1160, 2009.

Gijs D Mulders, Christoph Mordasini, Ilaria Pascucci, Fred J Ciesla, Alexandre Emsenhuber, and Dániel Apai. The exoplanet population observation simulator. ii. population synthesis in the era of kepler. *The Astrophysical Journal*, 887(2):157, 2019.

N Murray and B Chaboyer. Are stars with planets polluted? *The Astrophysical Journal*, 566(1): 442, 2002.

Taishi Nakamoto and Yoshitsugo Nakagawa. Formation, early evolution, and gravitational stability of protoplanetary disks. *The Astrophysical Journal*, 421:640–650, 1994.

N. Ndugu, B. Bitsch, and E. Jurua. Planet population synthesis driven by pebble accretion in cluster environments. *MNRAS*, 474(1):886–897, Oct 2017. ISSN 1365-2966. doi: 10.1093/mnras/stx2815. URL http://dx.doi.org/10.1093/mnras/stx2815.

Keiji Ohtsuki, Glen R Stewart, and Shigeru Ida. Evolution of planetesimal velocities based on three-body orbital integrations and growth of protoplanets. *Icarus*, 155(2):436–453, 2002.

Chris W Ormel. The emerging paradigm of pebble accretion. In *Formation, Evolution, and Dynamics of Young Solar Systems*, pages 197–228. Springer, 2017.

CW Ormel and HH Klahr. The effect of gas drag on the growth of protoplanets-analytical expressions for the accretion of small bodies in laminar disks. *A&A*, 520:A43, 2010.

S.-J. Paardekooper, C. Baruteau, A. Crida, and W. Kley. A torque formula for non-isothermal type I planetary migration - I. Unsaturated horseshoe drag. *MNRAS*, 401:1950–1964, January 2010. doi: 10.1111/j.1365-2966.2009.15782.x.

S-J Paardekooper, C Baruteau, and W Kley. A torque formula for non-isothermal type i planetary migration–ii. effects of diffusion. *Monthly Notices of the Royal Astronomical Society*, 410(1): 293–303, 2011.

Fausto Perri and Ao GW Cameron. Hydrodynamic instability of the solar nebula in the presence of a planetary core. *Icarus*, 22(4):416–425, 1974.

Giovanni Picogna, Barbara Ercolano, James E Owen, and Michael L Weber. The dispersal of protoplanetary discs–i. a new generation of x-ray photoevaporation models. *Monthly Notices of the Royal Astronomical Society*, 487(1):691–701, 2019.

James B Pollack, Olenka Hubickyj, Peter Bodenheimer, Jack J Lissauer, Morris Podolak, and Yuval Greenzweig. Formation of the giant planets by concurrent accretion of solids and gas. *Icarus*, 124(1):62–85, 1996.

Natalie Raettig, Hubert Klahr, and Wladimir Lyra. Particle Trapping and Streaming Instability in Vortices in Protoplanetary Disks. *ApJ*, 804:35, May 2015. doi: 10.1088/0004-637X/804/1/35.

Roman R Rafikov. Fast accretion of small planetesimals by protoplanetary cores. *The Astronomical Journal*, 128(3):1348, 2004.

Roman R Rafikov. Can giant planets form by direct gravitational instability? *The Astrophysical Journal Letters*, 621(1):L69, 2005.

Sean N Raymond and Andre Izidoro. Origin of water in the inner solar system: Planetesimals scattered inward during jupiter and saturn's rapid gas accretion. *Icarus*, 297:134–148, 2017.

Viktor Sergeevich Safronov. Evolution of the protoplanetary cloud and formation of the earth and the planets. *Israel program for scientific translations*, 1972.

VS Safronov and EV Zvjagina. Relative sizes of the largest bodies during the accumulation of planets. *Icarus*, 10(1):109–115, 1969.

Urs Schäfer, Chao-Chin Yang, and Anders Johansen. Initial mass function of planetesimals formed by the streaming instability. *A&A*, 597:A69, 2017.

M Schlecker, C Mordasini, A Emsenhuber, H Klahr, Th Henning, and R Burn. The new generation planetary population synthesis (ngpps). iii. warm super-earths and cold jupiters: A weak occurrence correlation, but with a strong architecture-composition link. *Astronomy & Astrophysics*, 2020.

M Schlecker, D Pham, R Burn, Y Alibert, C Mordasini, A Emsenhuber, H Klahr, Th Henning, and L Mishra. The new generation planetary population synthesis (ngpps). v. predetermination of planet types in global core accretion models. *arXiv preprint arXiv:2104.11750*, 2021.

Hilke E Schlichting, Cesar I Fuentes, and David E Trilling. Initial planetesimal sizes and the size distribution of small kuiper belt objects. *AJ*, 146(2):36, 2013.

Djoeke Schoonenberg and Chris W Ormel. Planetesimal formation near the snowline: in or out? *A&A*, 602:A21, 2017.

Andreas Schreiber. *Diffusion Limited Planetesimal Formation – Why asteroid and Kuiper-belt objects share a characteristic size*. PhD thesis, Ruperto-Carola University Heidelberg, 2018. URL http://www.ub.uni-heidelberg.de/archiv/24579.

Sara Seager, M Kuchner, CA Hier-Majumder, and Burkhard Militzer. Mass-radius relationships for solid exoplanets. *The Astrophysical Journal*, 669(2):1279, 2007.

Ni I Shakura and Rashid Alievich Sunyaev. Black holes in binary systems. observational appearance. *Astronomy and Astrophysics*, 24:337–355, 1973.

Jacob B Simon, Philip J Armitage, Rixin Li, and Andrew N Youdin. The mass and size distribution of planetesimals formed by the streaming instability. i. the role of self-gravity. *The Astrophysical Journal*, 822(1):55, 2016.

George Gabriel Stokes et al. On the effect of the internal friction of fluids on the motion of pendulums. 1851.

Hidekazu Tanaka and Shigeru Ida. Growth of a migrating protoplanet. *Icarus*, 139(2):350–366, 1999.

Hidekazu Tanaka, Taku Takeuchi, and William R Ward. Three-dimensional interaction between a planet and an isothermal gaseous disk. i. corotation and lindblad torques and planet migration. *The Astrophysical Journal*, 565(2):1257, 2002.

Amaury Thiabaud, Ulysse Marboeuf, Yann Alibert, Nahuel Cabral, Ingo Leya, and Klaus Mezger. From stellar nebula to planets: The refractory components. *Astronomy & Astrophysics*, 562: A27, 2014.

E. W. Thommes, M. J. Duncan, and H. F. Levison. Oligarchic growth of giant planets. *Icarus*, 161(2):431–455, February 2003. doi: 10.1016/S0019-1035(02)00043-X.

Dimitri Veras and Philip J Armitage. Outward migration of extrasolar planets to large orbital radii. *Monthly Notices of the Royal Astronomical Society*, 347(2):613–624, 2004.

Oliver Voelkel, Hubert Klahr, Christoph Mordasini, Alexandre Emsenhuber, and Christian Lenz. Effect of pebble flux-regulated planetesimal formation on giant planet formation. *Astronomy & Astrophysics*, 642:A75, 2020.

Oliver Voelkel, Rogerio Deienno, Katherine Kretke, and Hubert Klahr. Linking planetary embryo formation to planetesimal formation-i. the effect of the planetesimal surface density in the terrestrial planet zone. *Astronomy & Astrophysics*, 645:A131, 2021a.

Oliver Voelkel, Rogerio Deienno, Katherine Kretke, and Hubert Klahr. Linking planetary embryo formation to planetesimal formation-ii. the effect of pebble accretion in the terrestrial planet zone. *Astronomy & Astrophysics*, 645:A132, 2021b.

Oliver Voelkel, Hubert Klahr, and Christpoph Mordasini. On the multiple generations of planetary embryo formation. *Astronomy & Astrophysics*, submitted to A&A.

Kevin Walsh, Bryce Bolin, Chrysa Avdellidou, Alessandro Morbidelli, et al. Identification of a primordial asteroid family constrains the original planetesimal population. *Science*, 357(6355): 1026–1029, 2017.

Kevin J Walsh and Harold F Levison. Planetsimals to planets-revisiting terrestrial planet formation. In *DPS*, pages 302–05, 2015.

Kevin J Walsh and Harold F Levison. Terrestrial planet formation from an annulus. *The Astronomical Journal*, 152(3):68, 2016.

Kevin J Walsh and Harold F Levison. Planetesimals to terrestrial planets: Collisional evolution amidst a dissipating gas disk. *Icarus*, 329:88–100, 2019.

Kevin J Walsh, Alessandro Morbidelli, Sean N Raymond, David P O'Brien, and Avi M Mandell. A low mass for mars from jupiter's early gas-driven migration. *Nature*, 475(7355):206–209, 2011.

William R Ward. Protoplanet migration by nebula tides. *Icarus*, 126(2):261–281, 1997.

SJ Weidenschilling. Aerodynamics of solid bodies in the solar nebula. *Monthly Notices of the Royal Astronomical Society*, 180(2):57–70, 1977a.

SJ Weidenschilling. The distribution of mass in the planetary system and solar nebula. *Astrophysics and Space Science*, 51(1):153–158, 1977b.

SJ Weidenschilling. Initial sizes of planetesimals and accretion of the asteroids. *Icarus*, 214(2): 671–684, 2011.

Fred L Whipple. On certain aerodynamic processes for asteroids and comets. In *From plasma to planet*, page 211, 1972.

Joshua N Winn and Daniel C Fabrycky. The occurrence and architecture of exoplanetary systems. *ARA&A*, 53:409–447, 2015.

Andrew N Youdin and Jeremy Goodman. Streaming instabilities in protoplanetary disks. *The Astrophysical Journal*, 620(1):459, 2005.

Xiaochen Zheng, Douglas NC Lin, and MBN Kouwenhoven. Planetesimal clearing and size-dependent asteroid retention by secular resonance sweeping during the depletion of the solar nebula. *The Astrophysical Journal*, 836(2):207, 2017.

# Acknowledgments

I wish to thank the referees Hubert Klahr and Andreas Quirrenbach for investing their time to review this thesis. This research has been supported by the Deutsche Forschungsgemeinschaft Schwerpunktprogramm (DFG SPP) SPP 1992 “Exploring the diversity of extrasolar planets” contract : KL 1469/17-1 Consistent Planetesimal Formation from Pebbles for Synthetic Population Syntheses of Exo-Planets. Special thanks goes to Tina Rückriemen-Bez for her extraordinary effort within this program. At this point I also wish to thank the tax-payer for investing in fundamental research.

To my advisors Hubert Klahr and Christoph Mordasini I wish to say thank you for the guidance, trust and freedom you granted me. The past four years have without doubt been the most liberating, educative and productive period of my life. For this non self evident liberal framework and your continuous support I am deeply grateful. Special thanks for the wonderful collaborations goes to Rogerio Deienno and Alexandre Emsenhuber. Your support has been a tremendous help and I wish you all the best for your future careers. I also want to thank Christian Lenz and Remo Burn for the many helpful and guiding discussion. Remo, I wish you and Simone all the best, thank you for letting me be part of your lovely wedding. It was a pleasure to be part of the "Klahrgroup", specifically I wish to thank Martin Schlecker, Robert Latka, Vincent Carpenter, Simeon Doetsch, Paul Rosendahl and Jesper Tjoa for the entertaining group meetings.

Almost half of my PhD in Heidelberg was overshadowed by the Covid-19 Pandemic. I wish to thank everyone who with their continuous work and effort during that time enabled me to continue working on this project. Beyond the pandemic, this involves the entire MPIA and its infrastructure. To the technical department, the IT department, the cleaning staff, gardening, accounting, administration and everything else involved, thank you for making MPIA such a wonderful place to work at. Special thanks goes to Thomas Henning, Frank Witzel, Ulrich Hiller, Björn Binroth, Daniela Scheerer and Ingrid Apfel.

For proof reading the thesis and fruitful discussions to improve the manuscript I with to thank my brother Sebastian Völkel, David Fuksman, Tobias Moldenhauer and Jacob Isbell. Also I wish to thank all the wonderful people that I got to meet in Heidelberg as part of the IMPRS program and beyond, specifically Lizxandra Flores, Giancarlo Mattia, Marcello Barazza, Mischa Breuhaus, Vincent Carpenter, Francesco Conte, Camille Bergez-Casalou, Grigorii Smirnov-Pinchukov, Irina Smirnova-Pinchukova, Riccardo Franceschi, Melanie Kaasinen and Thomas Jackson. Regarding this I wish to thank Christian Fendt, who made this possible. Special gratitude for the wonderful time in Heidelberg goes to Gideon Yoffe, David Fuksman, Courtney Pereira and Siddhant Deshmuk. You are wonderful and wherever life will take you I wish you all the best.

To my (quite literal because we share the same apartment) closest friend in Heidelberg Jacob Isbell. It is a pleasure to have met you and my life in this city would not have been the same without you. For this and your hard work in our common project sci.an I want to say thank you. In this regard I also want to thank Tobias Moldenhauer and the crash-free sci.an backend. You guys are the perfect teammates.

Next to all the great scientists I got to meet over the last years, many others have inspired me along the way. Very notably Daniel Maslewski and Michael Kipnis. Their enthusiasm and passion for astronomy always helped me to remember the beauty of this field. Many wonderful vacations and adventures were taken, and hopefully many will follow with my good friend Achim Neff. For his supporting and reliable friendship throughout my entire life, I wish to thank Alexander Bitz.

My Brother Sebastian is the most skilled and passionate scientist I have ever met. He is the best role model one could have and working in theoretical astrophysics myself for a few years I begin to realize this more and more. There is no doubt in my mind that he will ascent to the great figures in science and that his name will be heard. For having a brother like you I am deeply grateful. Throughout my entire life I knew I could always rely on my parents Dorothea and Heinz. Their love and support has been a constant like no other. For motivating, inspiring and teaching me I wish to express my most honest gratitude. To you and my brother Sebastian, I could not be happier and more grateful to have you as my family.

Also I wish to thank my old friends around the group known as "Die Bank" and the most wonderful lively street in Heidelberg, the Untere Straße including my lovely neighbors.

To all of you: 10/10.

Background Image by Marcelo Barraza: Boceto Vórtice - Heidelberg 2020